DEVELOPMENT AND CHARACTERIZATION OF NOVEL DETECTORS FOR USE IN FLOW INJECTION ANALYSIS OR LIQUID CHROMATOGRAPHY

by

JOHN ALBERT ROUSH

Dissertation submitted to the Faculty of the

Virginia Polytechnic Institute and State University

in partial fulfillment of the requirements for the degree of

Doctor of Philosophy

in

Chemistry

Approved:

Mark R. Anderson, Chairman

James O. Glanville

Gary L. Long

John G. Mason

Harold M. McNair

Joseph S. Merola

September, 1992
Blacksburg, Virginia

c.2

DEVELOPMENT AND CHARACTERIZATION OF NOVEL DETECTORS FOR USE IN FLOW INJECTION ANALYSIS OR LIQUID CHROMATOGRAPHY

by
John Albert Roush
Committee Chairman: Mark R. Anderson
Chemistry

(Abstract)

A rapid scanning square wave voltammetric detector has been developed for use with high performance liquid chromatography.The electrochemical cell used in the detector was designed so that the HPLC effluent flows through the center of a large diameter platinum disk electrode and is then forced to flow radially across the electrode surface. The arrangement of the electrodes in the cell was intended to result in large analytical currents while minimizing electrical resistance and analyte band spreading in the detection zone. The detector was evaluated in terms of its minimum detectable quantity, linear dynamic range, electrochemical efficiency, and analyte band spreading. The MDQ was found to be in the low parts per billion range for hydroquinone. The detector was shown to provide data that is qualitatively superior to data obtained by amperometric detection and was shown to be compatible with gradient elution HPLC over a broad range of solvent compositions.

A sensor based on the quartz crystal microbalance was also developed for use in flowing solvent streams. Quartz crystals were treated with various compounds to produce close - packed monolayer coatings which could interact

with solutes entering the flow cell. The solute capacity was determined for one of the monolayer coatings and various factors that influence the magnitude of the QCM signal were investigated. These factors include the solvent flow rate, the solvent strength, solute molecular structure, and bonded phase molecular structure. The QCM sensor was found to be a convenient probe for conducting surface adsorption studies and the molar free energy of adsorption was determined for some chemically related solutes on an amine modified crystal.

Acknowledgements.

I would like to thank Professor Mark Anderson for his guidance, assistance, and support throughout the course of this research. This work is largely the result of many valuable discussions and challenging questions posed by Professor Anderson. I would also like to thank Dr. Thomas Floyd and Dr. Jack Hensley of Tennessee Eastman Company as well as professor Harold McNair for the use of laboratory equipment which was needed for many of the experiments performed in this research.

Finally, I would like to thank my wife Kathleen, whose love and friendship have been a constant source of happiness for me during the last fifteen years. Her kindness, understanding, and many personal sacrifices have made it possible to pursue this research. Her encouragement and belief in my abilities have provided the confidence and inspiration to continue working during times of personal doubt and anxiety.

TABLE OF CONTENTS

LIST OF FIGURES

FIGURE PAGE

LIST OF TABLES

Chapter 1. Introduction To Square Wave Voltammetric Detection For HPLC.

1.1 Overview of Electrochemical Detection For HPLC.

Electrochemical detection has been used in combination with high performance liquid chromatography for a wide variety of applications since the first commercial instruments became available in 1974. The advantages of electrochemical detection include greater selectivity and, often, lower limits of detection than is possible using spectroscopic methods. Although performance varies widely with the analyte and the conditions of analysis, limits of detection have been reported to be in the lower picogram range for several oxidizable compounds and about an order of magnitude higher for easily reducible analytes[1].

Several volumes would be required for a thorough review of the applications of electrochemical detection with liquid chromatography (LCEC). However, the applications can be generalized according to the electrochemical process occurring at the indicator electrode (oxidation or reduction) and by the classes of compounds most frequently studied. The most common oxidative applications involve phenols, aromatic amines, and thiols. Reductive LCEC applications are less common than those involving oxidation because of the need for removal of trace levels of oxygen. Reductive applications most often involve quinones and nitro compounds.

Many compounds of biological interest, including pharmaceuticals, plant phenolics, and catecholamines are phenolic and have been studied frequently[2].

Phenolic compounds are generally oxidizable on platinum, gold, or carbon electrodes. The oxidation potentials vary widely for these compounds, with hydroquinones and catechols being oxidized near +0.6 V versus SCE and cresols being oxidized at +1.0 V or higher. A number of methods have also been developed for phenolic compounds of industrial interest, such as antioxidants, antimicrobials, and agricultural chemicals[3].

Like phenols, aromatic amines are oxidized over a wide range of potentials. Among the most easily oxidized are phenylenediamines, benzidines, and amino-phenols. Numerous methods have been developed for these compounds[4].

Thiols are generally very easily oxidized to disulfides in solution, but the reaction is slow at most electrode surfaces[1]. LCEC methods for thiol determination generally depend on the behavior of these compounds on a mercury electrode surface at about +0.1 V. The reaction involves the formation of a stable complex between mercury and the thiol, and the mercury is actually the species that undergoes oxidation. This approach has been used to determine the amino acid cysteine as well as the tripeptide glutathione, and the pharmaceuticals penicillamine and captopril.

Other compounds that have been studied by oxidative LCEC include ascorbic acid and uric acid in complex matrices. Also, methods for some heterocycles of pharmaceutical interest, such as phenothiazines and imipramine have been developed.

The quinone group is considered to undergo a well behaved reversible reduction on carbon and mercury electrodes[1]. A large number of synthetic and natural products contain the quinone moiety and many of these are good candidates for selective determination by reductive LCEC. Unfortunately, several of the most important of these compounds are extremely hydrophobic due to the presence of long hydrocarbon side chains, leading to difficulty in developing adequate reverse-phase separation methods.

Aromatic nitro and nitroso compounds, as well as nitrate esters, nitramines, and nitrosamines are readily reducible at carbon and mercury electrodes. LCEC methods have been developed for many of the compounds that fall into these classes, including pharmaceuticals, explosives[5], and agricultural chemicals. The selectivity is often quite good in biological and environmental samples because of the low reduction potential of the nitro group and the rarity of this group in naturally occurring compounds. Reagents containing the nitro group have frequently been used to derivatize amines, aldehydes, ketones, and carboxylic acids to provide a more easily reducible handle for these compounds[6,7].

Many compounds which are normally difficult to detect by electrochemical means have been studied using post column derivatizations. A reagent is mixed with the column effluent to convert sample components into electroactive compounds. Alternatively, some methods measure changes in the concentration of the reagent itself. The most thoroughly investigated system involves the use of dual

electrodes, in which the reagent is generated at constant current at the upstream electrode and the consumption of the reagent is monitored at the downstream electrode[8]. One system of this type involves the generation of bromine from bromide at the upstream electrode, followed by the determination of bromine consumption by alkenes or aromatics.

The most common modes of electrochemical detection with HPLC are amperometry and coulometry. In the amperometric mode, the conversion of sample components is small (usually less than 5%), while coulometry involves essentially complete conversion (greater than 95%). These definitions are somewhat arbitrary, representing the extremes in the degree of sample conversion. In practice, many detectors fall in between these extremes and are referred to as quasi-amperometric detectors[1].

In general, coulometric detection is favored less than the amperometric mode, because of the ease of construction and lower detection limits of amperometric detectors. Coulometric detection is achieved using very large surface area electrodes which are constructed at the expense of greater cell dead volume and longer sample residence times. Furthermore, the background current also increases proportionally with the area of the electrode. Detector noise increases with the background current, resulting in a lower signal - to - noise ratio than is obtained by amperometric detection[1].

Voltammetry is another, less frequently used, mode of electrochemical

detection for HPLC. In voltammetry, the potential of the indicator electrode is changed rapidly and systematically between two chosen values and the current is measured at intervals. The potential may be scanned either linearly or in potential increments. A variety of nonlinear potential scanning methods are possible, including pulsed, stair case, and square wave voltammetry. Square wave voltammetry was the scanning method used with the detector developed for this research.

Figure 1.1 shows a typical wave form used in square wave voltammetry. The wave form consists of a combination of a stair case wave form with a potential pulse. The current is measured at the bottom (i_b) and top (i_a) of each potential step. The net current ($i_{NET} = i_a - i_b$) is the monitored value in this method.

Figure 1.2 shows a voltammogram generated from the square wave voltammetric method. The figure illustrates two important consequences of the method. First, the signal generated is a peak whose maximum corresponds to the oxidation (or reduction) potential of the analyte. Second, the differential current measurement results in a background current subtraction.

Rapid scanning square wave voltammetry offers some important advantages over amperometric or coulometric detection for HPLC. Current is monitored with respect to both time and potential, resulting in three-dimensional chromatograms which are qualitatively superior to those obatained by amperometric or coulometric detection. The three-dimensional aspect of square wave voltammetric

detection permits the resolution of coeluting analytes in the potential domain, provided that their oxidation or reduction potentials are sufficiently different. Furthermore, since square wave voltammetry measures a differential current, the method discriminates against non-faradaic processes; therefore, the net background current is near zero, regardless of the magnitude of the charging or resistive currents encountered.

Rapid scanning voltammetric techniques have been applied to high performance liquid chromatography (HPLC) previously by several groups[9-15]. Samuelsson et al.[9] were the first to describe the use of square wave voltammetry (SWV) with HPLC. They demonstrated the advantages of the method in terms of specificity of separations in both time and potential in the determination of N-nitrosodiethanolamine and N-nitrosoproline. Detection in this case however, was limited by flow pulsations and the geometry of the electrochemical cell. Goto and Shimada obtained superior results by using SWV and a carbon fiber electrode[12]. They described the analysis of several catecholamines by three-dimensional HPLC-SWV. More recently, Jorgenson et al.[10,13] demonstrated the qualitative and quantitative advantages of using microvoltammetric electrodes as detectors in liquid chromatography. In this application, Jorgenson et al. obtained a single square wave voltammogram for 10^{-7} M hydroquinone with a S/N of 5. Using a similar design, Kounaves and Young[14] obtained analogous results in

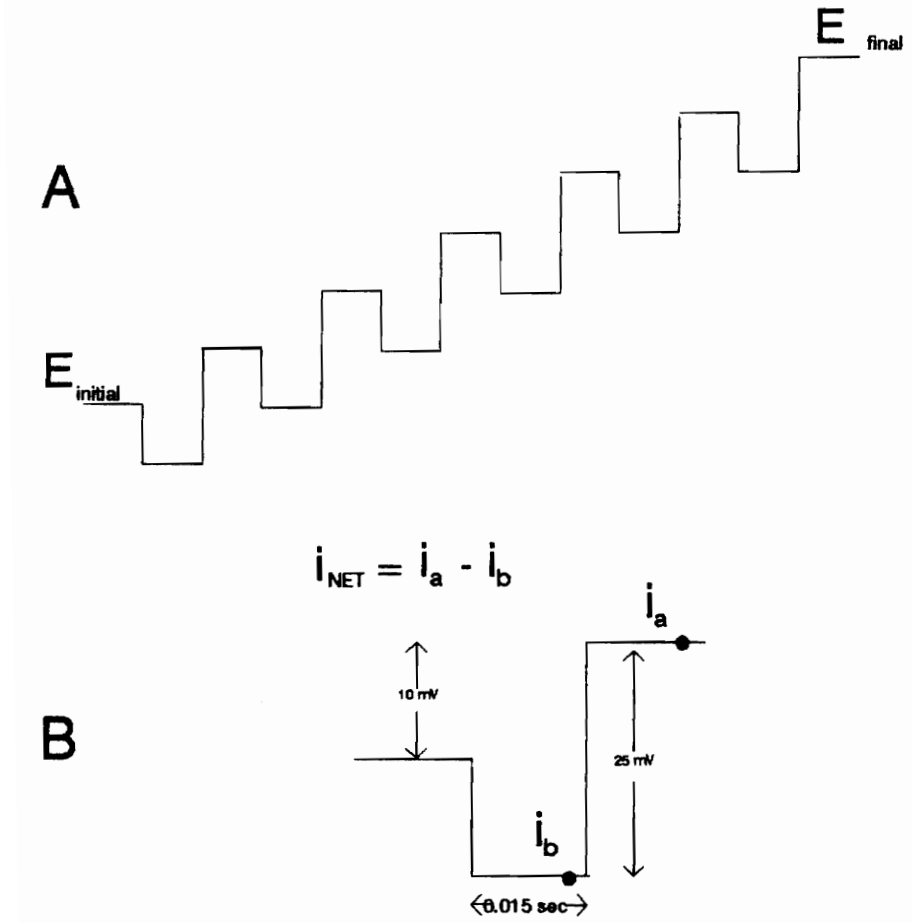

Figure 1.1 A) Illustrates the wave form used in square wave voltammetry for scanning between the initial potential $E_{initial}$ and the final potential E_{final}. B) Illustrates how current is measured in a single potential step and gives some typical parameters used for rapid scanning square wave voltammetry.

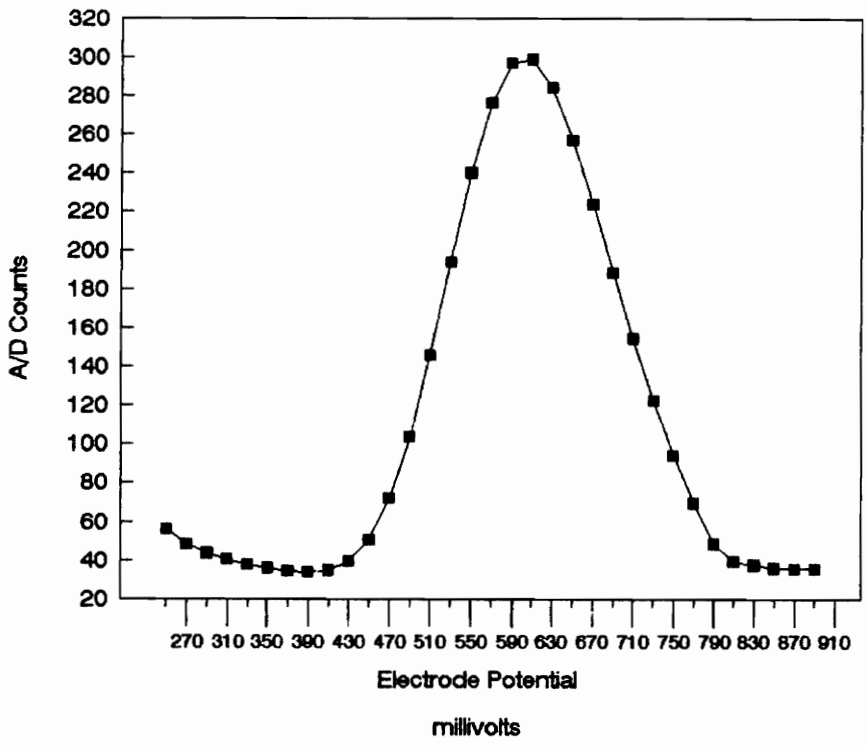

Figure 1.2 A square wave voltammogram obtained for a 5 ppm solution of hydroquinone used in this study. The solvent was 10% ethanol in water and contained 1 mM KBr and 1 mM $HClO_4$ as supporting electrolytes.

the separation and detection of several biogenic amines.

One of the major disadvantages of amperometric and coulometric detection for HPLC is the difficulty encountered when gradient elution methods are required. In general, the current measured by an electrochemical detector is a combination of Faradaic and non-Faradaic processes. The former is the result of the oxidation or reduction of electroactive analytes in the mobile phase and is the analytical current. The latter are a function of the solution composition and electrode placement. In electrochemical detectors, the non-Faradaic processes contribute to the chromatographic background noise. Because these background contributions are inherent to electrochemistry, electrochemical detection methods must minimize their influence to achieve reasonable detection limits. Gradient elution methods generally increase the background contribution because of the continuous compositional change.

With varying degrees of success, several researchers have developed methods which improve the compatibility of electrochemical detection with gradient elution HPLC [15-24]. Two basic approaches have been taken to reduce the magnitude of baseline shift. The first involves a modification of the detector in order to compensate for changes in the eluent. Tjaden and Jong[15] and Palmasano et al.[18] used a dual electrode detection system. In this configuration, the assumption is made that the current measured at the downstream electrode is entirely background current and can be subtracted from the current measured at

the upstream electrode to obtain the analytical current. However, the underlying assumption is not always true and only a partial correction is achieved. Gunasingham et al.[17] used a large volume wall jet cell in order to reduce the effect of the changing mobile phase composition on the detector. While this design reduces the magnitude of the baseline drift, it also contributes significantly to solute dispersion, reducing the gain in resolution that is normally expected with gradient elution.

A second approach involves the use of narrow mobile phase gradients in order to obtain the desired separation while minimizing the effect on the background current. Abell et al.[19] used an aqueous mobile phase containing 2-propanol and 1% acetic acid for the separation of amines. The concentration of 2-propanol was changed from 2.5% to 7.5% over several minutes. Drumheller et al.[20] used a water - acetonitrile gradient to separate two neuroactive peptides. In this case, the acetonitrile content of the mobile phase changed about 10% during the actual separation. Khaledi and Dorsey[21] and Bedard and Purdy[22] used surfactants as mobile phase modifiers and developed separations based on micellar gradients. In this application of mobile phase gradients the separation conditions are limited by the detector rather than by the sample as is normally the case.

These approaches dramatically compromise the chromatographic resolution in order to allow for the electrochemical detection. Recently, Oates and Jorgenson demonstrated the compatibility of voltammetric detection with gradient

elution for micro-capillary open tubular liquid chromatography [23,24]. Using a single carbon fiber working electrode that had been inserted into the outlet of the chromatographic system, they were able to obtain chromatovoltammograms which demonstrated very little change in the current baseline over the course of the mobile phase gradient.

1.2 Goals of The SWV Research.

The advantages of SWV detection for liquid chromatography have been demonstrated by others. However, the technique has not gained general acceptance because of several limitations. SWV detectors employing macroscopic indicator electrodes have been shown to have large minimum detectable quantities, in the low microgram range[9,30,31]. The detection limits for SWV detectors based on carbon fiber microelectrodes have been shown to be sufficiently low to make these instruments suitable for trace analysis. However, carbon fiber microelectrodes are difficult to prepare, are extremely fragile, and usually must be replaced when they become fouled. Furthermore, since current measurements are in the picoampere to nanoampere range, these systems require current amplification and are extremely vulnerable to interferences from environmental noises. These disadvantages make the use of microelectrode based SWV detectors impractical in most laboratory settings.

The primary goal of this research was the development and characterization

of a SWV detector for use with HPLC that would have a detection limit approaching those seen for microelectrode based detectors, but which would avoid the problems associated with microelectrodes. This goal was to be accomplished by incorporating a large diameter platinum disk indicator electrode in a detection zone of less than 1 μL, with the auxiliary and reference electrodes arranged in a way that would minimize the electrical resistance of the cell.

The detector characterization was to include the determination of the minimum detectable quantity in both the amperometric and voltammetric modes, as well as the linear dynamic range of the detector. Other characteristics to be assessed qualitatively included the ability to accurately control electrode potential and the effect of the detector dead volume on sample band spreading.

Other goals of this research included the demonstration of the qualitative superiority of the SWV data over data obtained amperometrically using isocratic HPLC. Finally, this research was intended to demonstrate the enhanced utility of electrochemical detection and the increased chromatographic resolution which is possible using macroscopic electrode based SWV detection with gradient elution HPLC.

Chapter 2. SWV Experimental.

2.1 The SWV Detector.

2.1.1 Electrochemical Apparatus.

The apparatus used in this study consisted of a conventional HPLC system, the SWV electrochemical cell, a microprocessor controlled potentiostat, and a personal computer which was used for overall control of the system and for data collection. Isocratic HPLC separations were performed using an EM Science MACS 100 pump (EM Science, Gibbstown, N. J.), a high pressure injection valve (Rheodyne Model 7120, Berkeley, Ca.) with a 20 μL sample loop, a pulse dampener, and a standard HPLC column, 4.6 X 250 mm, with 7 μm Zorbax ODS packing (Du Pont Instruments, Wilmington, De.). The gradient elution HPLC system consisted of two Waters model 501 pumps, a Waters model 660 solvent programmer, a high pressure injection valve (Rheodyne model 7010) with 20 μL sample loop, and a 4.6 X 250 mm HPLC column with 5 μm Econosil C18 packing (Alltech).

The SWV electrochemical cell is illustrated in figure 2.1 a - c. The cell is similar to the wall - jet design by Fleet and Little[25]. The principle differences with the new design are (i) the indicator electrode is the jet rather than the wall and (ii) the effluent may flow across the indicator electrode in any direction.

A 6 mm diameter platinum disk indicator electrode was prepared by drilling a 1/16" hole through the center of a Pt disk and the disk was then press fit onto

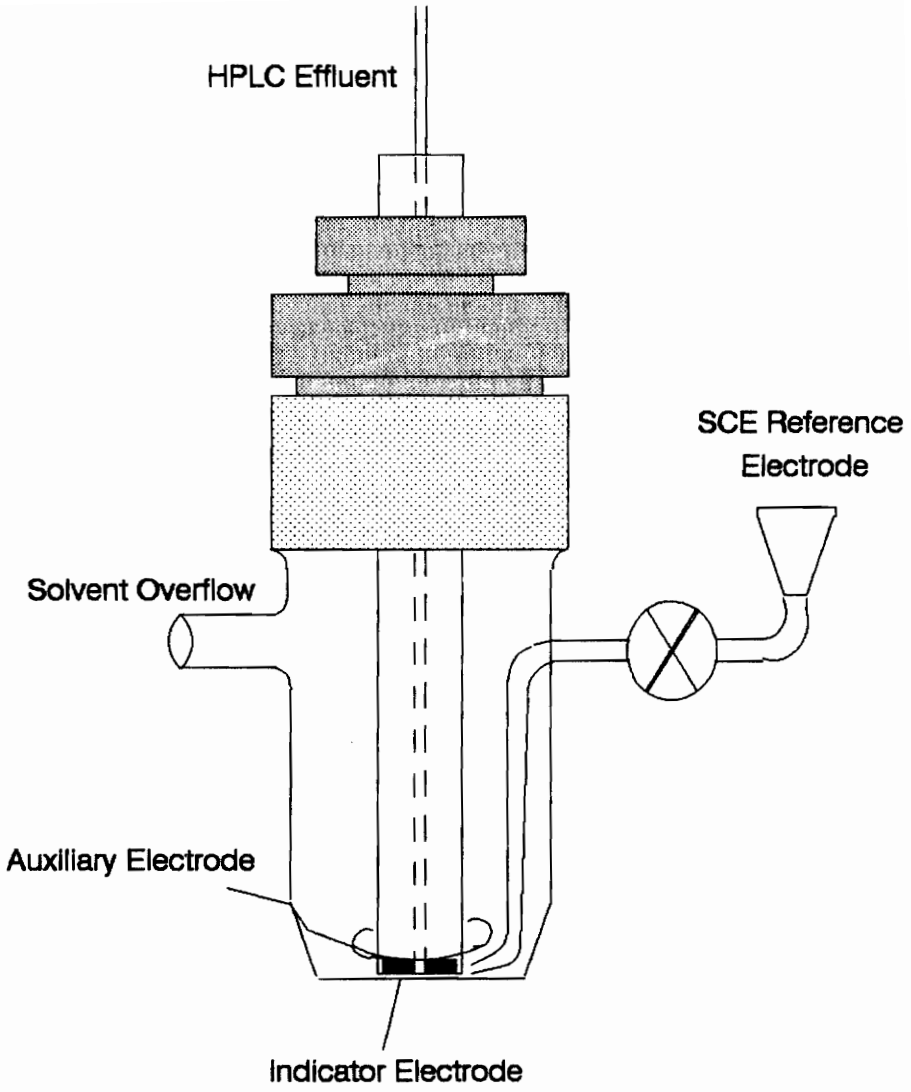

Figure 2.1 A) SWV Electrochemical Cell.

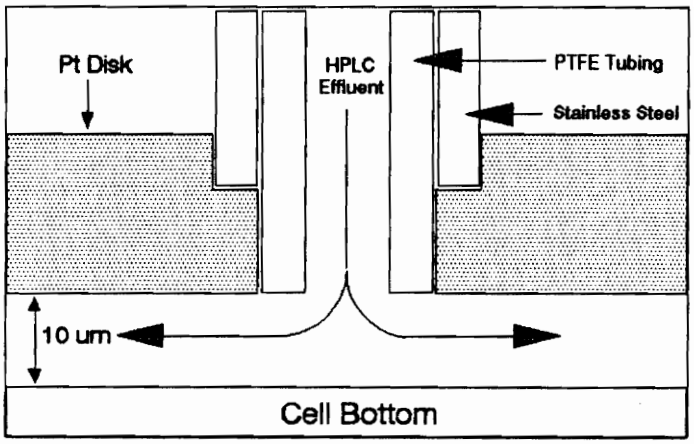

(B) Expanded View Of Detection Zone
Drawing Is Not To Scale.

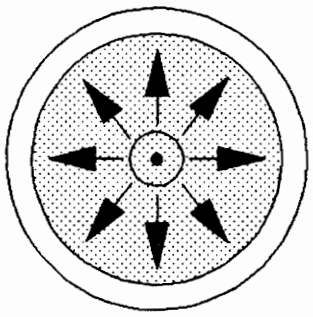

(C) View Of Flow Profile Across
The Indicator Electrode

the end of a stainless steel tube (1/8" o. d. X 1/16" i. d.) which served both as a conduit for the post column HPLC tubing and as the electrical connection for the indicator electrode. The electrode and tubing were embedded into a delrin rod (1.0 X 15 cm) and the post column PTFE LC tubing was inserted through the rod so that it terminated just past the opening in the indicator electrode. The PTFE tubing was the cut flush with the electrode face. The delrin rod was inserted into the cell with the indicator electrode pressed firmly against the cell bottom and was held in place by means of a compression nut and o - ring. In this arrangement, the HPLC effluent encounters a flat wall as it exits the tubing and is dispersed radially across the entire surface of the electrode (figure 2.1 C). The solution layer formed in this arrangement is similar in thickness to those found in other thin layer electrochemical measurements[26-28] and is estimated to be approximately 10 μm.

The reference electrode (SCE) was positioned so that the end of a Lugin capillary terminates adjacent to the working electrode. The counter electrode was comprised of a coiled length of platinum wire surrounding the indicator electrode. The cell was filled with the solvent which was used as the HPLC mobile phase and was kept at constant volume by drainage through a 3/8" i. d. overflow tube.

The electrode potential was controlled and the analytical current data was measured using an EG&G model 273 potentiostat/galvanostat (EG&G Princeton Applied Research, Princeton, N. J.). The potentiostat was controlled, in turn, by an IBM PS/2 model 50z personal computer through an IEEE - 488 interface.

2.1.2 Software.

The software used to control the potentiostat and to process and store the electrochemical data was written and compiled in - house using QuickBASIC version 4.5 (Microsoft, Redmond, Wa.). The software is multifunctional, allowing the user to specify several operating parameters, providing for rapid data acquisition and storage, and providing a real - time display of current/potential data. Figure 2.2 is a flow chart describing the various operations of the SWV controlling software. The actual BASIC source code can be found in the Appendix of this volume.

2.2 Reagents and Materials.

Hydroquinone and resorcinol were obtained from Eastman Chemical Company (Rochester, N. Y.). Phenylhydroquinone, bromohydroquinone, and catechol were obtained from Aldrich Chemical Company (Milwaukee, Wis.). All were used as received. Standard solutions were made for each compound in 0.001 M concentrations, using the mobile phase as solvent for the stock solution, and diluted as noted in the following chapter. Ethanol, USP 200 proof, was purchased from Aaper (Shelbyville, Ky.) and was filtered prior to use. High purity UV grade acetonitrile (Burdick & Jackson, Muskegon, Mi.) was used as received. All water used was purified by a Barnstead Nanopure II water purification system. Potassium bromide, acetic acid, and perchloric acid were purchased from Fisher

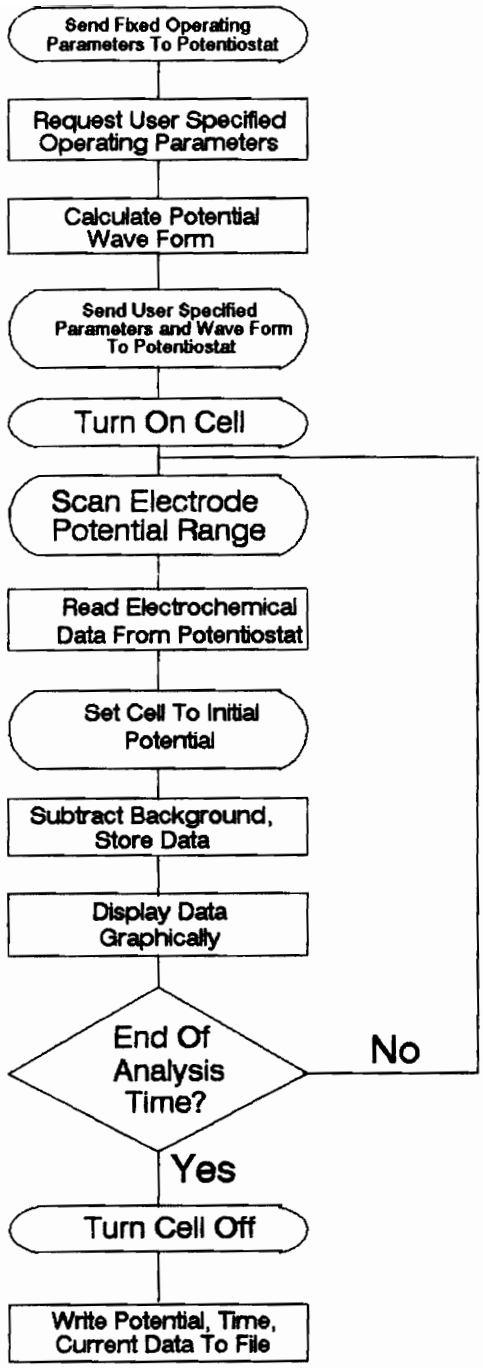

Figure 2.2 A flow chart illustrating the software routines used to control the SWV detector and process the data.

Scientific Company (Fairlawn, N. J.) and were used as received.

The extract of fennel seeds used in this study was prepared by extracting 1.728 g of fennel seeds with 25.0 mL of 20% acetonitrile, 80% water at room temperature for 10 minutes. The sample was filtered and the resulting filtrate was injected without additional treatment. Mainstream cigarette smoke was collected with a Phipps and Bird model 990 - 300 single port smoking machine (Phipps and Bird, Richmond, Va.), using the FTC procedure[29]. Five cigarettes were smoked per cambridge pad. The pad was then extracted with 20 mL of 1% acetic acid at room temperature for 10 minutes. The extract was then filtered and used without further treatment. It was found that cigarette extract samples degraded rapidly with time, so chromatographic analyses were performed within two hours of extraction. The cigarette brand used was "Cambridge".

2.3 SWV Electrochemical Procedures.

2.3.1 Electrode Preparation.

The platinum disk indicator electrode was initially received with a rough, nonplanar outer surface. The electrode was manually ground with 600 grit emery paper to obtain a planar electrode face which was normal to the length of the electrode shaft. The electrode was then polished successively with 1.0, 0.3, and 0.05 μm alumina suspensions in order to obtain a mirror finish. After the initial polishing procedure was completed, the electrode required only a light daily

polishing with 0.05 μm alumina suspension in order to ensure that the electrode had a smooth, mirror-like finish for each experiment.

2.3.2 Minimum Detectable Quantity.

The minimum detectable quantity (MDQ) was obtained from flow injection analysis data obtained in both the nonscanning and scanning modes of operation, using hydroquinone as the test analyte. The procedure used in the nonscanning mode was as follows: The solvent used was 10% ethanol, 90% water, containing 1.0 mM KBr and adjusted to pH 3 using perchloric acid. The solvent was allowed to pump through the SWV cell at a flow rate of 0.3 mL/minute for 24 hours prior to use. A stock solution containing 1000 ppm hydroquinone was prepared using the FIA solvent. The stock solution was used to prepare solutions containing various concentrations of hydroquinone, ranging from 500 ppm to 2 ppb. The cell potential was set to +0.6 V versus SCE approximately 15 minutes prior to the injection of any samples. Then beginning with the most dilute sample, the response was measured for the various samples. The number of injections per sample varied from fourteen injections for 5 ppb hydroquinone to five injections for concentrations higher than 10 ppm. The analytical current was measured at approximately one second intervals. The minimum detectable quantity was determined using MDQ = 3N, where N was the background noise observed for the data set corresponding to 5 ppb hydroquinone.

The procedure for the determination of the MDQ in the scanning mode of operation was essentially the same, with the exception that the cell was not permitted to equilibrate prior to being used. The electrode was scanned from 0 to 900 mV versus SCE with a scanning increment of 20 mV and a pulse height of 200 mV. The scanning frequency was 35 Hz. The minimum detectable quantity was obtained by determining the magnitude of the baseline fluctuations at 580 mV, which corresponded to the current maxima for hydroquinone under the experimental conditions.

2.3.3 Linear Dynamic Range.

The data obtained in the nonscanning mode, as described in section 2.3.2, was intended for the dual purpose of determining the minimum detectable quantity and the linear dynamic range of the SWV electrochemical detector. The data was plotted as the log of analytical current versus log of concentration. Deviations from linearity of greater than 5% were considered to be outside the linear range of the detector. Linear regression of the data obtained over the concentration range from the MDQ to 50 ppm hydroquinone was performed using Lotus 123 version 2.0. Current data was also obtained in the nonscanning mode for various concentrations of potassium ferrocyanide, from 100 ppb to 1000 ppm, using an aqueous solvent containing 1.0 mM KBr and 1.0 mM perchloric acid.

2.3.4 Isocratic HPLC.

The solvent used for the isocratic HPLC separation of test mixtures consisted of 5% ethanol, 95% water and contained 5.0 mM KBr. The pH was adjusted to 3 using perchloric acid. The solvent flow rate was set at 0.8 ml/minute and was allowed to pump through the SWV cell for approximately one hour each day prior to the injection of samples. The scanning method used for most isocratic separations involved an initial potential of 0.0 V and a final potential of 1.2 V versus SCE. The scan increment was 10 mV and the pulse height was 25 mV. The scanning frequency was 15 Hz. Using this potential program, the entire potential range could be scanned every 4.5 seconds.

2.3.5 Gradient Elution HPLC.

Gradient elution HPLC was performed using aqueous and acetonitrile solutions, each containing 1.0 mM KBr and 1.0 mM perchloric acid in order to maintain the solution pH and conductivity as constant as possible during solvent gradients. The solvent flow rate was set to 0.8 ml/minute and was pumped through the SWV cell for approximately one hour each day before the injection of any samples. Using a simple test mixture, numerous combinations of initial potential, final potential, potential increment, pulse height, and scan frequency were tested for use with gradient elution HPLC. The scanning method which appeared to result in the best overall chromatovoltammogram involved an initial potential of

0.0 V and a final potential of 1.2 V. The scan increment was 20 mV and the scan frequency was 35 Hz. Using this potential program, the entire potential range could be scanned every 3 seconds.

Chapter 3. SWV Detector Results.

3.1 Characterization of the SWV Electrochemical Detector.

The square wave voltammetric electrochemical detector developed for this work was designed to incorporate several desirable characteristics of commercially available electrochemical detectors with those attributed mainly to microelectrode based SWV detectors. Among these characteristics were high sensitivity to electroactive analytes, a large linear dynamic range, minimal cell resistance and minimal analyte band spreading in the detection zone. Furthermore, the detector was designed to avoid the difficulties associated with the preparation, use, and handling of microelectrodes; problems which make microelectrodes impractical for routine usage in most laboratory settings. Finally, the detector was intended to be compatible with the high solvent flow rates characteristic of conventional HPLC systems.

The platinum disk indicator electrode used in the SWV electrochemical cell is similar in dimensions to those used in commercially available electrochemical detectors. The analytical currents measured with such electrodes are generally in the microampere range, making current amplification unnecessary. Also, the platinum disk electrode allows for easy cleaning, either electrochemically or by physical polishing. Microelectrodes are usually replaced when they become fouled. The degree to which the SWV electrochemical detector meets the other design criteria is the subject of the following sections of this chapter.

3.1.1 Minimum Detectable Quantity.

The signal to noise ratio measured by the SWV electrochemical detector is affected by several variables. Among these are the diffusion rate of the analyte molecules in solution, the residence time of the analyte in the detection zone, and the magnitude of the background current. Small molecules with relatively large diffusion coefficients and low solvent flow rates generally have the effect of increasing the measured analytical current. The largest single contributor to the magnitude of the background current is the mode of detector operation. In the scanning mode the potential is changed in relatively large steps at a high frequency, resulting in the generation of a large charging current. Although the data acquisition method for the square wave voltammetric method results in a background correction, the large background change during a scan forces the potentiostat to be operated at a less sensitive current setting than would be required in a nonscanning mode. Also, in the scanning mode, the analytical current is affected by the scan frequency. An increase in scan frequency results in a larger measured current, generating greater analyte sensitivity. A limitation to this increase is observed however, because of the finite amount of time required for the working electrode to reach a desired potential setting because of resistance and capacitance effects in the electrochemical cell. At very high scan rates, the RC time constant of the cell may not permit the indicator electrode to reach a desired potential before a new potential is requested by the potentiostat.

The minimum detectable quantity (MDQ) was determined for both the scanning and nonscanning modes of operation using the standard definition, MDQ = 3N, where N is the background noise. The MDQ was determined using hydroquinone as the test analyte. Hydroquinone is a small molecule, capable of rapid diffusion in solution (diff. coef. = 1.57 E-5 cm^2/sec.). It was also used by Jorgenson et al., for the determination of the MDQ of a carbon fiber based SWV detector for use with open tubular liquid chromatography. The use of the same test analyte allows for a more meaningful comparison of the two detectors than would be possible otherwise. The flow rate used for the MDQ determination was 0.3 mL/minute. Figure 3.1 shows several replicate injections of 50 picograms of hydroquinone. The data was obtained using the cell in the nonscanning mode, with an electrode potential of +0.6 V versus SCE. From the figure, the background noise was determined to be 0.92 nA and the mean peak height was found to be 10.4 nA (RSD = 51%). The MDQ (3N) was found to be 13 picograms or 120 femtomoles. Similar calculations were done using data obtained for multiple injections of 100 pg and 250 pg amounts of hydroquinone. For the data obtained for 100 pg hydroquinone, the mean noise value was determined to be 0.80 nA and the mean peak height was found to be 14.3 nA (RSD = 30%), resulting in an MDQ of 17 pg. Likewise, for the 250 pg injections, the mean noise value was found to be 0.75 nA and the mean peak height was determined to be 26.0 nA (RSD = 9.5%), resulting in an MDQ of 22 pg. The data sets used for these

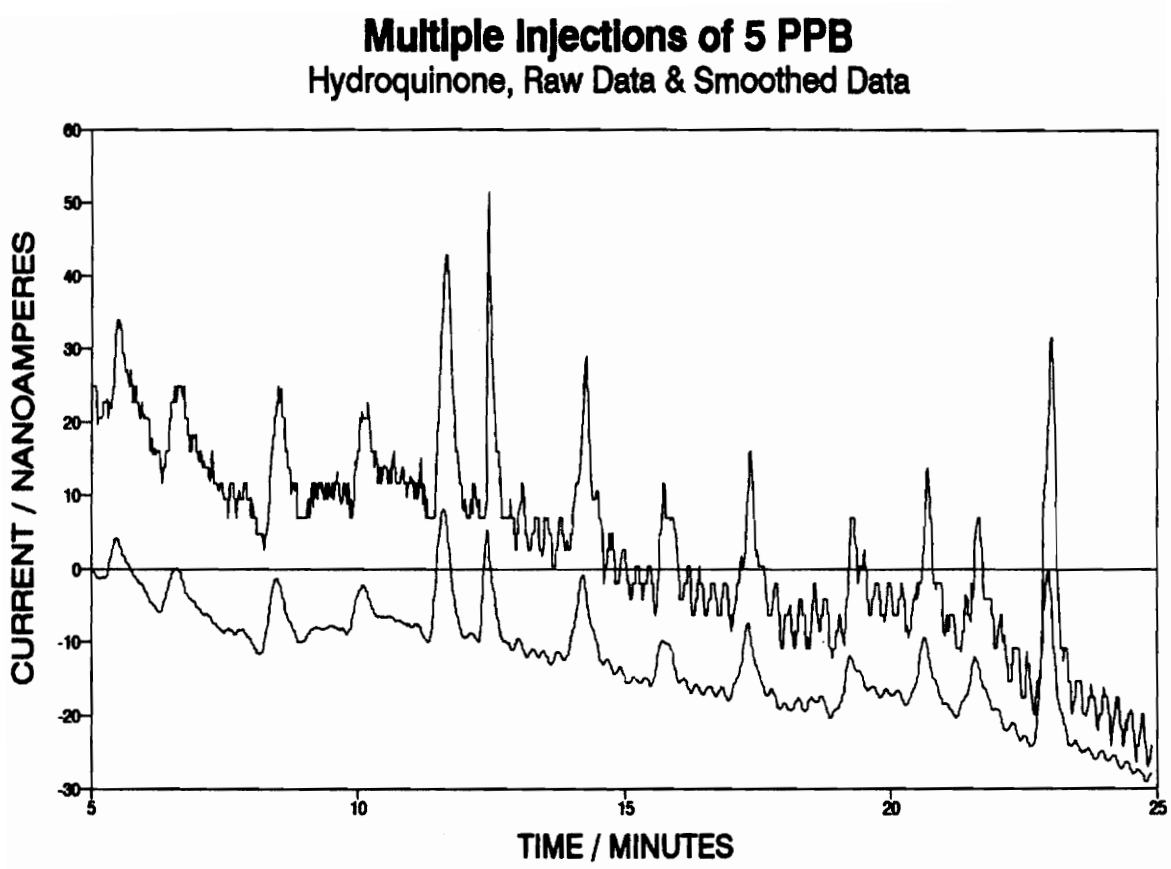

Figure 3.1 FIA data for the amperometric detection of 50 pg hydroquinone. The data was collected at +0.6 V. The data is shown in its original form (Top) and after smoothing by box car averaging (Bottom).The solvent was 10% ethanol in water and contained 0.001 M KBr and 0.001 M $HClO_4$. The solvent flow rate was 0.3 mL/minute. Using the smoothed data set, the mean peak height is 10.4 nA (RSD = 51%) and the mean noise value is 0.92 nA. The MDQ (3 X N) was calculated to be 13 pg.

calculations, including both the raw and smoothed data sets, are shown in Appendix D.

The MDQ was determined in the scanning mode using a pulse height of 200 mV and a frequency of 35 Hz. Figure 3.2 shows both the original data and the same data set after smothing for a two dimensional slice of a data set obtained in the scanning mode for four replicate injections of 1.0 ng of hydroquinone. The 2-D slice corresponds to an electrode potential of 580 mV. The mean peak height for the smoothed data set is 818 nA (RSD = 18.3%) and the mean noise value was determined to be 190 nA, resulting in a S/N ratio of 4.2. The MDQ was determined to be approximately 710 pg. Similar results were obtained using a data set corresponding to the injection of 2.5 ng quantities of hydroquinone. The mean peak height for this data set (shown in Appendix D) is 4550 nA (RSD = 14.6%) and the mean noise value was 570 nA. Using this data set, the MDQ was determined to be approximately 940 pg. These MDQ values are comparable to the MDQ reported by Kounaves for the SWV detection of epinephrine on a carbon fiber electrode[14]. The sample concentration used for the MDQ determination in the scanning mode was 100 ppb hydroquinone. This is nearly two orders of magnitude lower than the minimum detectable concentration, (5N), reported by Jorgenson et al.for the detection of hydroquinone[10].

The low minimum detectable quantity can be attributed largely to the cell geometry, in which there is no preferential flow path for the HPLC effluent across

the electrode face. This allows the entire electrode surface to be utilized for the detection of analytes. This is in contrast to conventional thin layer electrochemical cells that utilize macroscopic indicator electrodes. In these designs, the liquid inlet and outlet are on opposite side of the indicator electrode and are generally small openings. In such configurations, it is likely that the flow velocity across the electrode is nonuniform, with most of the liquid flowing near the center of the electrode. Since the analytical current is proportional to the surface area of the electrode that is exposed to the analyte solution, it is expected that a more efficient use of the electrode surface would result in superior signal to noise. The MDQ for the present system is approximately two orders of magnitude lower than has been reported for previous macroscopic electrode SWV detectors[9, 30-32].

3.1.2 Linear Dynamic Range.

On a plot of detector response versus concentration, the linear dynamic range is the ratio of the highest concentration for which the detector is linear to the MDQ. Figure 3.1.2.1 is a log - log plot of current versus concentration, using data obtained in the nonscanning mode of operation for the detection of hydroquinone. From the plot, the linear dynamic range was determined to be $10^{4.6}$ or 4.6 orders of magnitude. This value is comparable to those obtained from commercial amperometric detectors, which typically have a linear dynamic range of five orders of magnitude[1].

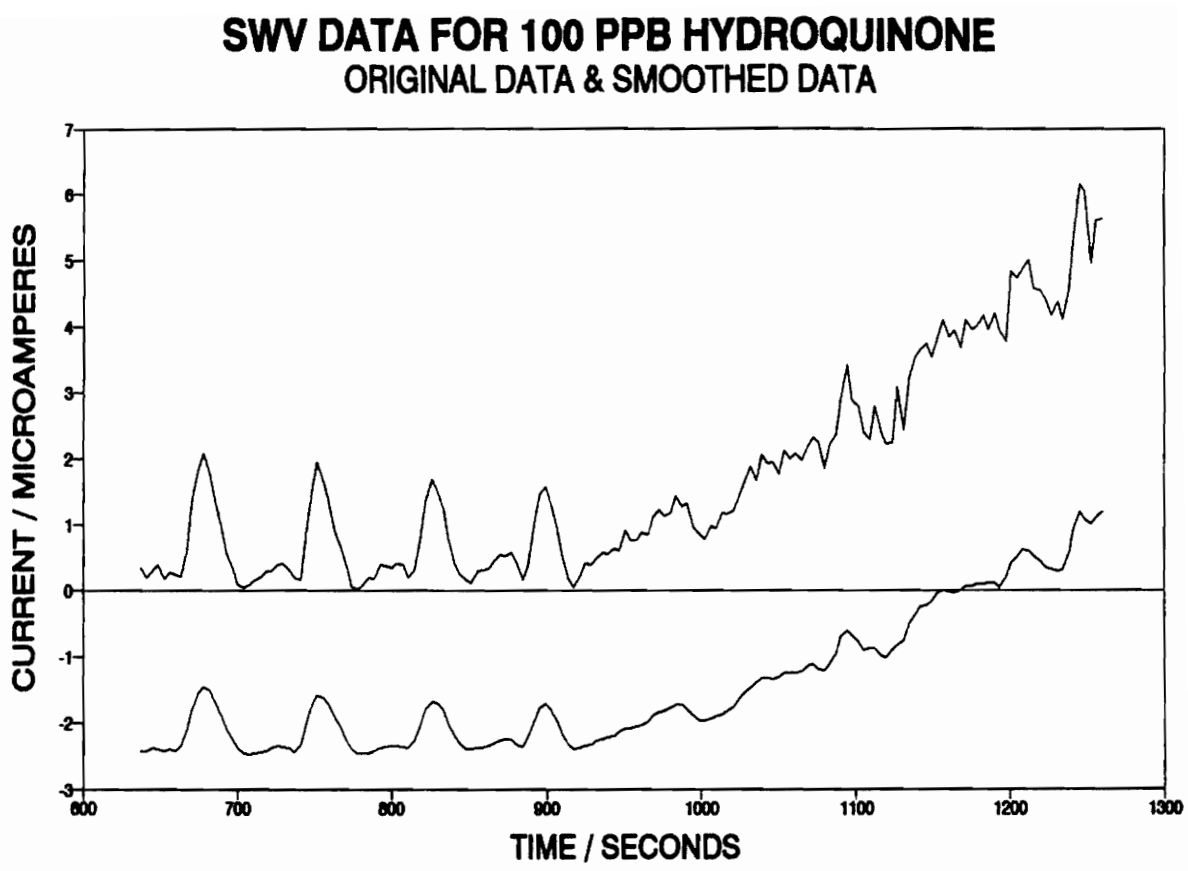

Figure 3.2 A two dimensional slice of SWV/FIA data for 100 ppb hydroquinone. The indicator electrode was scanned between 0 and 900 mV with a step height of 20 mV and a pulse height of 200 mV. The scan rate was 35 Hz. The top curve shows the data in its original form while the bottom curve shows the same data set after smoothing by box car averaging. Solvent conditions were the same as for Figure 3.1.

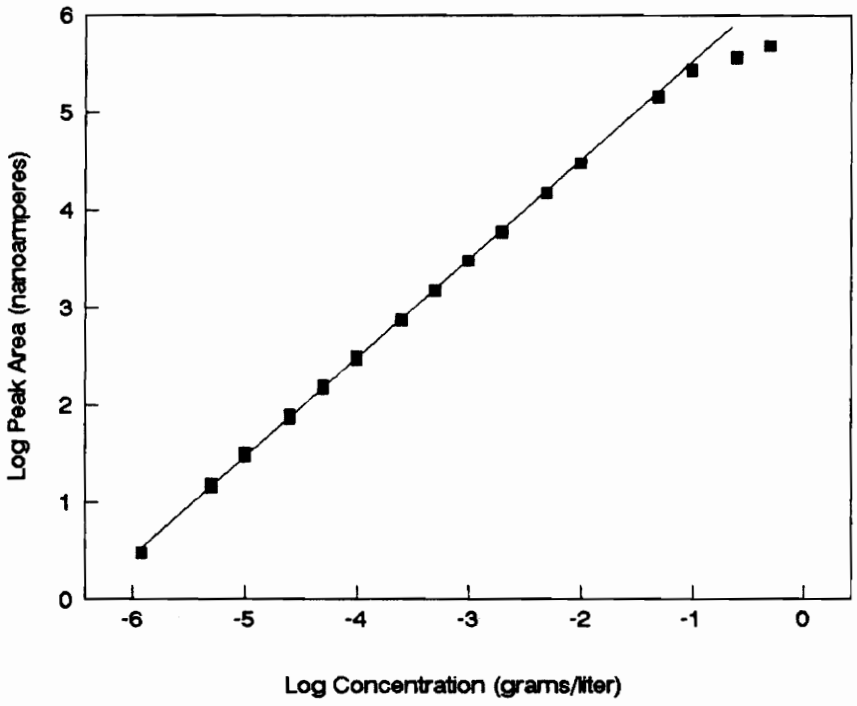

Figure 3.3 Log-log plot of the electrochemical detector response for various concentrations of hydroquinone. Variation in response is indicated by the height of the data points.
Electrode Potential: +0.6 V versus SCE.
Linear Dynamic Range: $10^{4.6}$
Number of Observations: 82
Degrees of Freedom: 80
Slope: 0.9996
Std. Error of Slope: 0.0014
Correlation Coefficient: 0.9998

For hydroquinone, the detector becomes nonlinear at concentrations above 50 ppm. This behavior might be explained if the electrochemical processes occurring at the electrode surface were sufficiently slow so that some of the sample was purgedfrom the detection zone prior to detection. The possibility of electrode fouling during the oxidation of hydroquinone was also considered.

The reproducibility of response at concentrations of 50 ppm and greater (see Appendix D) is evidence that electrode fouling is an unlikely cause for the nonlinearity at high concentrations. If significant fouling were to occur, the response would be expected to decrease for each succeeding injection of a particular sample. However, the possibility of electrode fouling could be completely eliminated by studying the behavior of the SWV detector using a reactant that is unlikely to adsorb. For this reason, the response of the SWV detector was obtained for various concentrations of potassium ferrocyanide. Figure 3.4 is a log-log plot of this data. It can be seen that the data for potassium ferrocyanide is similar to the data obtained for hydroquinone, with the response becoming nonlinear at concentrations higher than 80 ppm. Based on these results, electrode fouling does not appear to be an interference in the determination of the linear dynamic range of the SWV detector, using hydroquinone as the test analyte.

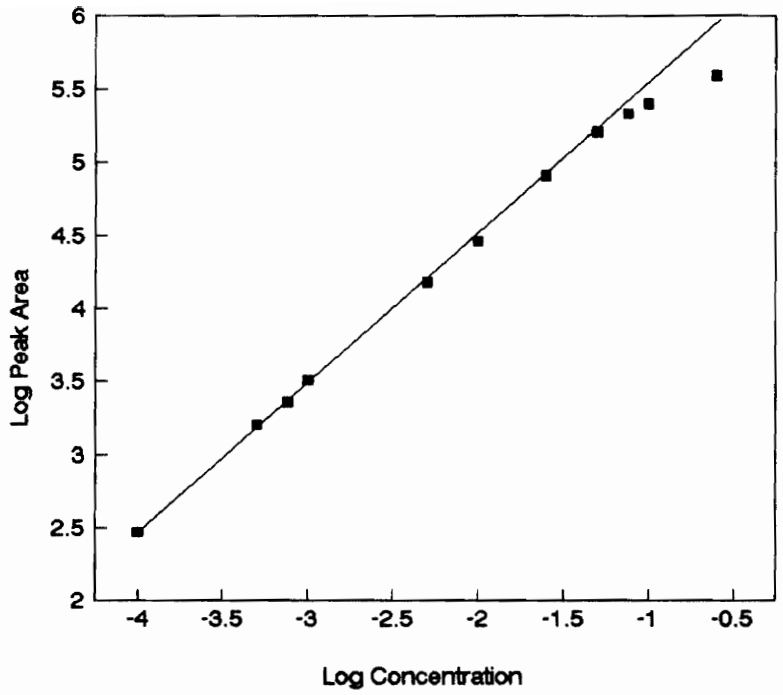

Figure 3.4 A Log-Log plot of the electrochemical detector response for various concentrations of potassium ferrocyanide. The data was obtained by pulsing the indicator electrode between +0.5 and +0.6 V versus SCE and taking the difference between the current measured at these two potentials.

3.1.3 Electrode Potential Control.

The purpose of this portion of the study was to determine whether the thin solution layer between the working electrode and the cell bottom introduces sufficient electrical resistance to interfere with the control of the working electrode potential. Increased resistance will increase the time response of the indicator electrode,resulting in poor potential control in thin layer cells; a problem associated with commercial LCEC detector cells[1]. In these cells, the auxiliary and reference electrodes are generally placed at some distance downstream from the indicator electrode, so that a significant portion of the iR drop exists along the surface of the indicator electrode. The result is a nonuniform potential across the electrode face, and poor potential control.

In square wave voltammetry, inadequate control of the electrode potential would be indicated by an apparent shift in the oxidation potential of a test compound in the thin layer relative to that which is observed under normal static solution square wave voltammetry. Figure 3.5 shows two individual square wave voltammograms obtained from a solution containing 0.001 M hydroquinone. Voltammogram A was obtained under nonflowing conditions with the working electrode pushed firmly against the cell bottom, as it would be if the cell were being used as a detector for liquid chromatography. Voltammogram B was obtained, using the same solution, with the working electrode pulled back approximately 1 cm from the cell bottom.

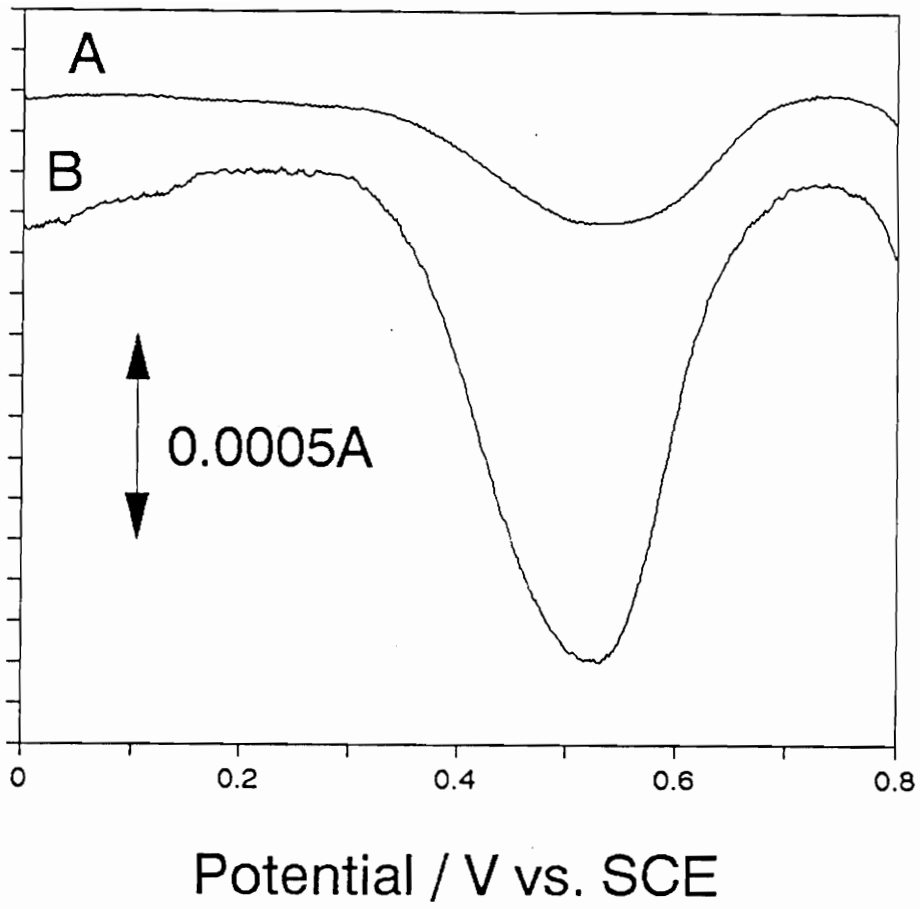

Figure 3.5 Voltammograms for hydroquinone obtained under nonflowing conditions. A) was obtained with the indicator electrode pressed firmly against the cell bottom. B) was obtained with the electrode pulled back 1 cm from the cell bottom.

Although the magnitude of the analytical current is greater for voltammogram B, it can be seen that the oxidation potential for hydroquinone is virtually the samein both cases. This is a clear indication that the thin solution layer between the working electrode and the cell bottom does not contribute enough to the total cell resistance to interfere with the control of the working electrode potential. The difference between the total analytical current observed for the two voltammograms may be accounted for by the depletion of analyte from the thin layer detection zone. Diffusion of analyte from the bulk solution to the detection zone is slow relative to the time required to complete a single voltammogram.

3.1.4 Chromatographic Efficiency Of The SWV Electrochemical Cell

One of the design criteria for the SWV cell was the need to limit analyte band spreading in the detection zone. In order to meet this specification, the cell was designed so that the solvent stream flows down the center of the indicator electrode shaft. When the effluent exits the tubing, it encounters a flat wall and is dispersed radially across the surface of the electrode (Figure 2.1). The solution layer formed in this arrangement is similar in dimensions to those frequently found in other thin layer electrochemical measurements[26-28]. In this configuration there is no preferential path for the liquid stream, so a uniform flow profile is established across the face of the electrode. The flow pattern was confirmed empirically by

injection of a red dye solution. It was observed visually that the dye rapidly covered the entire electrode surface upon entering the thin solution layer between the electrode and the cell bottom.

An indication of the degree of analyte band spreading in the detection zone is indicated by the degree to which data obtained by flow injection analysis approximates a Gaussian distribution. A close approximation of a Gaussian distribution implies that the cell performs as intended. Figure 3.6 is a comparison of a peak corresponding to the flow injection analysis of 10 μL of 50 ppb hydroquinone with a Gaussian curve. The experimental data closely approximates the Gaussian distribution, indicating that relatively little mixing occurs in the thin layer.

In a quantitative analysis of the analyte band spreading, a perpendicular line is drawn at the peak maximum and the peak width is measured on both sides of the line. The peak tailing factor is expressed as: Tailing Factor = (A/B) X 100%. The tailing factor was measured for the peak in figure 3.6 and was found to be 11.5%. The contributions of the sample injector and the 60 cm of post injector tubing were evaluated separately and were found to be 4.6% and 6.8%, respectively. The sum of these contributions is 11.4%, indicating that virtually all of the peak tailing can be attributed to these two contributions.

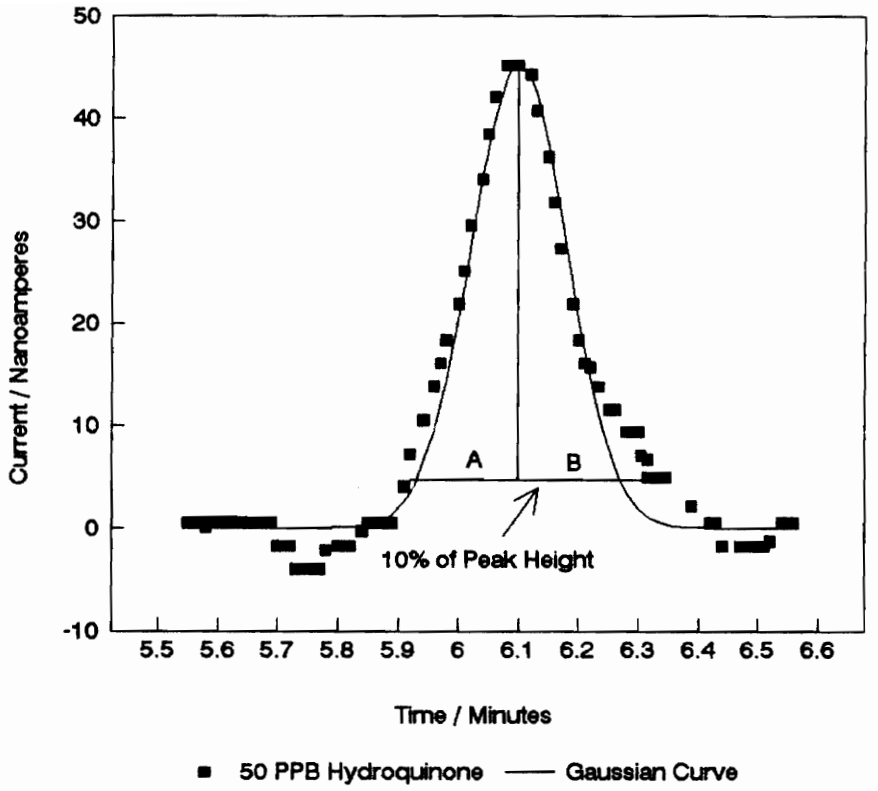

Figure 3.6 A comparison of a peak obtained from the FIA detection of 50 ppb hydroquinone with a Gaussian curve. The tailing factor (A/B X 100%) was measured at 10% peak height as was found to be 11.5%.

3.2 SWV Electrochemical Detection For Isocratic HPLC.

The application of the SWV electrochemical cell as a detector for HPLC results in three dimensional chromatovoltammograms that are qualitatively superior to chromatograms obtained using other electrochemical techniques. In the potential domain, the peak maxima correspond to the oxidation potentials of the various electroactive compounds eluted from the column. The square wave voltammetric technique also allows the electrochemical resolution of coeluting solutes, provided that they have different oxidation potentials. The combination of elution time, t_r, and oxidation potential, $E_{1/2}$, is specific for each electroactive component of the mixture and can greatly facilitate the proper identification of chromatographic peaks.

The three dimensional chromatovoltammogram shown in Figure 3.7 is for the isocratic separation of hydroquinone, resorcinol, catechol, and bromohydroquinone. The mixture was made so that the concentration of each component was approximately 15 ppm. The injection volume was 20 μL and the solvent flow rate was 0.8 mL/minute. The data was plotted with electrode potential on the X axis, time on the Y axis, and net analytical current on the Z axis. The individual components appear as single well defined peaks, with the exception of resorcinol, which exhibits two step oxidation as well as broad peak tailing.

The data obtained by SWV electrochemical detection can be presented in a variety of ways other than as a three dimensional plot, depending on the interests

of the researcher. Figure 3.8 is a contour plot of the same chromatovoltammogram shown in Figure 3.7. For simple chromatographic separations, it can be seen that the contour plot lends itself most easily to qualitative interpretation. Quantitation of the individual components was accomplished by integrating the total peak volume.

3.3 SWV Electrochemical Detection With Gradient Elution HPLC.

The application of amperometric electrochemical detection to gradient elution HPLC has been demonstrated by a few researchers[17-22]. However, The quality of the chromatograms generated is generally poor with drifting baseline, reduced signal to noise ratio, and loss of chromatographic peak resolution. Furthermore, severe restrictions are usually imposed on the separation method to accomodate the electro-chemical detector, rendering the technique impractical for many separations. The application of SWV electrochemical detection to gradient elution open tubular liquid chromatography was first described by Oates and Jorgenson[23,24]. This technique was shown to result in essentially no baseline drift over a wide range of solvent compositions. The signal to noise ratio and peak resolution were also unaffected by SWV electrochemical detection. In the present work, SWV electrochemical detection was adapted to conventional scale gradient elution HPLC.

One of the operational differences between SWV electrochemical detectors

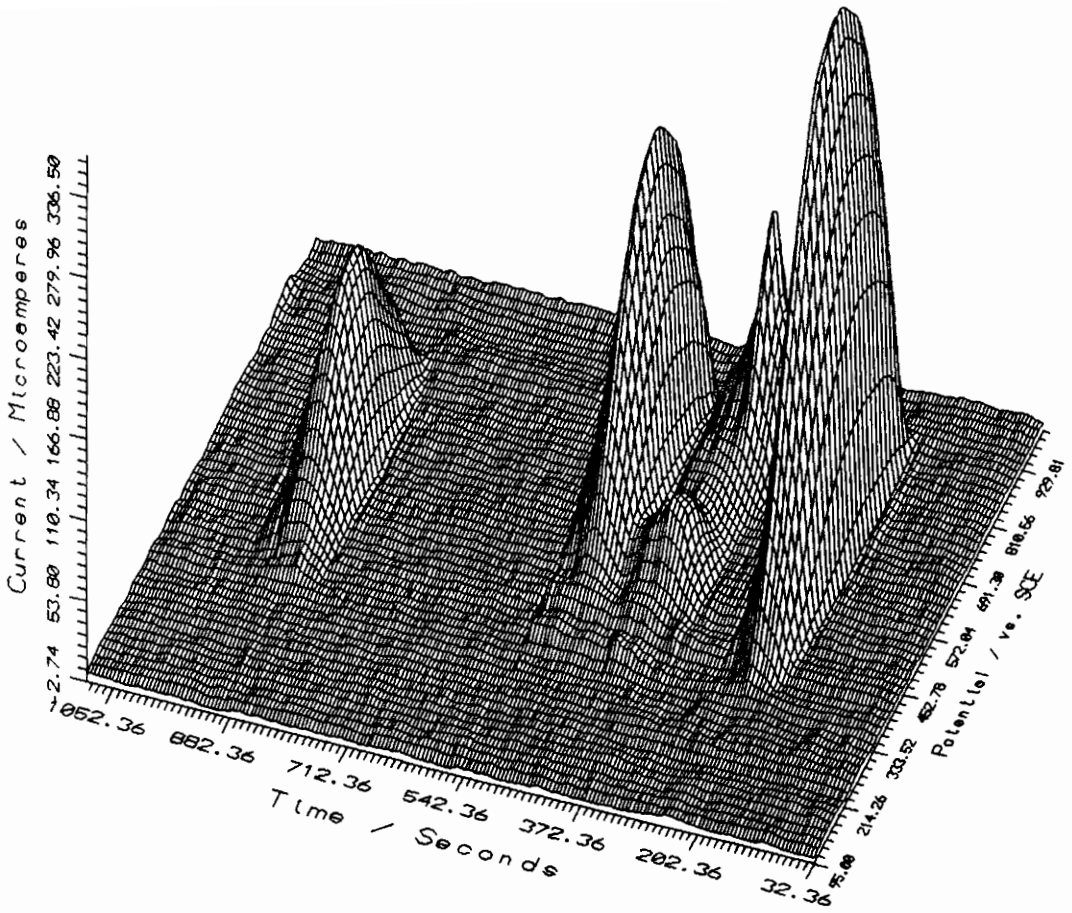

Figure 3.7 A Three dimensional chromatovoltammogram of a simple test mixture obtained under isocratic conditions. In order of increasing elution time, the components are: hydroquinone, resorcinol, catechol, and bromohydroquinone.

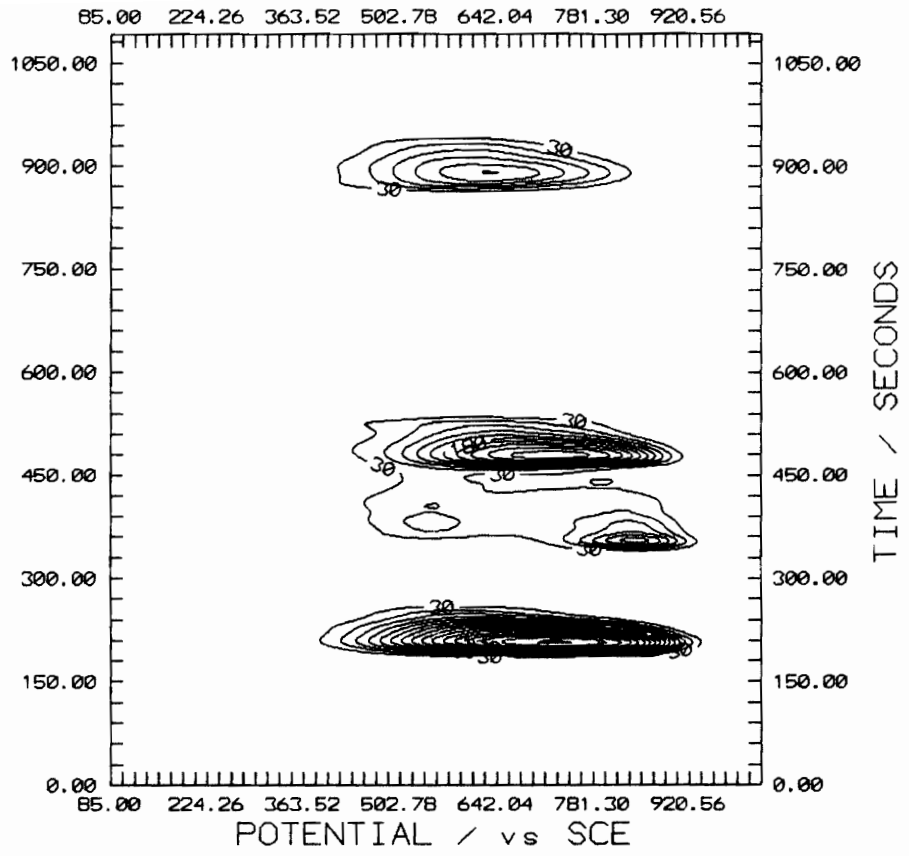

Figure 3.8 A two dimensional contour map of the chromatovoltammogram shown in Figure 3.7.

based on single carbon fibers and the macroscopic indicator electrode detector presented in this work is the potential scan rate of the electrode. For carbon fiber electrodes, scan rates are typically 100 Hz or greater. For macroscopic electrodes, due to solution resistance, the time required to reach a desired potential is much longer than for carbon fibers and the scan rate is consequently much slower. Since gradient elution HPLC results in substantially narrower chromatographic peaks than those obtained by isocratic elution, it is necessary to scan the entire potential range of the electrode in a shorter period of time in order to obtain optimum peak resolution. In the present case, any improvement in resolution in the time domain comes at the expense of resolution in the electrochemical domain. Therefore, adaptation of the macroscopic electrode SWV detector to gradient elution HPLC involves the adjustment of the scan rate and the scan interval in order to optimize resolution in both domains. Although some loss of electrochemical resolution occurs, the loss is more than offset by increased time resolution and shorter analysis time.

3.3.1 Separation Of A Test Mixture By Gradient Elution HPLC.

The scanning method required for SWV detection using gradient elution HPLC was developed using a test mixture containing 75 ppm each of hydroquinone, resorcinol, catechol, bromohydroquinone, and phenylhydroquinone. The first four components of the mixture are separable in a few minutes using a

weakly organic mobile phase. On the other hand, phenylhydroquinone can only be eluted from the column by a strong organic mobile phase. With these requirements, an efficient separation of all components of the mixture was not possible using any isocratic method. The best separation was obtained using a nonlinear mobile phase gradient that changed from 30% to 80% acetonitrile over 15 minutes. In this case, the mobile phase composition changed slowly over the first three to four minutes of the gradient and then more rapidly during the remaining time.

Various combinations of the scan rate and scan interval were tested in order to obtain the optimum resolution in time and potential. Figure 3.9 show the best overall chromatovoltammogram obtained for the test mixture, using a scan rate of 35 Hz and a scan interval of 20 mV. The pulse height was 25 mV. The chromatovoltammogram shows that nearly baseline resolution was obtained for all of the sample components. Although the baseline exhibits more noise than was seen in the previous isocratic separation, it should be noted that no discernable drift is evident in the baseline, even though the mobile phase composition was changed in an irregular fashion with respect to time. Figure 3.10 is a contour plot of the same chromatovoltammogram. Although the oxidation potentials of the five components of the mixture are similar, they are still distinguishable from one another. Comparing this contour plot to figure 3.8, it can be seen that the electrochemical resolution has not been severely degraded by the adjustments that

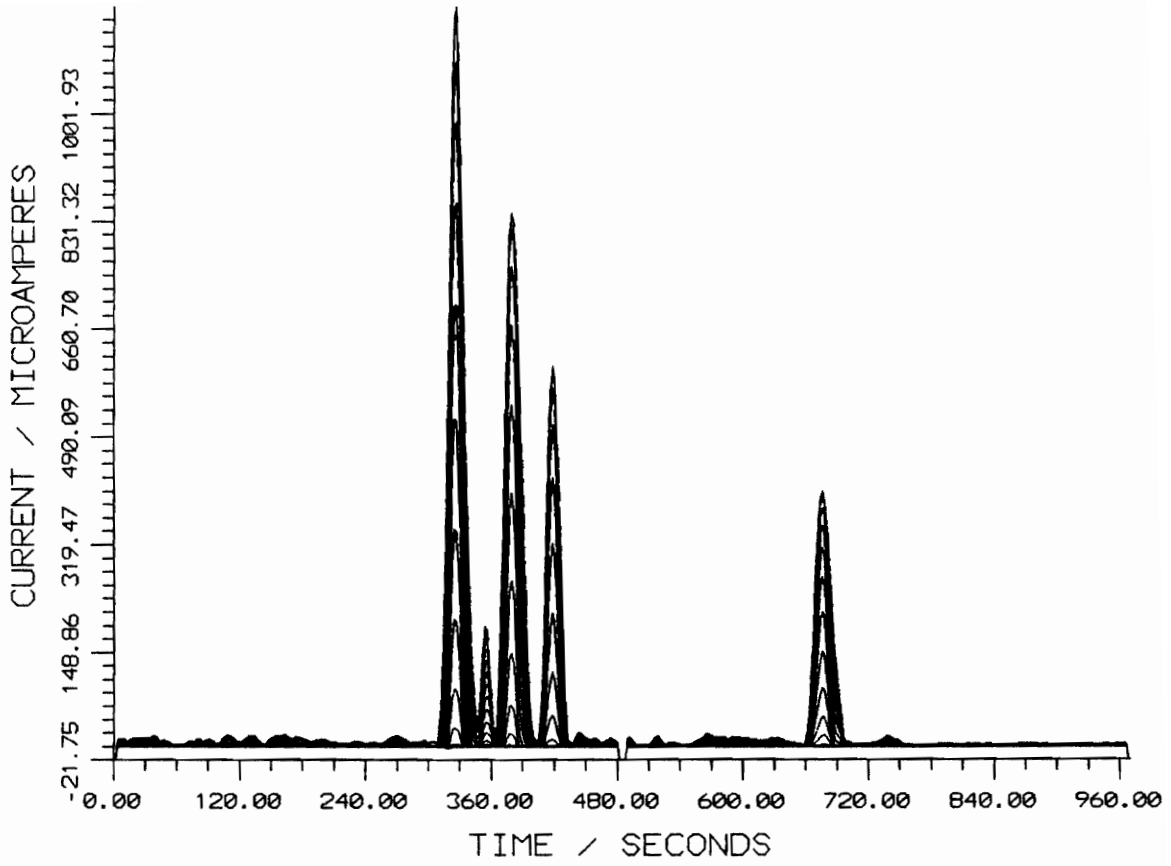

Figure 3.9 A chromatovoltammogram of a simple test mixture separated by gradient elution HPLC. In order of increasing elution time, the components are: hydroquinone, resorcinol, catechol, bromohydroquinone, and phenylhydroquinone.

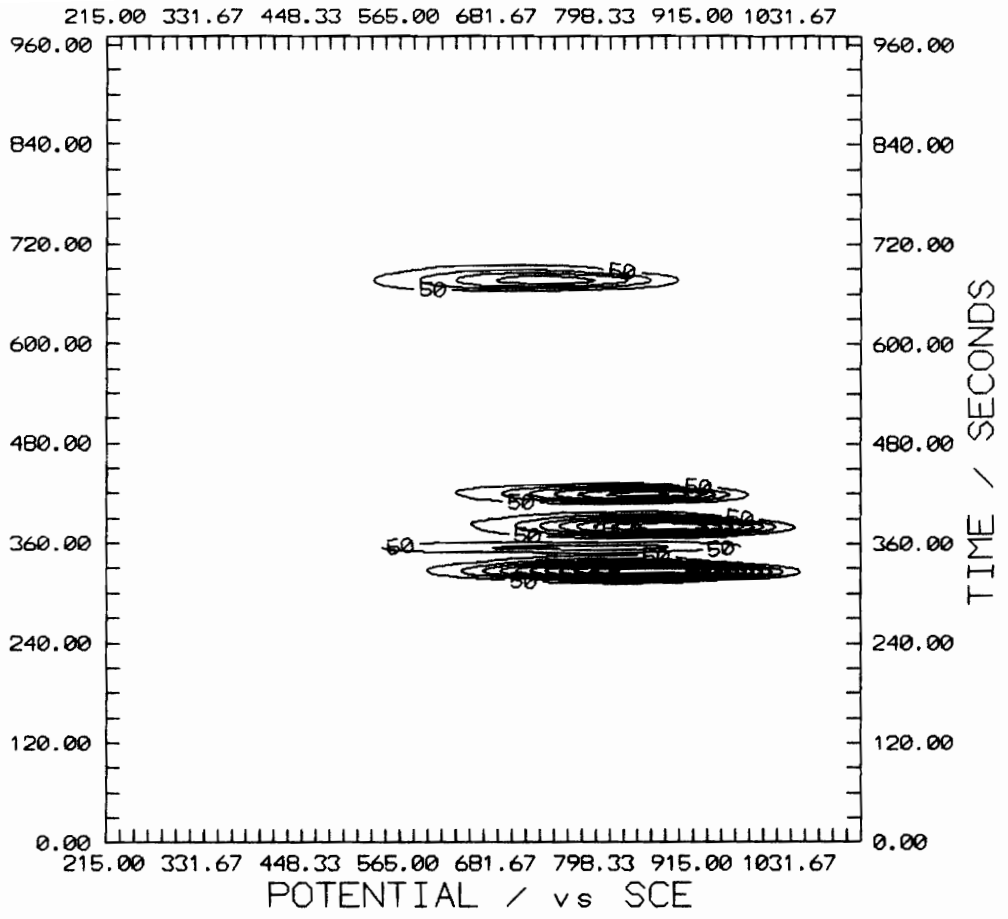

Figure 3.10 A two dimensional contour map of the chromatovoltammogram shown in Figure 3.9.

were made in the scanning method.

3.3.2 Separation Of Naturally Occurring Mixtures By Gradient Elution HPLC.

The application of SWV electrochemical detection to separations of complex, naturally occurring mixtures was quite straight-forward after the optimum scanning method was developed for use with gradient elution HPLC. The separations were performed in order to demonstrate the utility of the SWV electrochemical detector developed in this work, rather than for the identification of individual components of the mixtures.

Figure 3.11 is a chromatovoltammogram for the separation of an extract of fennel seeds. The separation was carried out using a linear mobile phase gradient with the composition changing from 20% to 80% acetonitrile over 15 minutes. In this separation, several components of the sample are apparently unresolved in the time domain but are resolved in the electrochemical domain. Furthermore, despite the large change in mobile phase composition over a short gradient time, there is no drift in baseline current.

The separation of an extract of mainstream cigarette smoke was carried out using a linear mobile phase gradient, with the composition changing from 10% to 90% acetonitrile over 30 minutes. The complexity of the sample was such that a three dimensional representation of the chromatovoltammogram is visually unresolvable. Under these circumstances, the data can only be represented as a contour plot such as Figure 3.12 or as a series of two dimensional chromatograms,

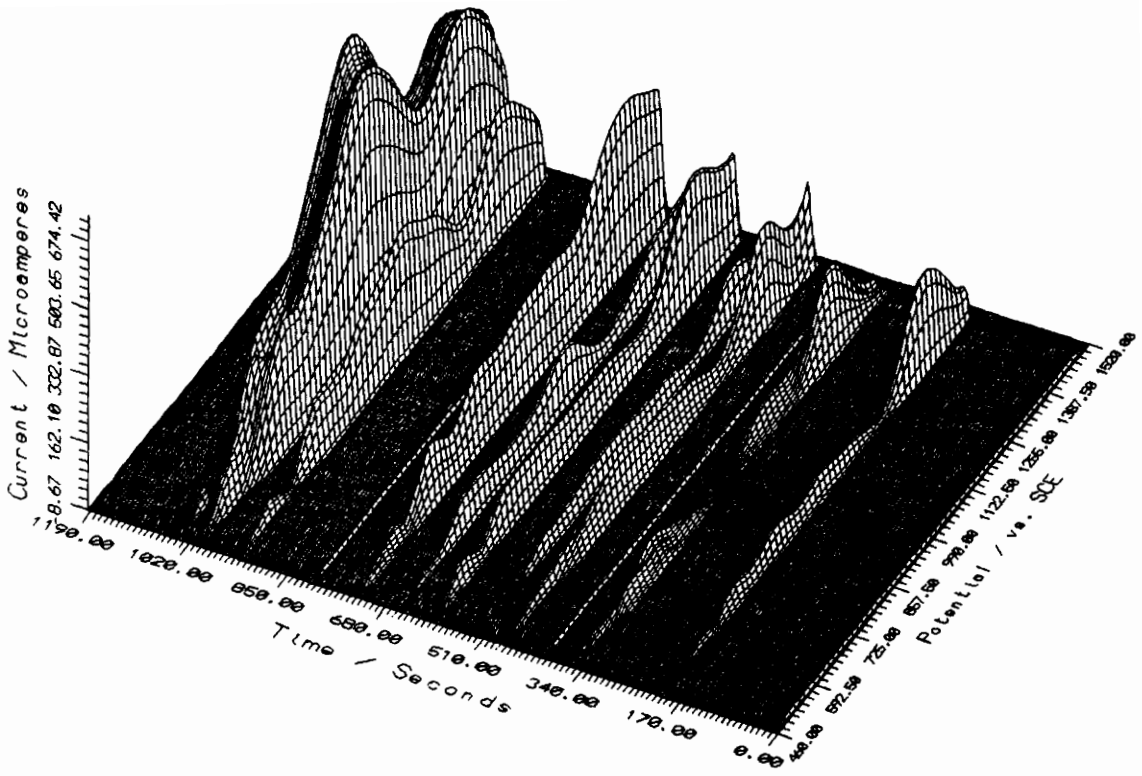

Figure 3.11 A 3-D chromatovoltammogram obtained for the separation of a fennel seed extract by gradient elution HPLC.

which are slices of the three dimensional data set corresponding to a single electrode potential (Figure 3.13 A-C). The contour plot shows the electrochemical resolution of several coeluting components of the mixture. Unfortunately, many chromatographically resolved peaks become blurred using the contour plot, so the actual number of peaks resolved in the time domain is obscured. The two dimensional plots, are the best demonstration of the utility of SWV electrochemical detection for the separation of complex mixtures. In contrast with other electrochemical detection methods, this technique is quite compatible with wide changes in mobile phase composition. The differential measurements of SWV eliminate background drift and most of the noise associated with the changing mobile phase. Furthermore, the degree of sample component resolution demonstrated with this detection method is unlikely to be possible in the same amount of time, using any single dimensional detection method.

3.4 Summary of SWV Electrochemical Detection.

A square wave voltammetric electrochemical detector has been developed for use with HPLC. The detector has been developed around a large diameter platinum disk indicator electrode, and it incorporates several desirable characteristics of commercially available electrochemical detectors with those of microelectrode based SWV detectors. Among the characteristics that the macroelectrode SWV detector has in common with commercial detectors are its

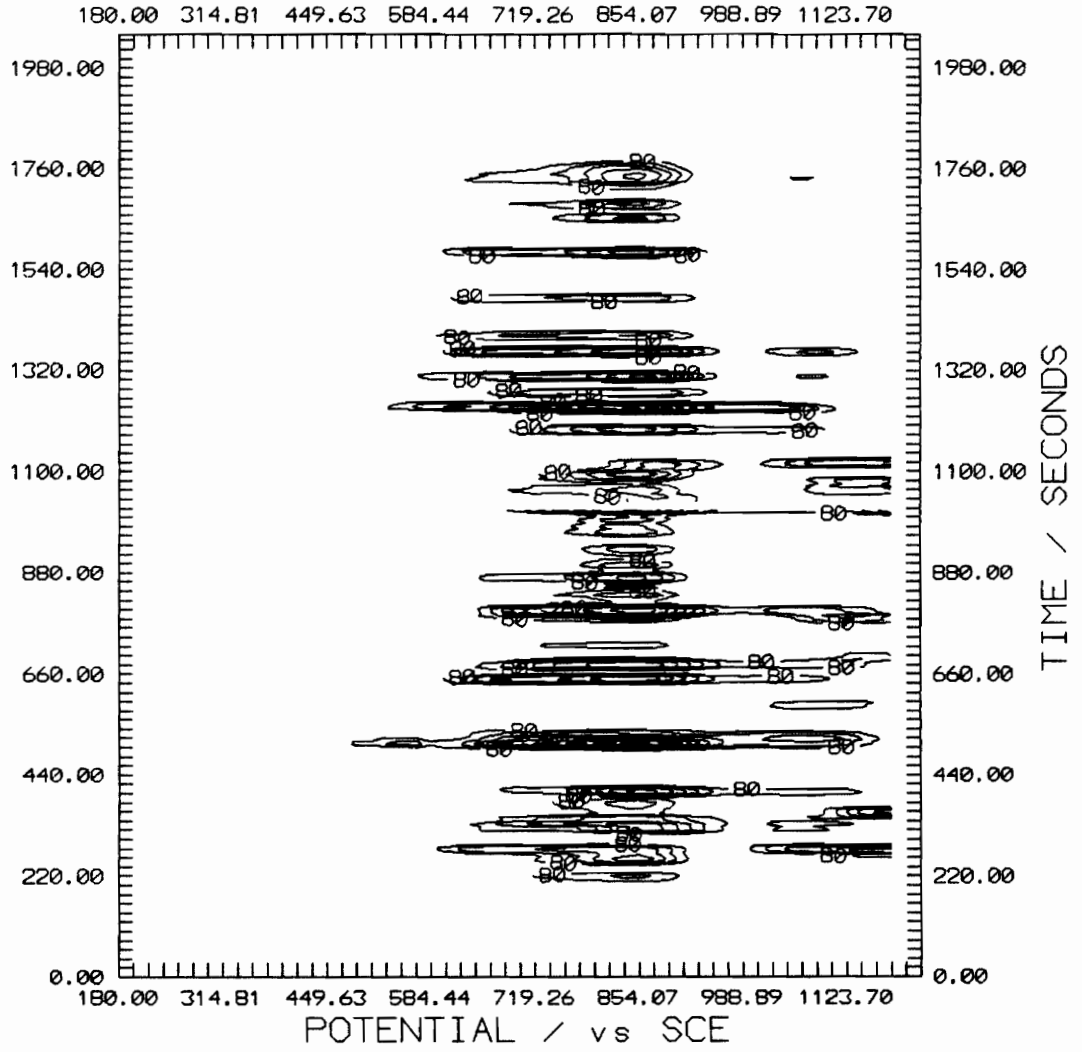

Figure 3.12 A contour map of a chromatovoltammogram obtained for the separation of an extract of mainstream cigarette smoke under gradient elution conditions.

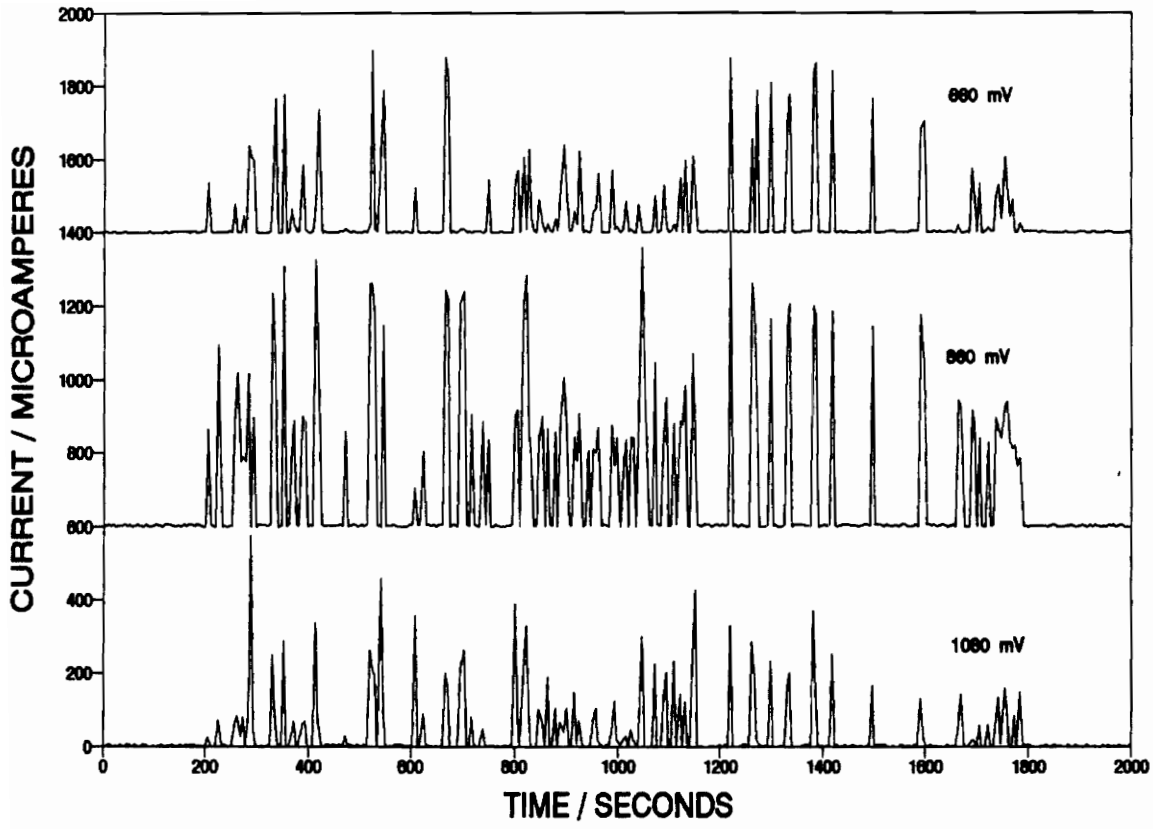

Figure 3.13 Two dimensional slices of the data shown in Figure 3.12 corresponding to individual electrode potentials. The potentials were 660 mV, 860 mV, and 1080 mV. The data illustrates the resolution that is possible using SWV detection with gradient elution HPLC.

physical ruggedness and its relative ease of maintenance. Analytical currents measured with large diameter electrodes are large compared to those measured with carbon fibers, so the need for amplificationand isolation has been avoided. Furthermore, large diameter electrodes are less sensitive to vibrations and rf noise than are carbon fibers. Finally, the SWV detector developed in this study is compatible with the solvent flow rates typically used with conventional HPLC systems.

The ability to operate an electrochemical detector employing a large diameter indicator electrode in a rapid scanning mode while maintaining accurate potential control is attributed to an electrochemically efficient cell geometry which results in lower internal resistance than is found in commercially available cells. The cell has also been shown to be chromatographically efficient, with relatively little analyte band spreading in the detection zone. This is largely due to the low volume of the detection zone, which has been estimated to be approximately 0.3 μL.

The minimum detectable quantity has been determined for both the scanning and nonscanning modes of operation. Using hydroquinone as the test analyte, the MDQ was determined to be in the low picogram range for the nonscanning mode and approximately 100 pg for the scanning mode. The limit of detection in the scanning mode is about the same as the best previously reported MDQ for a carbon fiber based SWV detector[14]. The linear dynamic range has

been determined to be 4.6 orders of magnitude.

The square wave voltammetric method combined with HPLC results in a three dimensional chromatovoltammogram, with current being monitored as a function of both time and electrode potential. The combination of elution time and oxidation/reduction potential is generally unique for a particular analyte under a given set of experimental conditions, increasing the likelihood of positive peak identification. The utility of the SWV detector has been demonstrated using both isocratic and gradient elution HPLC with simple test mixtures and complex, naturally occurring mixtures. The ability to use mobile phase gradients with only a slight modification to the scanning method is a result of the background correction which is inherent in square wave voltammetry. In separations that involved the use of broad mobile phase gradients, it was observed that essentially no background current drift occurred. The combination of square wave voltammetry with gradient elution HPLC vastly increases the degree of component resolution and the qualitative value of the information which can be obtained in a given time span, relative to that which can be obtained using conventional electrochemical detectors.

Chapter 4. Introduction To The Quartz Crystal Microbalance.

4.1 Theory of QCM Measurements.

It is well known that piezoelectric materials undergo a physical distortion when subjected to an electric field. In the presence of an oscillating electric field, piezoelectric materials will physically oscillate. Although numerous materials have this property, quartz is the most commonly used because of its low cost, mechanical strength, and chemical properties. The direction of crystal oscillation depends on the orientation of the crystal lattice in the electric field. In the quartz crystal microbalance, the predominant mode of oscillation is in the direction parallel to the surface of the quartz wafer. This shear wave oscillation is induced most efficiently in AT-cut quartz wafers[33].

The frequency of oscillation depends on several factors. Among these are the properties of the quartz (thickness, density, and shear modulus) and the properties of the environment in which the oscillation occurs. These include the density and viscosity of the phases in contact with the wafer, the pressure differences across the wafer, and temperature. Usually, efforts are made to keep these factors as constant as possible. Factors that are subject to change are the mass of the attached electrodes and/or the mass of an adsorbate attached to the electrodes.

Sauerbrey[34] developed a simple expression which relates changes in interfacial mass to changes in the QCM oscillating frequency:

(4.2.1) $$\Delta f = -2\Delta m f_o^2/(A(S_q d_q)^{1/2})$$

In this expression, Δf is the change in oscillating frequency, Δm is the change in interfacial mass on the oscillating surface, f_o is the fundamental oscillating frequency, A is the area of the oscillating surface, S_q and d_q are the shear modulus and density of quartz, respectively. It is known that the amplitude of the standing wave is most intense between the attached electrodes and that it decays exponentially with distance from the electrode edges[35]. This allows the use of the electrode area as an approximation of the area of the oscillating surface. The fundamental oscillating frequency is determined by the manufacturing process and the other variables in the Sauerbrey expression are readily available in the literature, making it easy to calculate the frequency change per unit mass change on the crystal surface.

The Sauerbrey expression is useful for many situations, but there are limitations to its applicability. One assumption implicit in the expression is that the material attached to the surface of the crystal must not experience any deformation during oscillation. This is a good assumption when thin, rigid layers of material are attached, but the validity of the assumption decreases with the increasing thickness and nonrigidity of the attached layer. A more complex theory known as the Z-match theory, which takes the density and shear modulus of the attached layer into account, has been shown to be applicable for cases in which

thick, nonrigid polymer layers are attached to a quartz crystal[36].

Recently, several research groups have developed detailed theoretical explanations for the behavior of uncoated piezoelectric crystals in the presence of liquids[37-43]. Kanazawa and Gordon developed a model based on the coupling of the shear wave in the quartz with a damped shear wave in the fluid, assuming negligible fluid elasticity[37,38]. The change in oscillating frequency is related to the material parameters describing the liquid and the quartz

(4.2.2) $$\Delta f = -2f_0^{3/2}(V_L d_L/S_q d_q)^{1/2}$$

where V_L is the viscosity of the liquid, d_L is the density of the liquid, and S_q and d_q are the shear modulus and density of the quartz, respectively.

Bruckenstein and Shay[39] derived an expression based on an analogy between the oscillating boundary adjacent to the crystal face and the thickness of an ac polarographic diffusion layer. The expression is

(4.2.3) $$\Delta f = -(2.26 \times 10^{-6})nf_{03/2}(S_L d_L)^{1/2}$$

where n is one or two, depending on the number of crystal faces exposed to the liquid. Hager[40] developed an expression in which Δf is a function of the dielectric constant as well as the density and viscosity of the liquid. Other expressions, which

are based on empirical observations, have also been offered[41-43].

4.2 Historical Overview of QCM Analysis.

The quartz crystal microbalance (QCM) is a very sensitive instrument which has been applied to numerous analytical problems in the gas phase. Among these applications are the measurement of the dew point of gases[44], the thickness of evaporated metal films[45], and adsorption of gases on quartz[46]. The QCM was first employed as a detector for gas chromatography by King[47]. Quartz crystals were coated with gas chromatographic substrates and mounted in a 20 μL flow cell. The sensor was found to be a selective detector, with sensitivity increasing linearly with respect to retention volume. The detection limit for a 15 MHz crystal was estimated to be about one picogram[47]. The quartz crystal microbalance is now a widely accepted sensor for chemical analysis in the gas phase. Guilbault and coworkers have published several reviews concerning the application of the QCM for detection of trace constituents in gases[48-51].

Extension of QCM measurements to the liquid phase has been slow because of several problems not encountered in gas phase applications[52,53]. Greater energy losses at the liquid - crystal interface make stable crystal oscillation more difficult to achieve in the presence of liquids. The oscillation frequency is sensitive to changes in the density and viscosity of the liquid at the interface. Therefore, slight variations in these properties results in increased noise and baseline drift.

Finally, progress has been hampered by the lack of coating procedures that result in stable and reproducible surfaces that are capable of strong interaction with analytes[52-54].

Konash and Bastiaans were the first to achieve reliable oscillation of quartz crystals in contact with solutions[53]. These researchers chemically bonded ocatadecyltrichloro-silane and docosodimethyl(dimethylamino) silane to the crystal surfaces exposed to solvent flow in an effort to simulate LC conditions. They were able to demonstrate the effect of surface adsorption of toluene on the QCM signal, exclusive of density effects. However, their detector compared poorly with other modes of LC detection. The authors attributed this poor performance to incomplete coverage of the quartz with the surface modifiers.

Perhaps the most significant use of the quartz crystal microbalance in the liquid phase has been the electro-gravimetric analysis of ions in solution (EQCM). The technique was first used ex-situ by Mieure and Jones[55]. These researchers used the electrodes on a quartz crystal as cathodes for the electrodeposition of cadmium ions. The crystal was then rinsed and dried before measuring the frequency change caused by the deposited metal. The sensor had a linear response in the range of 2×10^{-6} M to 2×10^{-4} M Cd^{+2}, with a relative standard deviation of about 3% for measurements at a single concentration.

Bruckenstein et al.[56] used a similar approach to measure the deposition of lead monolayers onto electrode surfaces. Using a process known as underpotential

deposition (UPD) they were able to create a single atomic layer of metal on the electrode surfaces. The crystal was then rinsed and dried and the mass of the metal was calculated from the EQCM frequency in air.

In a more recent study, Deakin and Melroy demonstrated the deposition and reoxidation of a submonolayer of lead using simultaneous voltammetric and QCM measurements[57]. The frequency change for the deposition of a monolayer of lead corresponded to a surface coverage of 1.5 nanomoles/cm^2. By plotting the surface coverage data versus the integrated current, the number of electrons transferred to each Pb atom was found to be 2, demonstrating that the EQCM responds to changes in the interfacial mass as predicted by the Sauerbrey equation.

The EQCM has also been used to study mass transport phenomena that accompany redox processes occurring in thin films on electrodes[58-60]. Mass changes in the film associated with the gain or loss of any species are detected with the EQCM. Since both electrochemical charge and mass changes are measured, independent calculations of the ion and solvent fluxes is possible. It has been shown that in these thin films, solvent transport occurs in a direction opposite to that of ion transport[60].

The QCM has also been used for several nonelectro-chemical analyses in solution. Nomura et al.[61-63] used coated quartz crystals for the selective determination of ionic species in solution. For the determination of lead, these researchers coated a quartz crystal with copper(II) oleate and then removed the

copper by passing an EDTA solution over the surface. With the remaining coating, lead could be determined in the range of 3 to 40 μM with good reproducibility[61]. A poly(vinylpyridine) coating was used for the determination of 5 to 35 μM solutions of copper(II)[62]. A coating of silicone oil was used for the determination of 5 to 100 μM solutions of iron(III) and aluminum(III) with a relative standard deviation of 3%[63].

Okahata et al.[64] used a lipid bilayer coating to provide a rapid and sensitive indicator for bitter substances in aqueous solutions. Charlesworth[52] used a poly(ethylenimine) coating for the determination of low levels of organic acids in nonpolar hydrocarbons. He demonstrated that the QCM frequency change is dependent on solute diffusion as well as the capacity of the coating. In general, thicker polymer coatings provided greater mass sensitivity, but also increased the indicator response time.

4.3 Purpose of The QCM Study.

One of the purposes of this study was the adaptation of existing procedures for the chemical modification of gold surfaces to produce stable, reproducible, monolayer coatings on the electrodes of quartz crystals. Gold surfaces modified with substituted thiols have been well characterized[65] and a large number of these compounds are either available commercially or are easily prepared, allowing the QCM to be modified for general or selective detection.

Additionally, the study was intended to develop an improved understanding of the factors that contribute to the total QCM signal using various chemically modified quartz crystals in a low volume flow cell. These factors include the capacity of the bonded monolayer coatings, the contribution of the density/viscosity term $(V_L d_L)^{1/2}$ and the effect of variations in the solvent flow rate. Other factors that effect the magnitude of the QCM signal include the nature of the solute - bonded phase interactions, structural differences in the substituents on similar solute molecules, and the relative solvent strength for various solutes.

Finally, the QCM was developed as a means of conducting surface adsorption studies. Using an amine bonded phase, isotherms were obtained for the adsorption of a single compound under conditions of varying solvent strength and for various solutes, using a single solvent composition. The isotherms were classified according to the system developed by Giles et al.[66-68], and the free energies of adsorption were determined for the compounds. The advantages of this method over older methods were also discussed.

Chapter 5. QCM Experimental.

5.1 QCM Apparatus.

Quartz crystals with 10 MHz resonant frequency were purchased from International Crystal Manufacturing Co., Inc. (Oklahoma City, Ok.). The crystals were lab monitor AT cut, measuring 11.4 mm in diameter, with a thickness of 0.25 mm. The crystals had centrally deposited gold electrodes 5 mm in diameter on each face.

The flow cell, which was machined from two delrin blocks, is illustrated in Figure 5.1. The cell was constructed so that the indicator quartz crystal was held between two o-rings which were partially recessed into the upper and lower halves of the cell. The two halves were held together by four 2 inch bolts (10-32 thread). The flow cavity consisted of the space between the upper face of the crystal and the top half of the flow cell and had an estimated volume of 5 μL. The cell was constructed so that the incoming solvent stream was directed normal to the center of the quartz crystal, flowing radially across the surface to two exit ports which were located at the outer edges of the flow cavity.

The electrical circuit used to measure crystal oscillation frequency was a modified version of that which was published by Bruckenstein and Shay[39]. The flow cell and related electrical circuit were isolated from vibrations.

The solvent delivery system consisted of an ISCO model 314 syringe pump and a Rheodyne model 7120 high pressure injection valve with a 20 μL sample

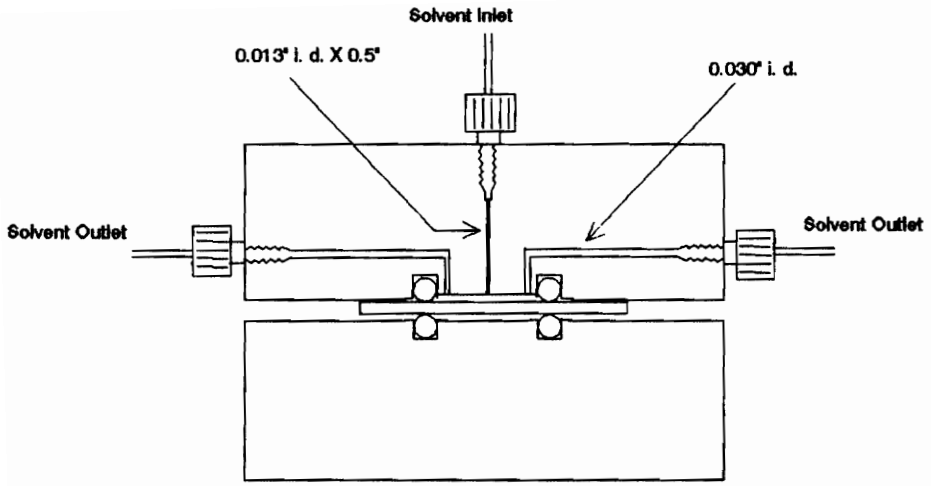

Figure 5.1 A cross sectional view of the QCM flow cell.

loop. All post-injector tubing was 0.010" i. d. teflon. Data was collected using a Servocorder model 6252 chart recorder.

5.2 Chemicals and Solvents.

The following chemicals were purchased from Aldrich Chemical Company (Milwaukee, Wis.) and were used without further purification:

p-thiocresol, ocadecylmercaptan, phenol, 4-ethyl-phenol, 4-isopropyl-phenol, 4-tert-butylphenol, 4-nitrophenol, fructose, pyridine, aniline, 4-ethyl-aniline, 4-isopropylaniline, 4-tert-butylaniline.

Other chemicals purchased from Aldrich include 4-amino-pyridine, 4-benzoylpyridine, 4-cyanopyridine, and 4-amino-thiophenol. The 4-aminothiophenol was purified by sublimation, while the substituted pyridines were recrystallized from ethanol prior to use. Sucrose was obtained as ordinary table sugar and used without further purification. 11-Mercaptodecanoic acid was prepared by the method described by Troughton et al.[69].

Experiments were conducted using acetonitrile-water mixtures as solvents. Acetonitrile was nonspectro grade (Burdick & Jackson, Muskegon, Mi.) and was used without further purification. All water was purified by a Barnsted Nanopure II water purification system.

5.3 Preparation of Chemically Bonded Crystals.

The procedure for surface modification followed standard self assembly techniques. Briefly, the quartz crystals were immersed in a warm solution of concentrated sulfuric acid and 30% hydrogen peroxide (4:1) in order to oxidize and remove surface contaminants. The crystals were then rinsed with deionized water, 95% ethanol, and chloro-form. After drying under a stream of dry nitrogen, the crystals were immersed in solutions of the organic mercaptan substrates (50 mM, in chloroform) and the spontaneous adsorption reactions were allowed to proceed at room temperature for 24 hours. After this period of time, the crystals were rinsed with chloroform and 95% ethanol, then allowed to dry before use in the flow cell. Surface coatings were confirmed by XPS measurements on the modified crystals.

Coating with 4-amino pyridine was performed within the flow cell, since this compound was found to adhere rapidly and irreversibly to the crystal's upper gold electrode. Clean crystals were installed in the flow cell and the cell was filled with a 1000 ppm solution of 4-amino pyridine in 20% acetonitrile, 80% water. This solution was allowed to remain in the cell for 30 minutes, after which the cell was purged with the solvent to be used in the experiment.

5.4 QCM Procedures.

Unless otherwise noted, the QCM experiments were conducted using a

solvent consisting of 20% acetonitrile and 80% water. The solvent was degassed in two separate operations. First, by exposure to ultrasonic vibrations and second, by exposure to subatmospheric pressure. Each time the flow cell was assembled, the solvent was pumped through the cell for a minimum of 20 hours prior to the performance of an experiment. The solvent flow rate was 40 μL/min. for experiments that were performed at a fixed flow rate. All samples were made using the same solvent batch as that which was being pumped through the flow cell.

For all experiments, the difference between the oscillation frequencies of the indicator and reference quartz crystals was set as close as possible to 2.0 kHz. Three to four measurements of the QCM response were made for each sample.

The QCM response per nanogram of material added to the surface of the crystal was determined by evaluating the Sauerbrey expression for the crystals used in these experiments. The response was determined to be a decrease of 0.81 Hz in the oscillating frequency per nanogram of material added to the surface. The surface capacity of the crystals was determined using the QCM response for various concentrations of KCl and $KClO_4$. The response initially increased rapidly with respect to increasing concentration until an apparent surface saturation point was reached. At concentrations greater than was required for surface saturation, the response was observed to increase much more slowly.

Chapter 6. QCM Results.

6.1 Capacity of the Chemically Bonded QCM Crystal Surface.

It was found during initial experiments that salts of sodium, potassium and calcium interacted strongly with 4-aminothiophenol modified crystals. Although the precise nature of the salt-surface interaction is not clearly understood, measurable signals were observed for potassium salts in the lower ppm range. Furthermore, the strength of the surface interaction provided a convenient method for determining the surface capacity of the modified crystals. The surface capacity of the quartz crystals was obtained by measuring the QCM response for injections of samples with varying concentrations of potassium salts. Figure 6.1 is a comparison of the QCM response to various concentrations of KCl using a bare quartz crystal (6.1 A) and a crystal modified with 4-aminothiophenol (6.1 B). For the bare crystal, the QCM response is small and was observed to be linear (slope = 290 Hz/(g/L)) for concentrations ranging from 1 to 1000 ppm KCl. For the 4-aminothiophenol bonded crystal, the QCM response was observed to be greater than for the bare crystal and the change in response with respect to increasing concentration was much greater for the range of 1 to 10 ppm KCl. At concentrations greater than 10 ppm KCl, the rate of change in QCM response with respect to increasing concentration slows dramatically and is linear in the range of 10 to 1000 ppm, having approximately the same slope as that observed for the nonbonded crystal.

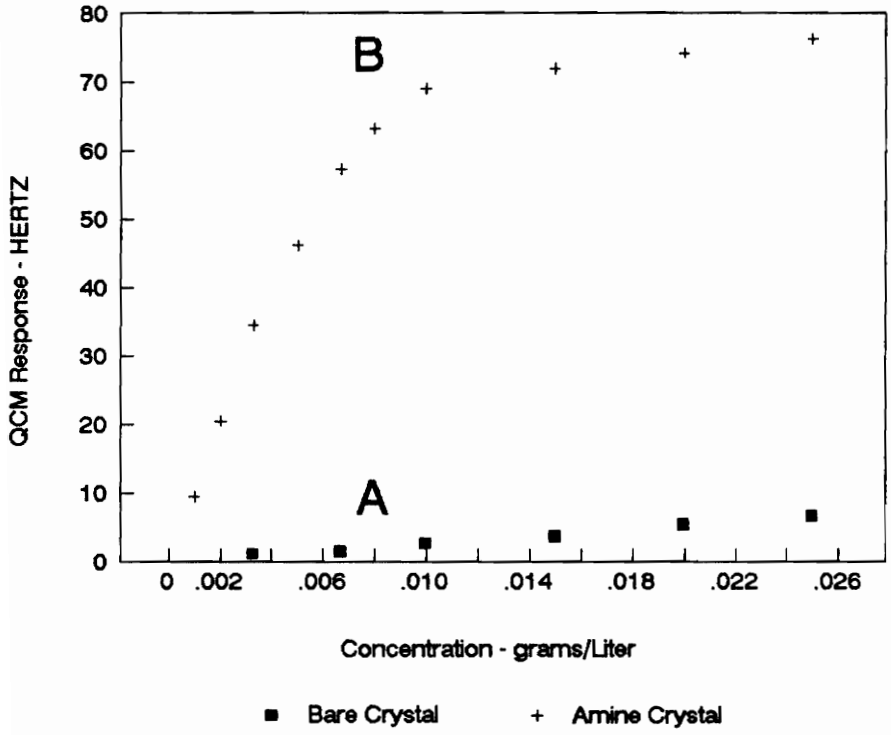

Figure 6.1 The QCM response for various concentrations of KCl using a bare quartz crystal and a 4-aminothiophenol modified crystal.

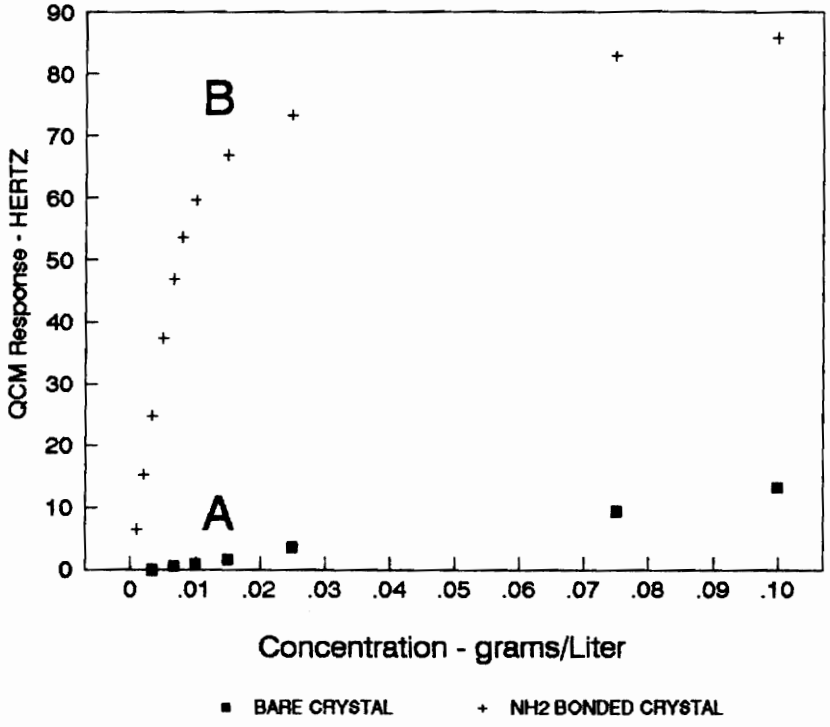

Figure 6.2 The QCM responses to various concentrations of $KClO_4$ using the same crystals as those used to obtain the data shown in figure 6.1.

A similar pattern was observed using various concentrations of potassium perchlorate using the same bare and 4-aminothiophenol modified crystals as those used for the detection of KCl solutions. Figure 6.2 is a comparison of the QCM response using these crystals. For the bare crystal, the response was observed to be small and increased linearly (slope = 185 Hz/(g/L)) with respect to concentration in the range of 1 to 1000 ppm $KClO_4$. For the 4-aminothiophenol modified crystal, the response increased much more rapidly with respect to concentration in the range of 1 to 18 ppm $KClO_4$ Above 18 ppm, the change in response increased linearly with respect to increasing concentration, having the same slope as that observed for the nonbonded crystal.

These observations indicate that at very low concentrations, the dominant contribution to the QCM signal is a physical interaction between KCl and the modified crystal surface. A surface saturation point appears to be reached at about 10 ppm or 3.4 nanomole/cm^2 for KCl, and approximately 18 ppm or 3.3 nanomole/cm^2 for $KClO_4$. These values are of the same order of magnitude as that which was determined by Crooks et al.[70], who reported a surface coverage of 2.5 nanomoles/cm^2 for 4-aminothiophenol on a gold surface.

6.2 Factors Effecting The Magnitude of The QCM Signal

6.2.1 Flow Rate Dependence of Solute - Surface Interactions.

Additional evidence for a mass interaction between solutes and the modified quartz crystal surface was obtained using 1000 parts per million solutions of sucrose and fructose dissolved in 20% acetonitrile, 80% water. The Quartz crystal was modified by bonding 4-aminothiophenol to the gold electrode surface. Figure 6.3 is a plot of the maximum QCM response for these sugars, using flow injection analysis, as a function of flow rate. It can be seen that in the interval from 13.3 to 150 μL/minute that the QCM response is strongly dependent on the carrier solvent flow rate. This is expected for a diffusion rate dependent solute - surface interaction, since the residence time for the solute in the flow cell is reduced at higher flow rates. On the other hand, a response to the bulk properties of the sample, such as density, viscosity, or refractive index, should be instantaneous, and therefore, immune to changes in the flow rate.

In the interval from 150 to 300 μL/minute, the QCM oscillating frequency changes only slightly with respect to increasing flow rate, indicating that the residence time in the flow cell is too short for a significant amount of solute to diffuse to the crystal surface. In this interval, the QCM response is primarily due to the bulk properties of the sample, which has a different density and viscosity than the carrier solvent.

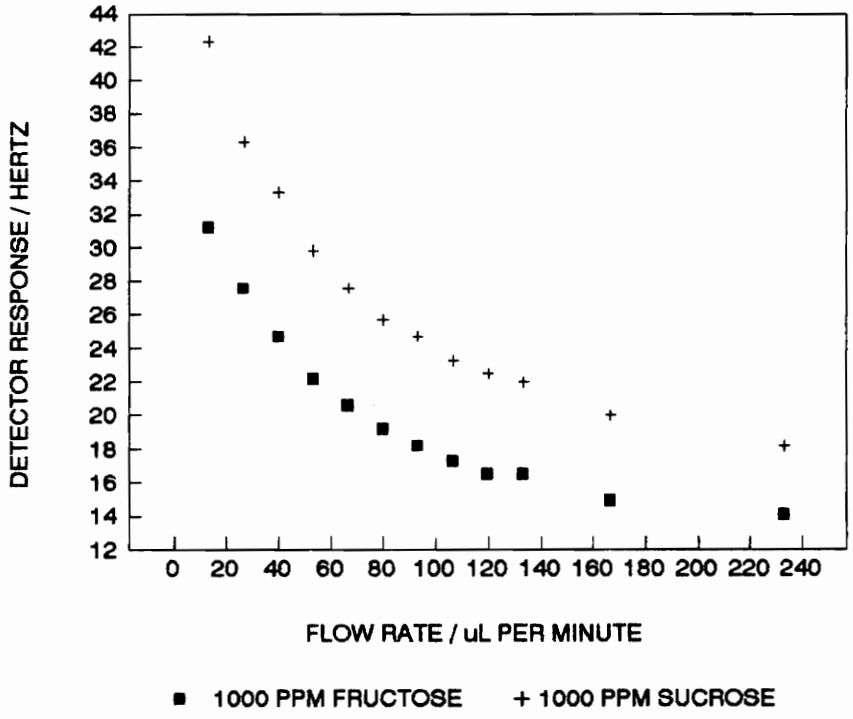

Figure 6.3 The QCM response as a function of solvent flow rate using a 4-aminothiophenol modified quartz crystal.

An attempt was made to demonstrate the instantaneous response of the QCM to density and viscosity changes using a nonbonded crystal and a 1000 ppm sucrose solution. However, no response was observed for sucrose under these conditions. This is not really surprising, since the QCM response is a result of changes in the density/viscosity term of equation 4.2.3 $(V_L d_L)^{1/2}$. For solutions of organic compounds, it is possible for the solution density to decrease with respect to that of the solvent, while the viscosity increases. The result is that the effect of one of these parameters can be canceled by the effect of the other.

6.2.2 The QCM Response Using Various Solutes And Bonded Phases

The magnitude of the QCM signal is dependent on the nature of both the solute and the bonded phase. Table 6.1[71,72] shows the QCM response for various test solutes using four different bonded phases. The concentration of each solute was 1000 ppm and the solvent used was 20% acetonitrile, 80% water.

From the table, two general patterns can be observed. With respect to decreasing signal magnitude, the bonded phases can be arranged as follows:

4-aminothiophenol > 4-aminopyridine, 1-mercapto-decanoic acid > octadecylmercaptan.

Likewise, the solute classes can be arranged with respect to decreasing signal magnitude: phenols > anilines > pyridines. A notable exception to the latter arrangement is 4-aminopyridine, which has the greatest affinity for all of the

Table 6.1 QCM response to various solutes using four different quartz crystal modifiers.

Solute (1000 ppm)	4-amino thiophenol	4-amino pyridine	C11COOH	C18 Alkyl
Phenol	8.9 Hz	4.2 Hz	0 Hz	19.2 Hz
4-Ethylphenol	32.5	17.8	11.7	12.7
4-i-Propylphenol	52.7	17.1	19.9	16.0
4-t-Butylphenol	138.8	51.6	51.5	16.3
4-Nitrophenol	0	5.7	0	4.8
Sucrose	33.3			
Fructose	24.7			
4-Aminopyridine	197.4	101.3	96.7	18.7
4-Benzoylpyridine	7.6	6.8	5.4	8.4
4-Cyanopyridine	4.2	3.0	3.0	3.0
Pyridine	5.1	4.6	4.6	4.0
Aniline	6.1	0	2.0	5.4
4-Ethylaniline	8.3	7.1	6.8	6.0
4-i-Propylaniline	14.1	9.8	8.8	10.3
4-t-Butylaniline	17.9	6.5	10.8	11.9

bonded phases used except octadecylmercaptan.

6.2.3 Studies of the role of surface acid - base interactions

It can be seen from the data presented in the previous section that, in general, the strongest QCM responses occur when the surface modifier contains a terminal functional group which is either acidic or basic. This raises the possibility of Bronsted-Lowry type acid-base interactions, in which some degree of proton transfer is possible. Alternatively, electron pair donation may occur between nonbonding pi orbitals of one species and empty electron orbitals of the other.

Table 6.2[71,72] gives the pK_a for the phenols, sugars, and the conjugate acids of the organic bases that were used as test solutes in this study. If the solute-surface interactions were primarily due to Bronsted-Lowry proton transfers, then the strongest QCM signal would be expected when the most acidic solute interacted with a basic surface modifier, and vice versa. For example, 4-nitrophenol (pK_a = 7.15) should cause a stronger response than any of the other solutes tested when the quartz crystal is modified with 4-aminothiophenol. Furthermore, 4-aminopyridine, which is the

Table 6.2 pK_a of test solutes in water. 25 °C

Compound	pK_a
Phenol	9.98
4-Ethylphenol	10.21
4-i-Propylphenol	10.24
4-t-Butylphenol	10.39
4-Nitrophenol	7.15
Sucrose	12.39
Fructose	12.21
Pyridine *	5.21
4-Aminopyridine *	9.11
4-Cyanopyridine *	1.90
4-Benzoylpyridine *	3.35
Aniline *	4.60
4-Ethylaniline *	5.00
4-i-Propylaniline *	4.85
4-t-Butylaniline *	4.95

* Indicates pK_a of the conjugate acid

most basic solute tested, would be expected to have a weak interaction with basic surface modifiers and a strong interaction with acidic surface modifiers. However, from Table 6.1 it can be seen that 4-nitrophenol did not cause a measurable response using either acid or base modified crystals. Furthermore, 4-aminopyridine caused the greatest response in all cases. A comparison of the maximum QCM response with the pK_a for the various test solutes reveals no correlation between the proton donating capability of solutes and the apparent strength of the solute - surface interaction. Therefore, it is unlikely that Bronsted-Lowry acid-base interactions make a significant contribution to the magnitude of the QCM response. This is contrary to the conclusion reached by Charlesworth[52], who determined that an acid-base interaction is the primary attractive force between a poly(ethylenimine) coating and various organic acids.

In order to determine the relative importance of electron pair donation between the bonded phase and the solutes, the QCM responses for several phenols were measured under conditions in which electron pair donation was thought to be possible and compared with the responses obtained under conditions in which electron pair donation was thought to be prevented. Specifically, the QCM responses were measured using a quartz crystal modified with 4-aminothiophenol to the surface of the gold electrodes. Afterward, several injections of a 1 mM HCl solution were made, in order to ensure the complete protonation of the amine groups of the bonded substrate. The QCM responses

were then measured using the same samples as those used prior to the surface protonation.

Figure 6.4 is a comparison of the QCM responses obtained before and after surface protonation. The responses obtained after protonation are much smaller than those obtained initially and are approximately the same magnitude as those obtained using a bare crystal. This indicates that the primary mode of interaction with the amine terminated modifier involves an electron pair donation between the surface and the solute, such as that which occurs in hydrogen bond formation. Figure 6.5 compares the QCM responses for the same phenols using a crystal modified with 1-mercaptododecanoic acid with those obtained using a crystal modified with 4-aminopyridine. The responses are similar for the two modifiers and they are a further indication that electron pair donation rather than Bronsted/Lowry acid-base interaction is the primary mode of interaction between the solute and the surface, since the former modifier is acidic and the latter is basic.

Electron pair donation is not possible for the octadecylmercaptan modifier. Van der Waal's forces, such as dipole-dipole and dipole-induced dipole forces, are the only possible forces of attraction between this modifier and solutes. These interactions are weaker than electron pair donation and the QCM response to most of the test solutes is consequently smaller compared to the response using modifiers capable of electron pair donation.

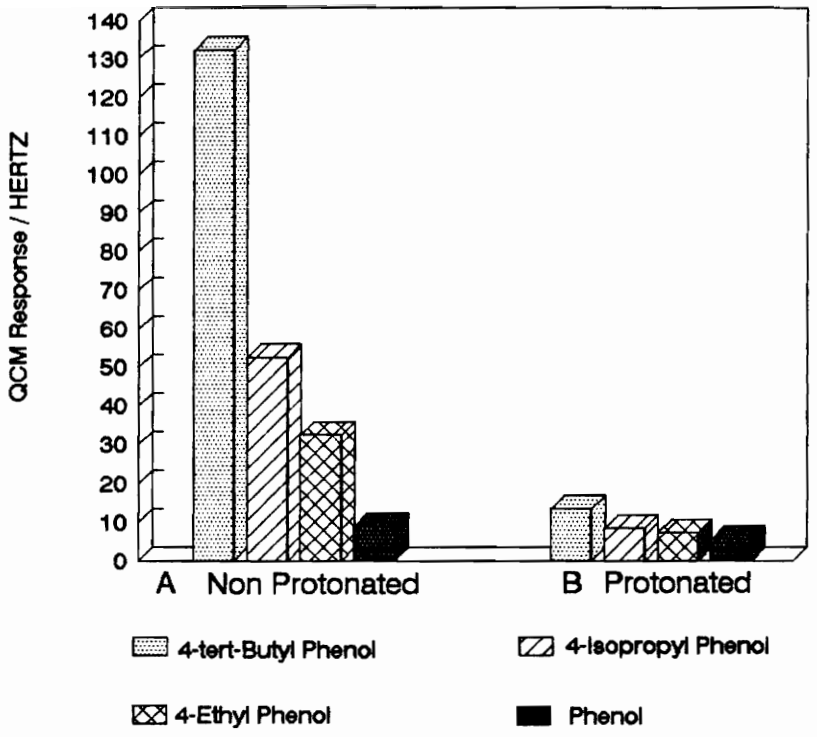

Figure 6.4 The QCM response for phenol and substituted phenols using a 4-aminothiophenol bonded crystal. The QCM responses were obtained A.) before protonation of the amine functional group and B.) after protonation of the amine functional group.

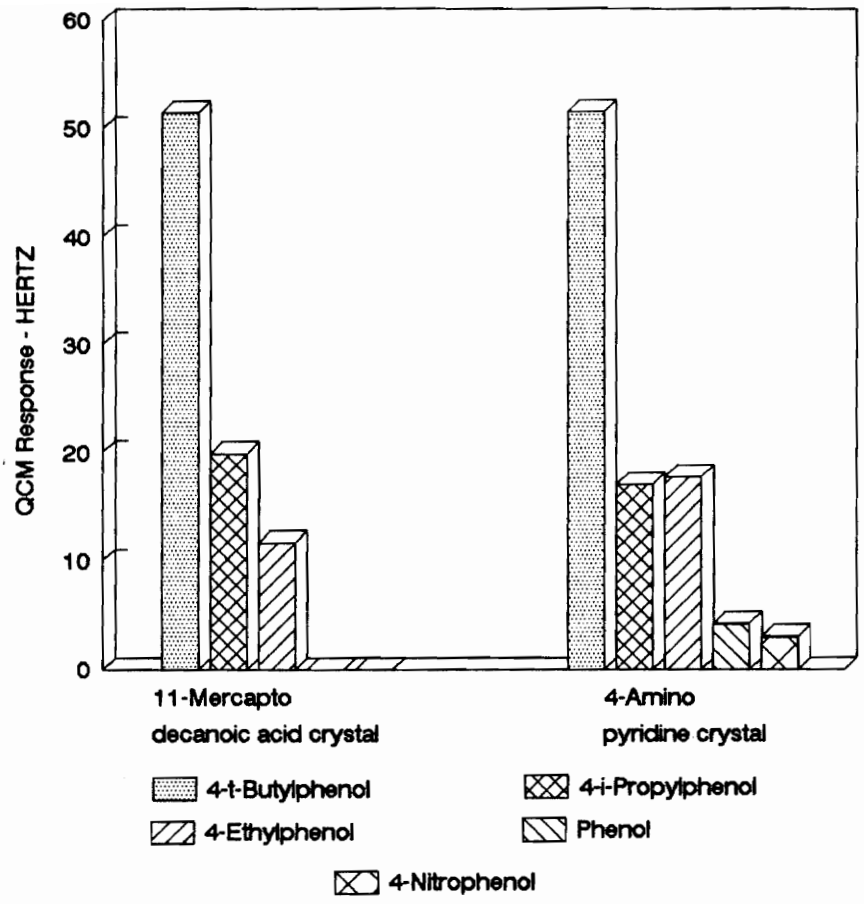

Figure 6.5 A comparison of the QCM responses for various phenols using a crystal modified with 11-mercaptodecanoic acid and a crystal modified with 4-aminopyridine.

6.2.4 Surface Adsorption As A Function of Solute Structure

Referring to Table 6.1, a general pattern can be seen for the adsorption of organic solutes from largely aqueous carrier solvents. Using the quartz crystal modifiers that permit adsorption through electron pair donation between the bonded phase and the solute molecules, the magnitude of the QCM response increases with increasing size of the hydrophobic portion of the solute molecules. This phenomenon can be understood partly as a manifestation of Traube's Rule, which states that a polar adsorbent will prefer-entially adsorb the more polar component of a nonpolar solution. The term polarity is used in the general sense of the ability to engage in hydrogen bonding or dipole-dipole interactions. A semiquantitative extension of Traube's Rule states that the adsorption of organic substances from aqueous solutions increases strongly and regularly with ascending species of a homologous series[73].

6.2.5 Surface Adsorption As A Function of Solvent Composition

Another manifestation of Traube's Rule is the inverse relationship between the extent of adsorption of a species and its solubility in the solvent used. Figure 6.6 shows a series of isotherms for 4-t-butylphenol using three different solvent compositions. The isotherms illustrate the fact that when solubility in a particular solvent is limited, a small change in solvent composition can have a dramatic effect on the amount of solute adsorbed. Reduced concentration, C_r = C/C0, where C0

is the solubility of the solute in the particular solvent, may be a potentially more useful parameter than absolute concentration, since solubility differences are accounted for.

Table 6.3 give the solubility of 4-t-butylphenol for each of the solvent compositions used as well as the reduced concentration corresponding to each absolute concentration value. The table makes it easy to understand why the amount of solute adsorbed varies with the organic content of the solvent. For example, in 30% acetonitrile, 70% water, an absolute concentration of 1.00 gram/liter corresponds to a reduced concentration of 0.178. If the QCM response is a function of the reduced concentration, then this sample would be expected to cause approximately the same response as a sample that was 0.250 gram/liter dissolved in 20% acetonitrile, 80% water. An examination of Figure 6.6 verifies that this is the case. More significantly, all three data sets are superimposable when the amount of adsorbed solute is plotted as a function of reduced concentration, as seen in figure 6.7. This demonstrates that the amount of solute adsorbed is a function of the reduced concentration of the solute.

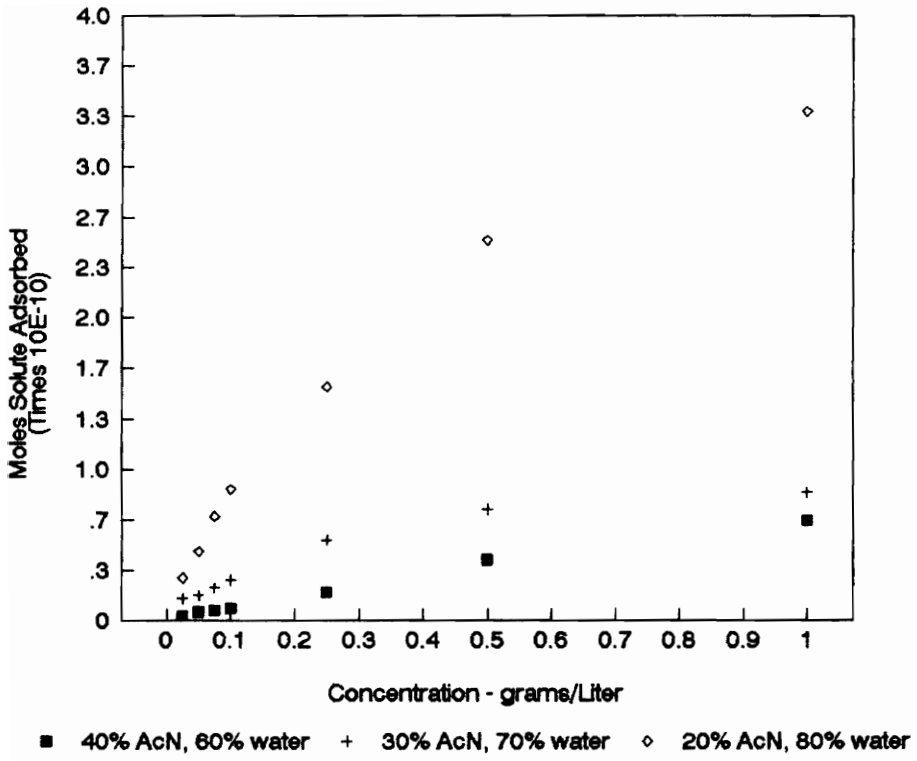

Figure 6.6 Isotherms for 4-t-butylphenol obtained by QCM measurements in various solvent compositions.

Table 6.3 Reduced concentrations of 4-t-butylphenol determined as C_R = C/Solubility. The solubilities given were measured experimentally.

Solvent	Concentration (g/liter)	Measured Solubility (g/liter)	Reduced Concentration
20% AcN	.025	1.40	.018
80% Water	.050		.036
	.075		.054
	.100		.071
	.200		.179
	.500		.357
	1.00		.714
30% AcN	.025	5.6	.0045
70% Water	.050		.0089
	.075		.013
	.100		.018
	.250		.045
	.500		.089
	1.00		.178
40% AcN	.025	21.4	.0012
60% Water	.050		.0023
	.075		.0035
	.100		.0047
	.250		.012
	.500		.023
	1.00		.047

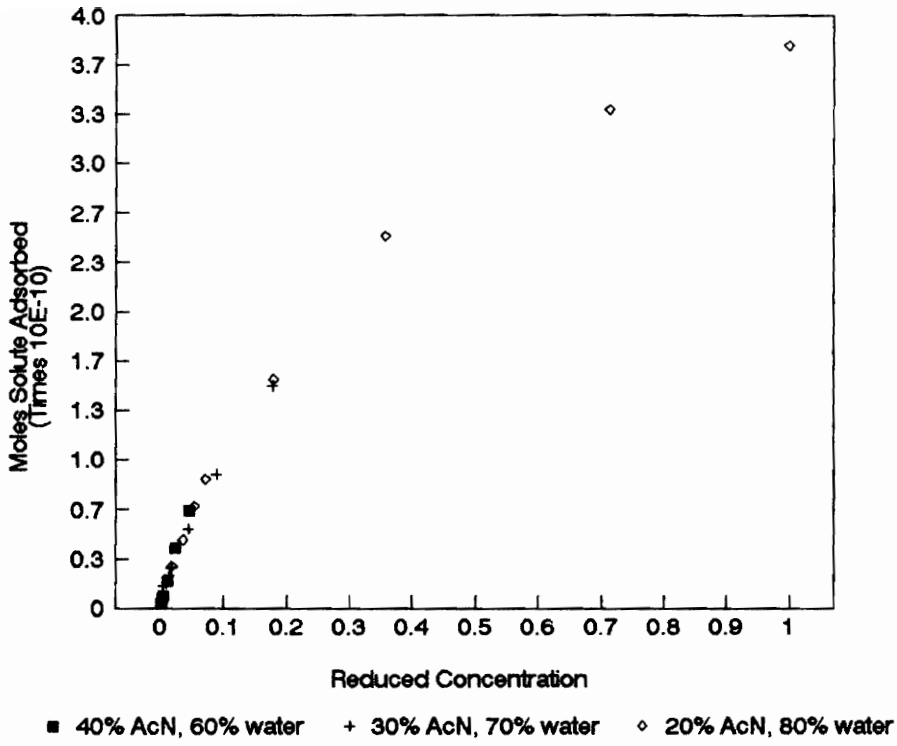

Figure 6.7 Isotherms for 4-t-butylphenol plotted as a function of reduced concentration.

6.3 Determination of Molar Free Energy of Adsorption.

The isotherms shown in section 6.2.4 suggest the possibility of determining the energy of adsorption for various solutes on the crystal surface. Many methods have been developed for conducting surface adsorption studies in liquids. One common method for determining the energy of adsorption of a solute on a solid surface involves the addition of a known quantity of a finely divided adsorbent into a stirred solution containing a known concentration of solute. The solution is allowed to reach equilibrium with the adsorbent and then the change in solute concentration is determined by titration, uv/vis absorbance, or by some other means. The experiment is repeated using solutions of various solute concentrations and the data is plotted as the amount of solute adsorbed per gram of adsorbent versus solute concentration. Among the most commonly studied solutes are fatty acids, aromatic acids, and esters. Typical adsorbents include alumina, silica gel, various forms of carbon, and some organic compounds such as sugars and starches[73].

The traditional methods understandably require relatively large samples and gram size quantities of adsorbent. By contrast, the use of the quartz crystal microbalance allows the study of samples in the hundreds of nanograms to microgram range. Furthermore, the same adsorbent is used throughout the experiment, eliminating the repetitive weighing of adsorbent samples as a possible source of experimental error. Finally, the range of chemical modifiers available for

the quartz crystals allows the researcher to tailor the adsorbent surface for a much broader range of applications than are possible using traditional adsorbents.

The isotherms shown in section 6.2.4 are of the L1 (Langmuirian) type described by Giles, et al.[66-68], having an initial region which is concave with respect to the concentration axis and a nonzero slope up to the limit of solubility. The general shape of the isotherms allows one to draw some important conclusions concerning the adsorption process. Most significantly, the L shape indicates that the activation energy for adsorption is independent of solute concentration; i. e., there is no interaction between solute molecules adsorbed at the surface[67]. Furthermore, the L shape is an indication of a homogeneous adsorbent surface. This is an important advantage of chemically modified gold surfaces, since many adsorbents contain a variety of different adsorption sites which may interact with the solute by several different mechanisms.

The adsorption data can be fitted to a modified version of the Langmuir expression, where solute concentration replaces the pressure term used in gas phase studies:

$$(6.2.1) \qquad Y = Y_m bC_r/(1+BC_r)$$

where Y is the number of molecules of solute adsorbed per square centimeter, Y_m is the number of molecules of solute per square centimeter forming a complete

monolayer, C_r is the reduced solute concentration, and b is a term which contains the molar free energy of adsorption:

(6.2.2) $$b = (K/Y_m)\exp(\Delta G/RT).$$

The molar free energy of adsorption can be calculated from equation 6.2.3:

(6.2.3) $$\Delta G = -RT\ln K$$

The constant K in the expressions above is determined by assuming that the QCM response arises from a competition for active surface sites between water molecules and the solute of interest. The Expression for K then becomes:

(6.2.4) $$K = X1_S X2_L / X1_L X2_S$$

where $X1_S$ and $X2_S$ denote the mole fractions of solute and water adsorbed on the surface, respectively. The variable $X2_L$ denotes the mole fraction of water in solution. The variable $X1_L$ is the reduced mole fraction of the solute in solution,

(6.2.5) $$X1_L = X_L(C_r/C)$$

where X_L is the actual mole fraction of solute in solution and the term (C_r/C) accounts for differences in the solvent strength.

Calculation of the molar free energy of adsorption is straight forward since all of the variables in equation 6.2.5 are either known or are readily measurable. The monolayer capacity, Y_m, was determined from the adsorption data for KCl and $KClO_4$ using a 4-aminothiophenol modified crystal. The amount of solute adsorbed can be readily measured since a 0.81 Hz decrease in frequency corresponds to 1 ng of material adsorbed. Evaluation of the molar free energy of adsorption, using equation 6.2.5 and the data shown in Figure 6.6 results in a mean free energy of ΔG = -23.7 +/- 0.6 kj/mole. Figure 6.8 is a comparison of the experimentally obtained isotherms with isotherms that were calculated using this molar free energy. Figure 6.9 shows a series of isotherms for 4-t-butylphenol, 4-isopropylphenol, and 4-ethylphenol. The molar free energy was evaluated for the latter two compounds by the same method. For 4-ethylphenol, ΔG = -21.3 +/- 0.3 kj/mole and for 4-isopropylphenol, ΔG = -20.4 +/- 0.2 kj/mole.

The equilibrium constant K can also be used to determine the enthalpy and entropy for the adsorption of solutes on the QCM surface since K can be expressed as:

(6.2.6) $$\ln(K) = \Delta S/R - \Delta H/RT$$

These values can be determined by generating isotherms at various temperatures. A plot of ln(K) versus 1/T would then be linear with a slope of -ΔH/R and an intercept equal to ΔS/R. Unfortunately, this procedure requires a means of controlling the temperature precisely. Unfortunately, no adequate means of controlling the temperature was available so these values were not determined in this study.

Adsorption may occur by one of two processes. The first is physisorption, which involves weak molecular interactions such as dipole interactions or hydrogen bonding. The second process is known as chemisorption and it usually involves the formation of a covalent bond. Typical enthalpies of physisorption are in the range of -20 to -40 kj/mole while the enthalpies measured for chemisorption may be in the range of -200 kj/mole[74]. Therefore, the values obtained for the free energy of adsorption for the substituted phenols on a 4-aminothiophenol substrate are indicative of physisorption, consistent with our description of the primary mode of surface interaction (i. e. electron pair donation).

6.4 QCM Summary

A procedure which is based on standard self assembly techniques, has been employed to generate reproducible, homogeneous chemically modified surfaces of piezoelectric quartz crystals. A low volume flow cell has been designed which allows for reduced detector response time and decreased solute band spreading

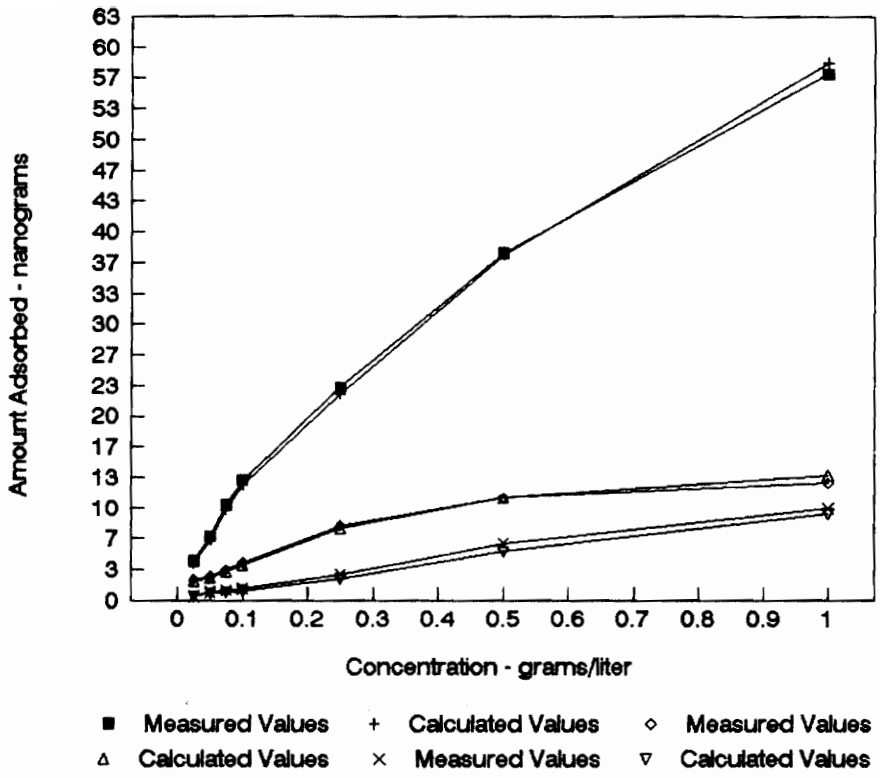

Figure 6.8 Experimentally measured and calculated isotherms for 4-t-butylphenol.

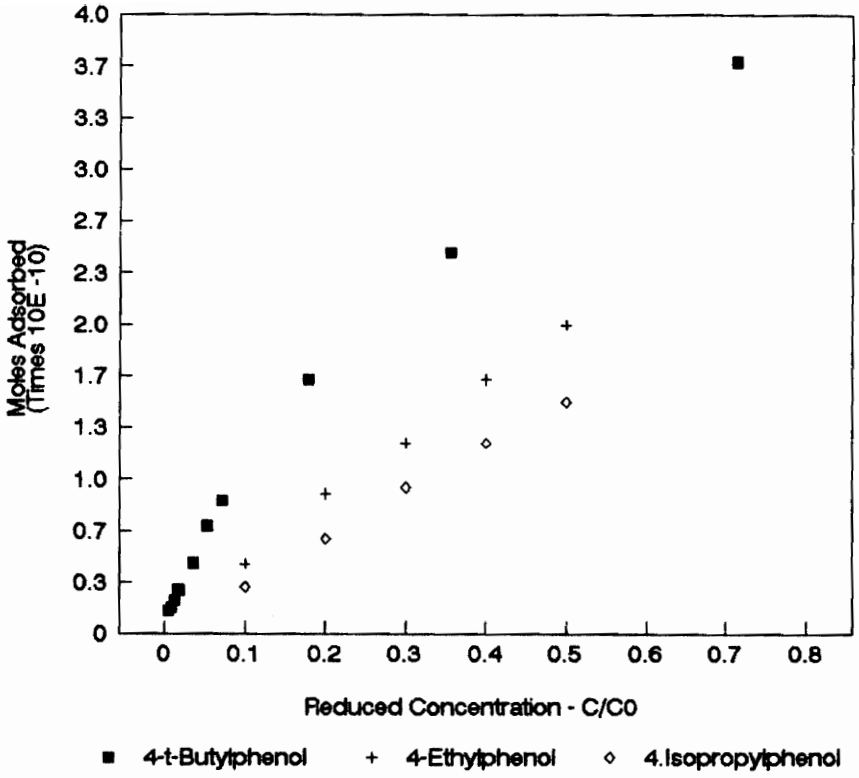

Figure 6.9 Isotherms for 4-t-butylphenol, 4-i-propylphenol, and 4-ethylphenol using a 4-amino-thiophenol modified crystal. Isotherms are plotted as a function of reduced concentration.

relative to previously described flow cells[52]. Reproducible oscillation behavior has been observed for the chemically modified crystals in contact with highly polar solvents under flowing conditions.

Definite surface interactions between solutes and the bonded phase have been demonstrated using a variety of solutes and surface modifiers. When chemically modified quartz crystals are used, the magnitude of the QCM signal has been shown to be a function of both the mass interaction at the crystal surface and of the bulk properties of the sample. At low solute concentration, the dominant contribution to the QCM response is from the mass interaction at the crystal surface. At higher solute concentrations, the QCM signal changes predominantly with respect to the changing bulk properties of the sample.

Several additional factors have been shown to effect the magnitude of the QCM response. For solutes that interact strongly with the modified crystal surface, the response is dependent on the carrier solvent flow rate. At very low flow rates, the residence time of the solute in the flow cell is sufficiently long for solute molecules to diffuse to the crystal surface and be adsorbed. At flow rates exceeding 150 μL per minute, the solute is apparently purged from the flow cell before a significant amount can diffuse to the bonded phase.

The chemical nature of the solute and the bonded phase also dramatically affect the magnitude of the QCM response. In general, the greatest responses were observed when electron pair donation between the solute and substrate was

possible. An exception to this generalization was found for the response of 4-nitrophenol using polar crystal modifiers. Although it would seem reasonable to expect strong electron donation between the solute and surface, the QCM response was generally weak. No satisfactory explanation for this behavior is currently available, although it has been noted in Chapter 4 that the material adjacent to the crystal must be a rigid, thin layer. It may be possible that 4-nitrophenol in aqueous solution does not meet this condition when interacting with polar crystal modifiers. Weak responses were generally observed where hydrophobic attraction was the dominant mode of surface interaction. Within a class of solutes, the QCM response was seen to increase strongly with the increasing size of the hydrophobic portion of the solute molecules. This is a manifestation of Traube's rule and is an indication of the relative solubility of the solutes in the particular solvent used. The QCM signal was shown to decrease with increasing solvent strength, but isotherms generated for a particular compound using various solvent compositions are superimposible when the amount of solute adsorbed is plotted versus reduced concentration. This is an indication that the strength of the solute-surface interaction is constant regardless of the solvent used. Isotherms generated for various compounds, having different free energies of adsorption, are not superimposible.

Finally, isotherms generated from the QCM response to various concentrations of substituted phenols have been observed to be of the L1 type

according to the Giles classification system. The isotherms can be fitted to a modified version of the Langmuir expression, with good agreement between the measured and calculated curves. Rearrangement of the Langmuir expression allows one to calculate the molar free energy of adsorption using data obtained from QCM measurements. Enthalpies and entropies can also be determined by the method presented assuming that some adequate means is available to control the temperature of the QCM. The molar free energy was evaluated for the adsorption of substituted phenols on 4-aminothiophenol modified crystals. For 4-t-butylphenol, the free energy of adsorption was determined using three solvent compositions and was found to be independent of solvent composition. The values obtained were consistent with the description of physisorption of analyte to the modified crystal surface through a lone electron pair interaction.

Chapter 7. Research Summary and Future Research Areas.

Two new detectors have been developed and characterized for use with flow injection analysis of HPLC. The first detector is a rapid scanning square wave voltammetric detector which employs a large diameter platinum disk indicator electrode in a wall-jet type electrochemical cell. The second detector is based on the mass sensitivity of the quartz crystal microbalance and employs chemically modified crystals in a low volume flow cell.

The SWV detector developed in this research represents a significant enhancement in the utility of electrochemical detection for liquid chromatography. It combines the ruggedness and ease of maintenance inherent in macroscopic electrodes with the high sensitivity normally associated with microelectrode based SWV cells. Analytical current is measured with respect to both time and potential, resulting in chromatographic data that is qualitatively superior to that which is obtainable by conventional electrochemical detection methods. Furthermore, The detector has been shown to be completely compatible with gradient elution separation methods. This is the first successful application of square wave voltammetry with analytical scale gradient elution HPLC. This combination has been shown to permit greater component resolution than is possible using previously developed electrochemical detection methods.

The development of new separation methods using gradient elution HPLC for the analysis of trace quantities of electroactive compounds is probably the most

promising area for future research involving the SWV detector. The technique should be particularly useful for environmental, biological, and other very complex samples for which high resolution and selective detection are requirements.

The quartz crystal microbalance detector was also originally intended for use with HPLC. Quartz crystals used in the QCM detector were chemically modified using existing procedures to produce homogeneous, reproducible, monolayer coatings capable of selective interaction with analytes. The magnitude of the QCM signal to a particular analyte was found to be influenced by several variables other than sample concentration. Among these variables are the density and viscosity of the sample, the solvent strength and solvent flow rate, the nature of the surface-solute interaction, and the structure of substituents on chemically related analytes.

Although the QCM was found to be a poor candidate for an HPLC detector, it was found to be useful for conducting surface adsorption studies. Langmuirian type isotherms can be generated from QCM data and the data can be used to calculate the thermodynamic quantities associated with solute adsorption.

A future area of research for the QCM detector will involve the tailoring of quartz crystals for more selective or specific analyte detection. This will involve the immobilization of chiral modifiers such as cyclodextrins and various enzymes for analyte determination via FIA. Controlled temperature surface adsorption studies

will allow the determination of enthalpies and entropies associated with the interactions of these coatings with analytes while using very limited sample quantities.

References.

1. P. T. Kissinger in *Laboratory Techniques In Electroanalytical Chemistry*, P. T. Kissinger and W. R. Heineman editors, Marcel Dekker, inc., New York, 1984.
2. P. T. Kissinger, C. S. Bruntlett, and R. E. Shoup, *Life Sci.*, **28**, 455, 1981.
3. P. T. Kissinger, K. Bratin, W. P. King, and J. R. Rice, *ACS Symp. Ser.*, **136**, 57, 1980.
4. *Recent Reports On Liquid Chromatography/ Electrochemistry*, R. E. Shoup, editor, BAS Press, West Lafayette, Ind., 1982.
5. K. Bratin and R. C. Briner, *Curr. Sep.*, **2**, 1, 1980.
6. W. R. Heineman and P. T. Kissinger, *Anal. Chem.*, **50**, 166R, 1978; and **52**, 138R, 1980.
7. D. L. Rabenstein and R. Saetre, *Anal. Chem.*, **49**, 1036, 1977.
8. W. P. King and P. T. Kissinger, *Clin. Chem.*, **26**, 1484, 1980.
9. R. Sammuelson, J. J. O'Dea, J. Osteryoung, *Anal. Chem.*, **52**, 2215-2216, 1980.
10. L. A. Knect, E. J. Guthrie, J. W. Jorgenson, *Anal. Chem.*, **56**, 479-482, 1982.
11. W. L. Caudill, A. G. Ewing, S. Jones, and R. M. Wightman, *Anal. Chem.*, **55**, 1877-1881, 1983.
12. M. Goto, and K. Shimada, *Chromatographia*, **21**, 631-634, 1986.

13. J. G. White, R. L. St. Clair, J. W. Jorgenson, *Anal. Chem.*, **58**, 293-298, 1986.

14. S. P. Kounaves and J. B. Young, *Anal. Chem.*, **61**, 1469-1472, 1989.

15. U. Tjaden and J. de Jong, *J.Liq.chromatogr.*, **6**, 2255-2274, 1983.

16. M. Hadj-Mohammadi, J. Ward and J. Dorsey, *J. Liq. Chromatogr.*, **6**, 511-526, 1983.

17. H. Gunasingham, B. Tay, K. Ang and L. Koh, *J. Chromatogr.*, **285**, 103-114, 1984.

18. F. Palmisano, P. Zambonin, A. Visconti and A. Bottalico, *Chromatographia*, **27**, 425-429,1989.

19. R. St. Claire III, G. Ansari and C. Abell, *Anal. Chem.*, **54**, 186-189, 1984.

20. A. Drumheller, H. Bachelard, S. St-Pierre and F. Jolicoeur, *J. Liq. Chromatogr.*, **8**, 1829-1843, 1985.

21. M. Khaledi and J. Dorsey, *Anal. Chem.*, **57**, 2190-2196, 1985.

22. P. Bedard and W. Purdy, *J. Liq. Chromatogr.*, **9**, 1971-1984, 1986.

23. M. Oates and J. Jorgenson, *Anal. Chem.*, **61**, 431-435, 1989.

24. M. Oates and J. Jorgenson, *Anal. Chem.*, **61**, 1977-1980, 1989.

25. B. Fleet and C. J. Little, *J. Chromatogr. Sci.*, **12**, 747-752, 1974.

26. J. O'M. Bockris and B. J. Yang, *J. Electroanal. Chem.*, **252**, 209-214, 1988.

27. R. J. Nichols and A. Bewick, *Electrochimica Acta*, **33**, 1691-1694, 1988.

28. J. K.Foley and S. Pons, *Anal. Chem.*, **57**, 945A-956A, 1985.

29. H. C. Pillsbury, C. C. Bright, K. J. O'Conner, and F. W. Irish, *J. Assoc. Off. Anal. Chem.*, **52**, 458-62, 1969.

30. M. Stastny, R. Volf, H. Benadikiva and I. Vit, *J. Chromatogr. Sci.*, **21**, 18-24, 1983.

31. K. Stulik and V. Pacakova, *CRC Crit. Rev. Anal. Chem.*, **14**, 297, 1984.

32. R. J. Rucki, *Talanta*, **27**, 147,1980.

33. W. P. Mason, *Piezoelectric Crystals and Their Application To Ultrasonics*, Van Nostrand, New York, 1956.

34. G. Sauerbrey, *Z. Phyzik*, **155**, 206, 1959.

35. *R. D. Mindlin and Applied Mechanics*, G. Herrmann editor, Pergamon Press, New York, 1974.

36. C. Lu and O. Lewis, *J. Appl. Phys.*, **43**, 4385, 1972.

37. K. K. Kanazawa, J. G. Gordon, *Anal. Chem.*, **57**, 1771-1772, 1985.

38. K. K. Kanazawa, J. G. Gordon, *Anal. Chim. Acta*, **175**, 99-105, 1985.

39. S. Bruckenstein, M. Shay, *Electrochim. Acta*, **30**, 1295-1300, 1985.

40. H. E. Hager, *Chem. Eng. Commun.*, **43**, 25-38, 1986.

41. H. Muramatsu, E. Tamiya, I. Karube, *Anal. Chem.*, **60**, 2142-2146, 1988.

42. T. Nomura, M. Okuhara, *Anal. Chim. Acta*, **142**, 281-284, 1982.

43. S. Z. Yao, T. A. Zhou, *Anal. Chim. Acta*, **212**, 61-72, 1988.

44. K. S. Dyke, U. S. Patent 257,171, July 4, 1945.

45. P. Oberg and J. Longensjo, *Rev. Sci. Instr.*, **30**, 1053, 1959.

46. L. J. Slutsky and W. H. Wade, *J. Chem. Phys.*, **36**, 2688-92, 1962.

47. W. H. King, *Anal. Chem.*, **36**, 1735-1739, 1964.

48. L. M. Webber, J. Hlavay, and G. G. Guilbalt, *Mikrochim. Acta*, **1**, 351, 1978.

49. G. G. Guilbalt, *Anal. Proc.*, **19**, 68, 1982.

50. J. Hlavay and G. G. Guilbalt, *Anal. Chem.*, **49**, 1890, 1977.

51. G. G. Guilbalt, *Ion Sel. Electrode Rev.*, **2**, 3, 1980.

52. J. M. Charlesworth, *Anal. Chem.*, **62**, 76-81, 1990.

53. P. L. Konash, G. J. Bastiaans, *Anal. Chem.*, **52**, 1929-1931, 1980.

54. M. R. Deakin and D. A. Buttry, *Anal. Chem.*, **61**, 1147A - 54A, 1989.

55. J. P. Mieure and J. L. Jones, *Talanta*, **16**, 149-50, 1969.

56. S. Bruckenstein and S. Swathirajan, *Electrochimica Acta*, **30**, 851, 1985.

57. M. R. Deakin and O. Melroy, *J. Electroanal. Chem.*, **239**, 321, 1988.

58. B. Feldman and O. Melroy, *J. Eelctroanal. Chem.*, **234**, 213, 1987.

59. S. Bruckenstein, C. Wilde, M. Shay, A. Hillman, and D. Loveday, *J. Electroanal. Chem.*, **258**, 457, 1989.

60. S. Lasky and D. A. Buttry, *J. Am. Chem. Soc.*, **110**, 6258, 1988.

61. T. Nomura, T. Okuhara, T. Hasegawa, *Anal. Chim. Acta*, **183**, 261-265, 1986.

62. T. Nomura, M. Sakai, *Anal. Chim. Acta*, **183**, 301-305, 1986.

63. T. Nomura, M. Ando, *Anal. Chim. Acta*, **172**, 353-357, 1985.

64. Y. Okahata, H. Ebatao, K. Taguchi, *J. Chem. Soc., Chem. Commun.*, 1363-67, 1987.

65. R. Murray in *Electroanalytical Chemistry,* A. J. Bard editor, **13**, 191-368, Marcel Dekker, New York, 1984.

66. C. H. Giles, T. H. MacEwan, S. N. Nakhwa, and D. Smith. *J. Chem. Soc.*, London, 3973, 1960.

67. C. H. Giles, D. Smith, and A. Huitson. *J. Colloid and Interface Sci.*, **47**, 755-765, 1974.

68. C. H. Giles, A. P. D'Silva, and I. A. Easton, *J. Colloid and Interface Sci.*, **47**, 766- 78, 1974.

69. E. B. Troughton, *Langmuir,* **4**, 365-385, 1988.

70. L. Sun, R. C. Thomas, and R. M. Crooks, *J. Am. Chem. Soc.*, **113**, 8550-8552, 1991.

71. *Ionization Constants of Organic Acids In Aqueous Solution,* IUPAC Chemical Data Series No. 23, Pergamon Press, New York, 1979.

72. *Dissociation Constants of Organic Bases In Aqueous Solution,* IUPAC, Butterworth & Co. Ltd., London, 1965.

73. A. W. Adamson, *Physical Chemistry of Surfaces*, 4th edition, John Wiley & Sons, 1982.

74. P. W. Atkins, *Physical Chemistry,* W. H. Freeman and Co., San Francisco, 1978.

Appendix A.

SWV Data Acquisition Program (SQ-WAVE.BAS)

Written and Compiled in Microsoft QuickBASIC v. 4.5

```
DECLARE SUB FRAME()
DECLARE SUB DATAGET()
DECLARE SUB TIMEBASE()
DECLARE SUB NUMOFPOINTS()
DECLARE SUB GETPARAMETERS()
DECLARE SUB WAITING()
DECLARE SUB GPIB(PSTAT%, WRT$)

COMMON SHARED F, I, INC, C, R, T, T1, T2, N1, SCANS,
COMMON SHARED CURVE$, A%(), PA%()

REM $INCLUDE: 'C:\MC-GPIB\QBDECL4.BAS'

DIM A%(6144), PA%(900)

SCREEN 9
COLOR 14,1
CLS

CALL FRAME
LOCATE 12,20: PRINT "SQUARE WAVE VOLTAMMETRIC LC
DETECTION"

UDNAME$ = "PSTAT" : CALL IBFIND(UDNAME$, PSTAT%)
FOR Z=1 TO 15
      CALL WAITING
NEXT Z

CLS
CALL FRAME
LOCATE 12, 25: PRINT " SENDING COMMANDS TO M273..."
FOR Z=1 TO 5
      CALL WAITING
NEXT Z

WRT$ = "AR 0": CALL GPIB(PSTAT%, WRT$)
WRT$ = "MM 2": CALL GPIB(PSTAT%, WRT$)
WRT$ = "MR 2": CALL GPIB(PSTAT%, WRT$)
WRT$ = "INTRP 0": CALL GPIB(PSTAT%, WRT$)
WRT$ = "DCV 0": CALL GPIB(PSTAT%, WRT$)
WRT$ = "SCV 2": CALL GPIB(PSTAT%, WRT$)
WRT$ = "AUXGAIN 1": CALL GPIB(PSTAT%, WRT$)
```

```
WRT$ = "EGAIN 1": CALL GPIB(PSTAT%, WRT$)
WRT$ = "IGAIN 1": CALL GPIB(PSTAT%, WRT$)
WRT$ = "ISUP 0": CALL GPIB(PSTAT%, WRT$)
WRT$ = "MODE 2": CALL GPIB(PSTAT%, WRT$)

CALL GETPARAMETERS
WRT$ = "FP 0": CALL GPIB(PSTAT%, WRT$)

N = ABS(F - I) * 2 / INC) + 2
IF N > 997 THEN CALL NUMOFPOINTS

N1 = INT(N)
WRT$ = "LP " +STR$(N1 - 1) : CALL GPIB(PSTAT%, WRT$)
WRT$ = "FLT 0": CALL GPIB(PSTAT%, WRT$)
WRT$ = "I/E " + STR$(R) : CALL GPIB(PSTAT%, WRT$)
WRT$ = "SIE 1" : CALL GPIB(PSTAT%, WRT$)

            '---PULSE HEIGHT, DAC COUNTS
P = ABS(P)
P1 = P * 4
IF F< I THEN P1 = -P1

            '---SCAN INCREMENT DAC COUNTS
INC = ABS(INC)
INC1 = INC * 4
IF F < I THEN INC1 = -INC1

            '---TIMEBASE (TMB), SAMPLES/POINT (S/P)
            '---AND FREQUENCY (= 1/(TMB*INC/(P*2))
T2 = 1
T1 = 500000! / T / 2 / T2
CALL TIMEBASE
WRT$ = "TMB " + STR$(T1) : CALL GPIB(PSTAT%, WRT$)
WRT$ = "PCV 2" : CALL GPIB(PSTAT%, WRT$)
WRT$ = "CLR" : CALL GPIB(PSTAT%, WRT$)

            '---CALCULATE WAVE FORM AND SEND TO
POTENTIOSTAT.
CLS
CALL FRAME
LOCATE 12,25: PRINT "DOWN LOADING THE SOURCE CURVE..."
```

```
PA%(0) = I * 4
PA%(1) = (I * 4) + P1
PA%(2) = (I * 4) - P1

FOR X = 0 TO 2
WRT$ = "LC " + STR$(X) + "1 " + STR$(PA%(X))
CALL GPIB(PSTAT%, WRT$)
NEXT X

DIM V(N1)
FOR X = 3 TO N1
PA%(X) = PA%(X - 2) + INC1
WRT$ = "LC " + STR$(X) + "1 " +STR$(PA%(X))
CALL GPIB(PSTAT%, WTR$)
NEXT X

MILLIVOLT$ = "D:MILLIVOLT.DAT"
OPEN MILLIVOLT$ FOR OUTPUT AS #5
X=1
DO WHILE X <= N1
V(X) = PA%(X) / 4
PRINT #5, V(X)
X = X + 2
LOOP
CLOSE #5

WRT$ = "BIAS " + STR$(I * 4) : CALL GPIB(PSTAT%, WRT$)
WRT$ = "PAM 0" : CALL GPIB(PSTAT%, WRT$)
WRT$ = "SAM 1" : CALL GPIB(PSTAT%, WRT$)
WRT$ = "BW 0" : CALL GPIB(PSTAT%, WRT$)
WRT$ = "S/P " + STR$(T2) : CALL GPIB(PSTAT%, WTR$)


SUB DATAGET
DIM A2(N1), D(INT(N1 / 2)), B#(N1), BG#(N1), PA#(N1)
BLANK$ = STRING$(50, " ")
SOLVENT$ = "C:\QB45\SOLVENT.DAT"
TIMEKEEP$ = "D:TIMEKEEP.DAT"
OPEN TIMEKEEP$ FOR APPEND AS #3
CLOSE #3

WRT$ = "DCV 0" : CALL GPIB(PSTAT%, WRT$)
```

```
WRT$ = "PCV 0" : CALL GPIB(PSTAT%, WRT$)
WRT$ = "CLR" : CALL GPIB(PSTAT%, WRT$)

CLS CALL FRAME
LOCATE 12, 25 : PRINT BLANK$
LOCATE 12, 25 : PRINT "INJECT SAMPLE AND STRIKE <ENTER> ..."
DO
LOOP UNTIL INKEY$ = CHR$(13)
LOCATE 12,25 : PRINT BLANK$
LOCATE 12,25 : PRINT "COLLECTING DATA FILE..."
FOR X = 1 TO 4
CALL WAITING
NEXT X

WRT$ = "CELL 1" : CALL GPIB(PSTAT%, WRT$)
OPEN TIMEKEEP$ FOR OUTPUT AS #3
DURVE$ = "D:DATA"
OPEN DURVE$ FOR APPEND AS #1
CLS



''''''''''''''''''''''''''''''''''''''''''''''DATACOLLECTION ROUTINE''''''''''''''''''''''''
''''''''''''''''''''''''''''''''''''''''''''''''''''''''''''''''''''''''''''''''''''''''''''''''

FOR SCNNUMBER% = 1 TO SCANS
WRT$ = "NC" : CALL GPIB(PSTAT%, WRT$)
WRT$ = "TC" : CALL GPIB(PSTAT%, WRT$)
WAITINTERVAL = INT(12 * (N1 / 100) * (5 / T))
FOR X = 1 TO WAITINTERVAL
CALL WAITING
NEXT X

IF SCNNUMBER% = 8 THEN SECOND1# = TIMER
IF SCNNUMBER% >= 8 THEN
SECOND# = (TIMER - SECOND1#)
PRINT #3, SECOND#
LOCATE 25,15 : PRINT "SCAN # "; SCNNUMBER%; "TIME "; SECOND#
END IF

WRT$ = "DC 0 " + SRT$(N1) : CALL GPIB(PSTAT%, WRT$)
SLICE$ = "D:SLICE"
```

```
UDNAME$ = "PSTAT" : CALL IBFIND(UDNAME$, PSTAT%)
RD$ = SPACE$(N1 * 6)
CALL IBRD(PSTAT%, RD$)
OPEN SLICE$ FOR OUTPUT AS #2
PRINT #2, RD$
CLOSE #2

IF SCNNUMBER% = 7 THEN
BG$ = "D:BG$"
OPEN BG$ FOR OUTPUT AS #4
OPEN SLICE$ FOR INPUT AS #2
FOR I% = 1 TO N1
LINE INPUT #2, RD1$
BG#(I%) = VAL(RD1$)
PRINT #4, BG#(I%)
NEXT I%
CLOSE #2, #4
END IF

IF SCNNUMBER# >= 8 THEN
BG$ = "D:BG$"
OPEN BG$ FOR INPUT AS #4
OPEN SLICE$ FOR INPUT AS #2
FOR I% = 0 TO N1 - 1
LINE INPUT #2, P1$
LINE INPUT #4, BG$
B#(I%) = (VAL(P1))
BG#(I%) = (VAL(BG$))
NEXT I%
FOR I% = 2 TO N1 - 3
BG#(I%) = (BG#((I% - 2) + BG#(I%) + BG#(I% + 2)) / 3
PA#(I%) = (B#(I% - 2) + B#(I%) + B#(I% + 2)) / 3
A%(I%) = (PA#(I%) - BG#(I%))
NEXT I%
CLOSE #2, #4
END IF

N2 = INT((N1 - 3) / 2)
IF SCMNNUMBER% >= 8 THEN
FOR I = 7 TO N2
A2#(I) = ((A%(2 * I) - A%(2 * I - 1)))
D(I) = A2#(I)
```

```
IF SCNNUMBER% >= 8 AND I >= 8 AND I <= N2 -3 THEN
PRINT #1, D(I)

LINE (((1250/N1) * (I-1)), -D(I-1) + 250)
                                    - (((1250/N1) * I), -D(I) + 250)
END IF
NEXT I

END IF
NEXT SCNNUMBER%

WRT$ = "CELL 0" : CALL GPIB(PSTAT%, WRT$)
CLOSE #1, #3
```

ASSEMBLY OF DATA FILE

```
''''''''''''''''''''''''''''''''''''''''''''''''''''''''''''''''''''''''''''''''''''''''''''''''''''''
MILIVOLT$ = "D:MILIVOLT.DAT"
COMPILE$ = "C:\" + CURVE$
OPEN TIMEKEEP$ FOR INPUT AS #3
OPEN COMPILE$ FOR APPEND AS #4
OPEN DURVE$ FOR INPUT AS #1
FOR Y = 8 TO SCANS
LINE INPUT #3, SECOND$
SECOND# = VAL(SECOND$)
OPEN MILIVOLT$ FOR INPUT AS #5
FOR X = TO N2 - 3
LINE INPUT #5, VOLT$
VOLT# = VAL(VOLT$)
IF X >= 8 THEN
LINE INPUT #1,POINT$
ROUGH# = VAL(POINT$)
PRINT #4, USING "#######.##"; VOLT#; SECOND#; ROUGH#
END IF
NEXT X
CLOSE #5
NEXT Y
CLOSE #1, #3, #4
KILL DURVE$, TIMEKEEP$

SCREEN 0
```

```
END SUB


SUB FRAME
TR = 2
BR = 24
LC = 3
RC = 78
BLANK$ = STRING$(80, " ")
LOCATE 1 : PRINT BLANK$
LOCATE 25 :PRINT BLANK$
LOCATE TR, LC : PRINT CHR$(201)
LOCATE TR, RC : PRINT CHR$(187)
LOCATE BR, LC : PRINT CHR$(200)
LOCATE BR, RC : PRINT CHR$(188)

FOR VERTLINE% = TR + 1 TO BR - 1
LOCATE VERTLINE%, LC : PRINT CHR$(186)
LOCATE VERTLINE%, RC : PRINT CHR$(186)
NEXT VERTLINE%

HORIZLENGTH% = RC - LC - 1
HORIZLINE$ = STRING$(HORIZLENGTH%, 205)
LOCATE TR, LC : PRINT HORIZLINE$
LOCATE BR, LC : PRINT HORIZLINE$;
END SUB


SUB GETPARAMETERS
CLS
CALL FRAME
LOCATE 4, 15 :PRINT "INITIAL E (+/- 1900 mV) ==> "; INPUT I
LOCATE 6, 15 :PRINT "FINAL E (+/- 1900 mV) ==> "; INPUT F
LOCATE 8, 15 :PRINT "SCAN INCREMENT (1 TO 20 mV) ==> ";
INPUT INC
LOCATE 10, 15:PRINT "PULSE HEIGHT (1 TO 100 mV) ==> ";
INPUT P
LOCATE 12, 15 :PRINT "FREQUENCY (1 TO 100 Hz) ==> "; INPUT T
LOCATE 14, 15 :PRINT "CURRENT RANGE EXPONENT (0 TO -7) ==> ";
INPUT R
LOCATE 18, 15 :PRINT "HOW MANY SCANS FOR THIS ANALYSIS ==>";
INPUT SCANS
```

```
LOCATE 22, 15 :PRINT "FILE NAME FOR THIS DATA SET ==> ";
INPUT CURVE$

END SUB

SUB GPIB(PSTAT%, WRT$) STATIC
CALL WAITING
CALL IBWRT(PSTAT%, WRT$)
END SUB

SUB NUMOFPOINTS
N = ABS((F - I) * 2 / (INC + 2))
DO WHILE N > 997
CLS
CALL FRAME
LOCATE 12, 22 :PRINT "ERROR! MORE THAN 1024 DATA POINTS!"
FOR Z = 1 TO 10
CALL WAITING
NEXT Z
CALL GETPARAMETERS
N = ABS((F - I) * 2 / (INC + 2))
LOOP
END SUB


SUB TIMEBASE
IF T1 > 10000 THEN
DO WHILE T1 > 10000
T2 = T2 + 1
T1 = 500000! / T / 2 / T2
LOOP
END IF
END SUB


SUB WAITING
FOR Z = 1 TO 3500
W = Z
NEXT Z
END SUB
```

Appendix B.

Amperometric Data Acquisition Program (AMP-LC.BAS)
Written and Compiled in Microsoft QuickBASIC v. 4.5

```
DECLARE SUB FRAME()
DECLARE SUB DATAGET()
DECLARE SUB TIMEBASE()
DECLARE SUB NUMOFPOINTS()
DECLARE SUB GETPARAMETERS()
DECLARE SUB WAITING()
DECLARE SUB GPIB(PSTAT%, WRT$)

COMMON SHARED F, I, R, T, T1, T2, N1,
COMMON SHARED CURVE$, A%(), PA%(), BOX#, LASTTYME#

REM $INCLUDE: 'C:\MC-GPIB\QBDECL4.BAS'

DIM A%(6144), PA%(900)

SCREEN 9
COLOR 14,1
CLS

CALL FRAME
LOCATE 12,20: PRINT "AMPEROMETRIC LC DETECTION"

UDNAME$ = "PSTAT" : CALL IBFIND(UDNAME$, PSTAT%)
FOR Z=1 TO 15
      CALL WAITING
NEXT Z

CLS
CALL FRAME
LOCATE 12, 25: PRINT " SENDING COMMANDS TO M273..."
FOR Z=1 TO 5
      CALL WAITING
NEXT Z

WRT$ = "AR 0": CALL GPIB(PSTAT%, WRT$)
WRT$ = "MM 2": CALL GPIB(PSTAT%, WRT$)
WRT$ = "MR 2": CALL GPIB(PSTAT%, WRT$)
WRT$ = "INTRP 0": CALL GPIB(PSTAT%, WRT$)
WRT$ = "DCV 0": CALL GPIB(PSTAT%, WRT$)
WRT$ = "SCV 2": CALL GPIB(PSTAT%, WRT$)
WRT$ = "AUXGAIN 1": CALL GPIB(PSTAT%, WRT$)
WRT$ = "EGAIN 1": CALL GPIB(PSTAT%, WRT$)
```

```
WRT$ = "IGAIN 1": CALL GPIB(PSTAT%, WRT$)
WRT$ = "ISUP 0": CALL GPIB(PSTAT%, WRT$)
WRT$ = "MODE 2": CALL GPIB(PSTAT%, WRT$)

CALL GETPARAMETERS
WRT$ = "FP 0": CALL GPIB(PSTAT%, WRT$)

WRT$ = "LP 4" : CALL GPIB(PSTAT%, WRT$)
WRT$ = "FLT 1" : CALL GPIB(PSTAT%, WRT$)
WRT$ = "I/E " + STR$(R) : CALL GPIB(PSTAT%, WRT$)
WRT$ = "SIE 1" : CALL GPIB(PSTAT%, WRT$)
WRT$ = "PCV 2" : CALL GPIB(PSTAT%, WRT$)
WRT$ = "CLR" : CALL GPIB(PSTAT%, WRT$)

CLS
CALL FRAME
LOCATE 12, 25 : PRINT "DOWN LOADING THE SOURCE CURVE..."
FOR I = 0 TO 4
PA%(I) = 2400
WRT$ = "LC " + STR$(I) + "1 " + STR$(PA%(I))
NEXT I

WRT$ = "PAM 0" : CALL GPIB(PSTAT%, WRT$)
WRT$ = "SAM 1" : CALL GPIB(PSTAT%, WRT$)
WRT$ = "BW 0" : CALL GPIB(PSTAT%, WRT$)
WRT$ = "S/P 1" : CALL GPIB(PSTAT%, WRT$)
CALL DATAGET



SUB DATAGET
BLANK$ = STRING$(50, " ")
WRT$ = "DCV 0" : CALL GPIB(PSTAT%, WRT$)
WRT$ = "PCV 0" : CALL GPIB(PSTAT%, WRT$)
WRT$ = "CLR" : CALL GPIB(PSTAT%, WRT$)

CLS
CALL FRAME
LOCATE 12, 25 : PRINT BLANK$
LOCATE 12,25 : PRINT "INJECT SAMPLE AND STRIKE <ENTER>...";
DO
LOOP UNTIL INKEY$ = CHR$(13)
```

```
LOCATE 12, 25 : PRINT BLANK$
LOCATE 12, 25 : PRINT "COLLECTING DATA FILE..."
FOR X = 1 TO 4
CALL WAITING
NEXT X

WRT$ = "CELL 1" : CALL GPIB(PSTAT%, WRT$)
W = 1
DURVE$ = "D:DATA"
OPEN DURVE$ FOR APPEND AS #1
SECOND1# = TIMER
DIM SAMPCURR#(BOX#), CHROM#(2000), MIN#(2000)
REFCURR# = 0
REP = 1
TYME# = 0
POINT$ = "D:POINT.DAT"
LCSUM# = 0
UCSUM# = 0
DIM LC(BOX#), UC(BOX#)
CLS

''''''''''''''''''''''''''''''''''''''''''''''DATACOLLECTION ROUTINE''''''''''''''''''''''
''''''''''''''''''''''''''''''''''''''''''''''''''''''''''''''''''''''''''''''''''''''''''''''''''''''''''''''''''''''''''''''''

DO UNTIL TYME# >= LASTTYME#
WRT$ = "NC" : CALL GPIB(PSTAT%, WRT$)
WRT$ = "TC" : CALL GPIB(PSTAT%, WRT$)
TYME# = (TIMER - SECOND1#) / 60
WRT$ = "DC 0, 5" : CALL GPIB(PSTAT%, WRT$)
UDNAME$ = "PSTAT" : CALL IBFIND(UDNAME$, PSTAT%)
RD$ = SPACE$(100) : CALL IBRD(PSTAT%, RD$)
OPEN POINT$ FOR OUTPUT AS #2
PRINT #2, RD$
CLOSE #2

OPEN POINT$ FOR INPUT AS #2
FOR X = 1 TO BOX#
LINE INPUT #2, UC$
UC(X) = VAL(UC$)
UCSUM# = UCSUM# + UC(X)
NEXT X
CLOSE #2
```

```
C# = (UCSUM#) / BOX#
UCSUM# = 0
IF TYME# >= 1.1 AND TYME <= 1.33 THEN
REFCURR# = REFCURR# +C#
REP = REP +1
END IF

RC# = (REFCURR# / REP)
SAMPCURR# = C# - RC#

IF TYME# >= 1.33 THEN

PRINT #1, USING "#######.##"; TYME#; SAMPCURR#
MIN#(W) = TYME#
CHROM#(W) = SAMPCURR#
LOCATE 1, 30 : PRINT " TIME "; USING "###.##"; TYME#
PSET(15 * (MIN#(W) - 1.33), CHROM#(W) + 200)
END IF
W = W + 1
END IF
LOOP
CLOSE #1


''''''''''''''''''''''''''''''''''''''''''''''''DATAFILE ASSEMBLY ROUTINE''''''''''''''''''''''''
''''''''''''''''''''''''''''''''''''''''''''''''''''''''''''''''''''''''''''''''''''''''''''''''''''''''''''''''''''''''''''''''

COMPILE$ = "C:\" + CURVE$
OPEN COMPILE$ FOR APPEND AS #4
OPEN DURVE$ FOR INPUT AS #1
DO UNTIL EOF(1)
LINE INPUT #1, DATA$
PRINT #4, DATA$
LOOP
CLOSE #1, #4
KILL DURVE$
SCREEN 0
END SUB



SUB FRAME
TR = 2
```

```
BR = 24
LC = 3
RC = 78
BLANK$ = STRING$(80, " ")
LOCATE 1 : PRINT BLANK$
LOCATE 25 :PRINT BLANK$
LOCATE TR, LC : PRINT CHR$(201)
LOCATE TR, RC : PRINT CHR$(187)
LOCATE BR, LC : PRINT CHR$(200)
LOCATE BR, RC : PRINT CHR$(188)

FOR VERTLINE% = TR + 1 TO BR - 1
LOCATE VERTLINE%, LC : PRINT CHR$(186)
LOCATE VERTLINE%, RC : PRINT CHR$(186)
NEXT VERTLINE%

HORIZLENGTH% = RC - LC - 1
HORIZLINE$ = STRING$(HORIZLENGTH%, 205)
LOCATE TR, LC : PRINT HORIZLINE$
LOCATE BR, LC : PRINT HORIZLINE$;
END SUB



SUB GETPARAMETERS
CLS
CALL FRAME
LOCATE 4, 15 : PRINT "ELECTRODE POTENTIAL = +0.600 V";
LOCATE 6, 15 : PRINT "NUMBER OF POINTS PER BOXCAR = 5";
BOX# = 5
LOCATE 12, 15 : PRINT "CURRENT RANGE EXPONENT (0 TO -7) ==> ";
INPUT R
LOCATE 18, 15 : PRINT "HOW LONG WILL THE ANALYSIS BE
(MINUTES)                                    ==> "; INPUT LASTTYME#
LOCATE 22, 15 : PRINT "ENTER THE DATA FILE NAME ==> ";
INPUT CURVE$
END SUB



SUB GPIB(PSTAT%, WRT$) STATIC
```

```
CALL WAITING
CALL IBWRT(PSTAT%, WRT$)
END SUB


SUB WAITING
FOR Z = 1 TO 2500
W = Z
NEXT Z
END SUB
```

Appendix C

Amperometric Data Smoothing Routine (BOXCAR.BAS)
Written and Compiled in Microsoft QuickBASIC ver. 4.5

```
CLS
LOCATE 10, 10: PRINT "THIS PROGRAM IS INTENDED TO SMOOTH
DATA BY BOX CAR AVERAGING"
LOCATE 11, 10: PRINT "NAME OF THE ANALYTICAL CURRENT DATA
FILE ==> ";
INPUT CURFILE$
LOCATE 12, 10:PRINT "NAME OF THE TIME DATA FILE ==> ";
INPUT TIMFILE$
LOCATE 13, 10:PRINT "NAME OF THE OUTPUT (TIME/CURRENT) FILE
==> ";
INPUT OUTFILE$

DIM TIM(2000), CUR(2000)
SCREEN 9

OPEN CURFILE$ FOR INPUT AS #1
OPEN TIMFILE$ FOR INPUT AS #2
OPEN OUTFILE$ FOR OUTPUT AS #3
X = 1
CURRENT = 0

DO UNTIL EOF(1)
LINE INPUT #1, CURDAT$
CUR(X) = VAL(CURDAT$)

LINE INPUT #2, TIMDAT$
TIM(X) = VAL(TIMDAT$)

X = X + 1

IF X >= 21 THEN
        FOR Z = X-20 TO X
        CURRENT = CURRENT + CUR(Z)
        NEXT Z
        CUR(X-10) = CURRENT / 21
        PRINT #3, USING "###.#######"; TIM(X-10); CUR(X-10)
        PSET (20 * TIM(X-10), -(5 * CUR(X-10)) + 150)
        CURRENT = 0
END IF
IF EOF(1) THEN EXIT DO
LOOP
CLOSE #1, #2, #3
```

APPENDIX D

Electrochemical Data For The SWV Detector

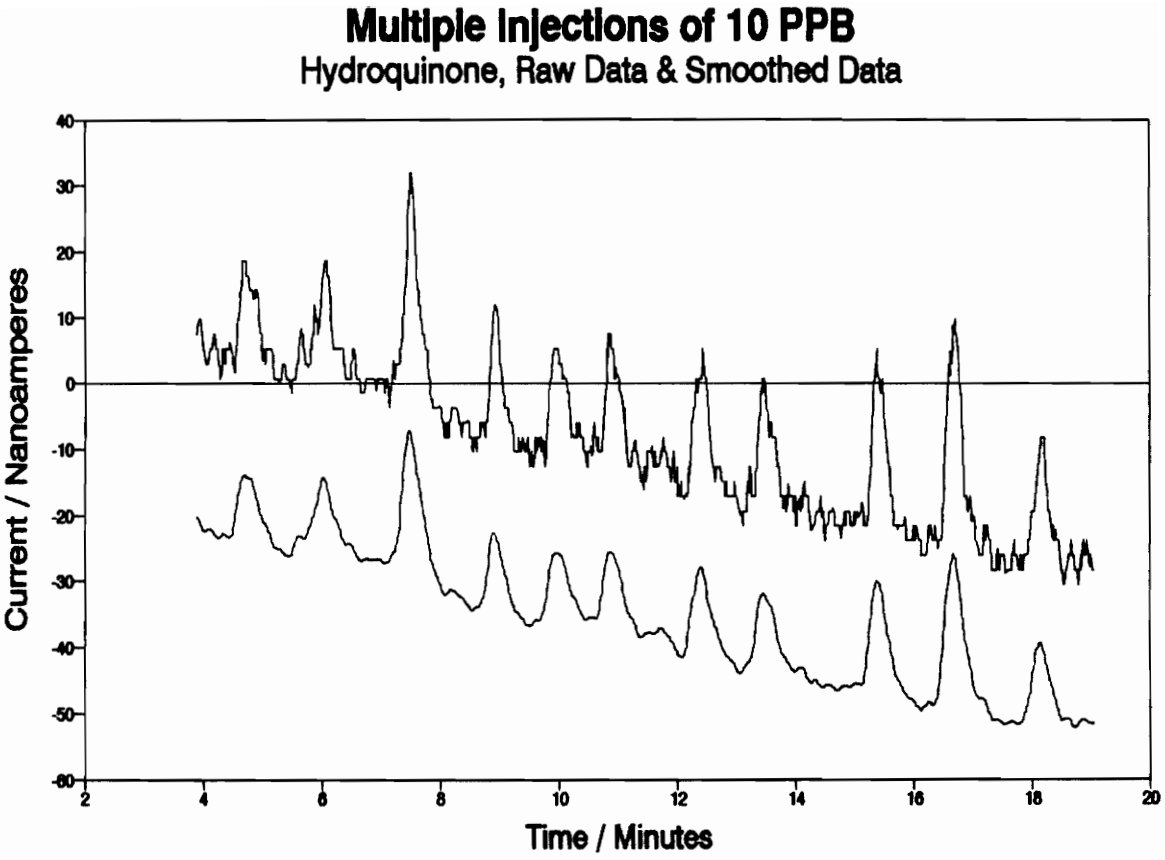

Smoothed Data Set Was Used For MDQ Calculation.
Mean Noise Value = 0.80 nA
Mean Peak Height = 14.3 nA
Std. Dev. Peak Height = 4.2 nA
RSD = 30%
N = 11
Mean S/N = 17.9
MDQ = 17 pg

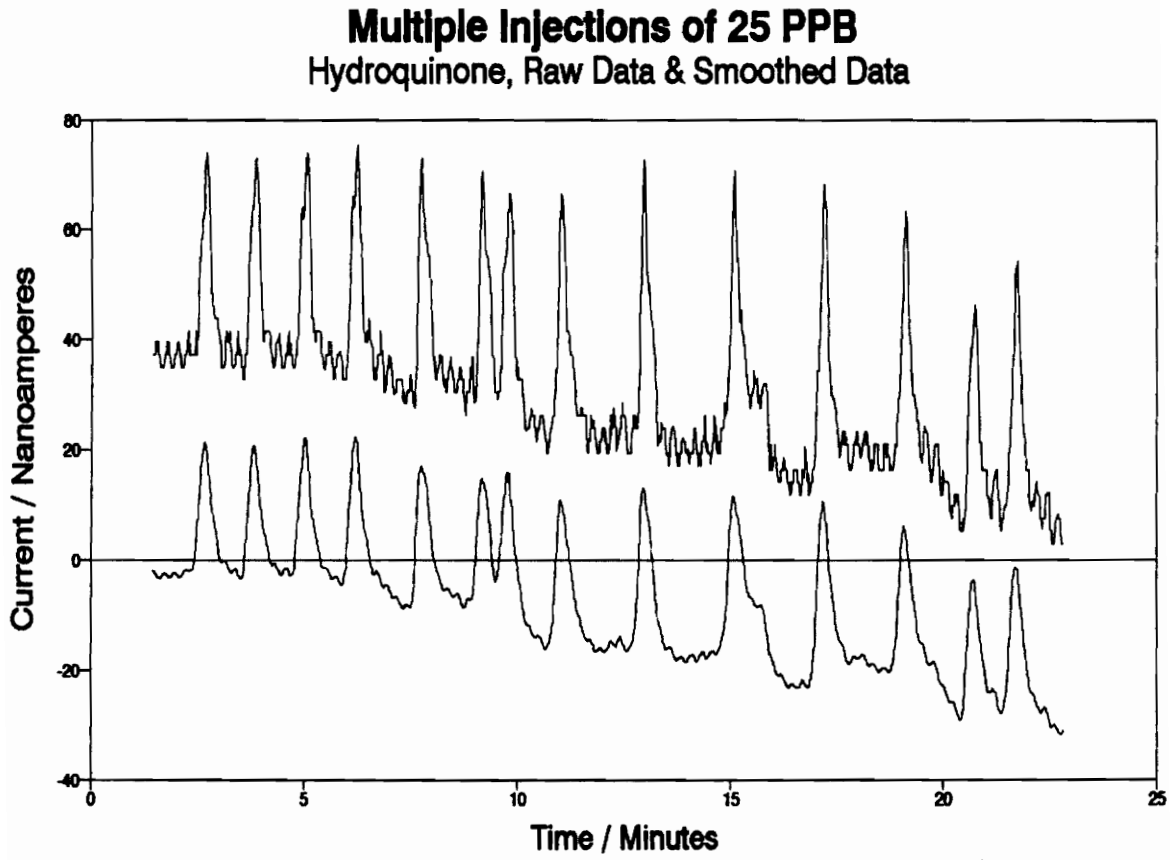

Smoothed Data Set Was Used For MDQ Calculations
Mean Noise Value = 0.75 nA
Mean Peak Height = 26.0 nA
Std. Dev. of Peak Height = 2.5 nA
RSD = 9.5%
N = 13
Mean S/N = 34.7
MDQ = 22 pg

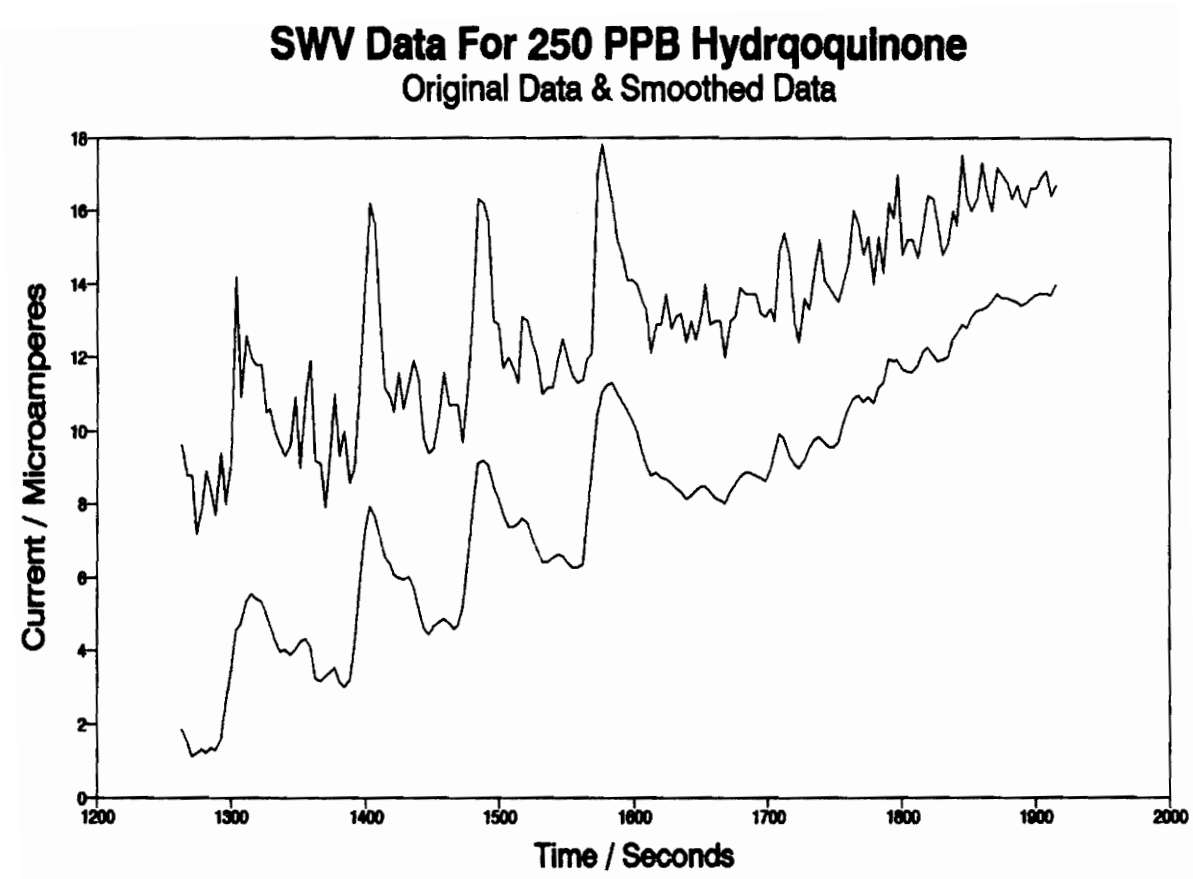

Smoothed Data Set Was Used For MDQ Calculation
Mean Noise Value = 570 nA
Mean Peak Height = 4550 nA
Std. Dev. of Peak Height = 665 nA
RSD = 14.6%
N = 4
Mean S/N = 8
MDQ = 940 pg

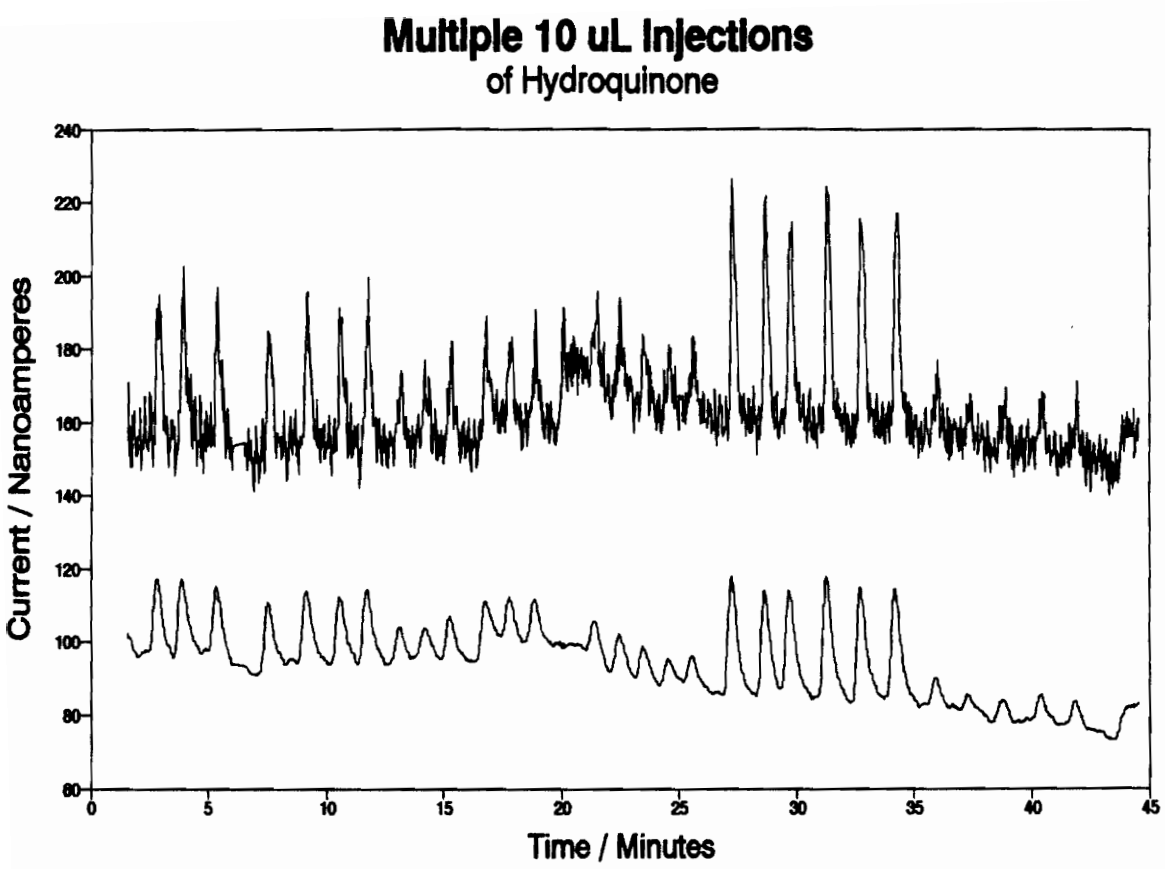

Smoothed Data Set Used For Linear Dynamic Range Measurement
Sample Concentration (Left to Right)
25 ppb X 7 injections
10 ppb X 6 injections
5 ppb X 5 injections
50 ppb X 6 injections
5 ppb X 5 injections

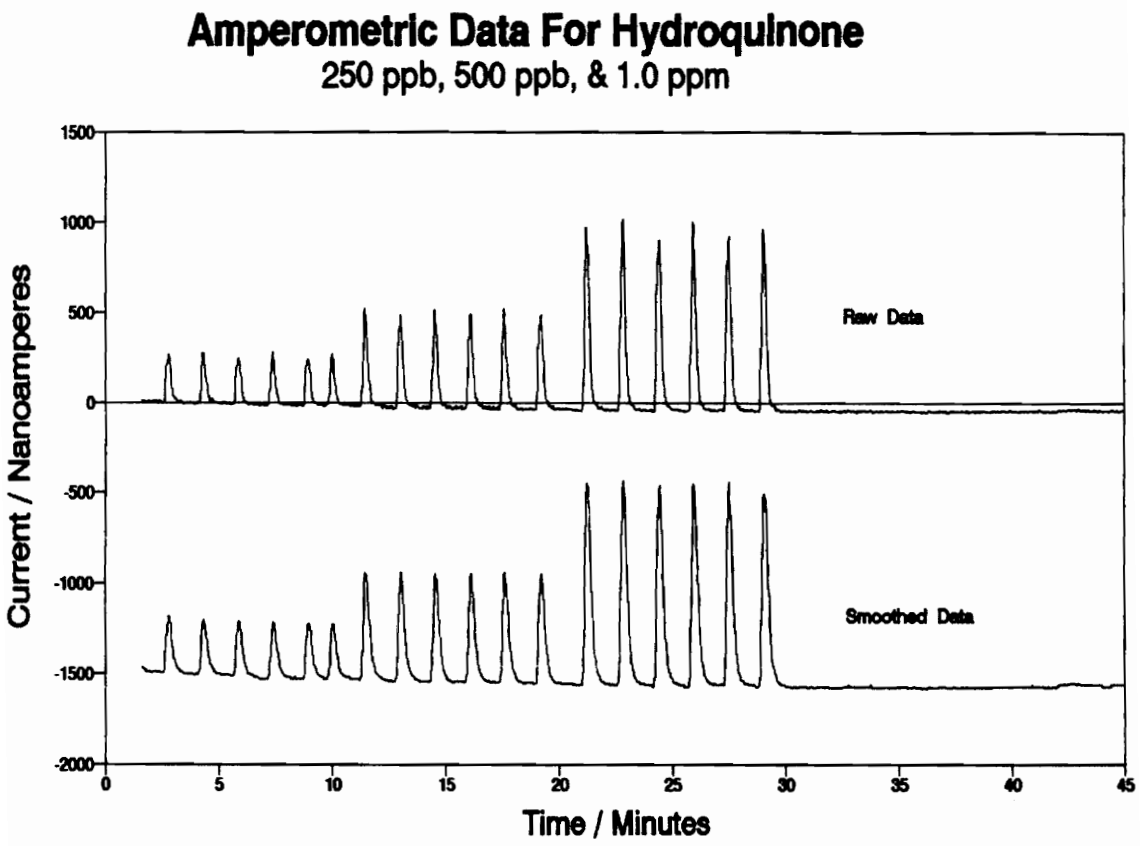

Data Set Used For Linear Dynamic Range Measurement
Sample Concentration (Left to Right)
250 ppb X 6 injections
500 ppb X 6 injections
1.00 ppm X 6 injections

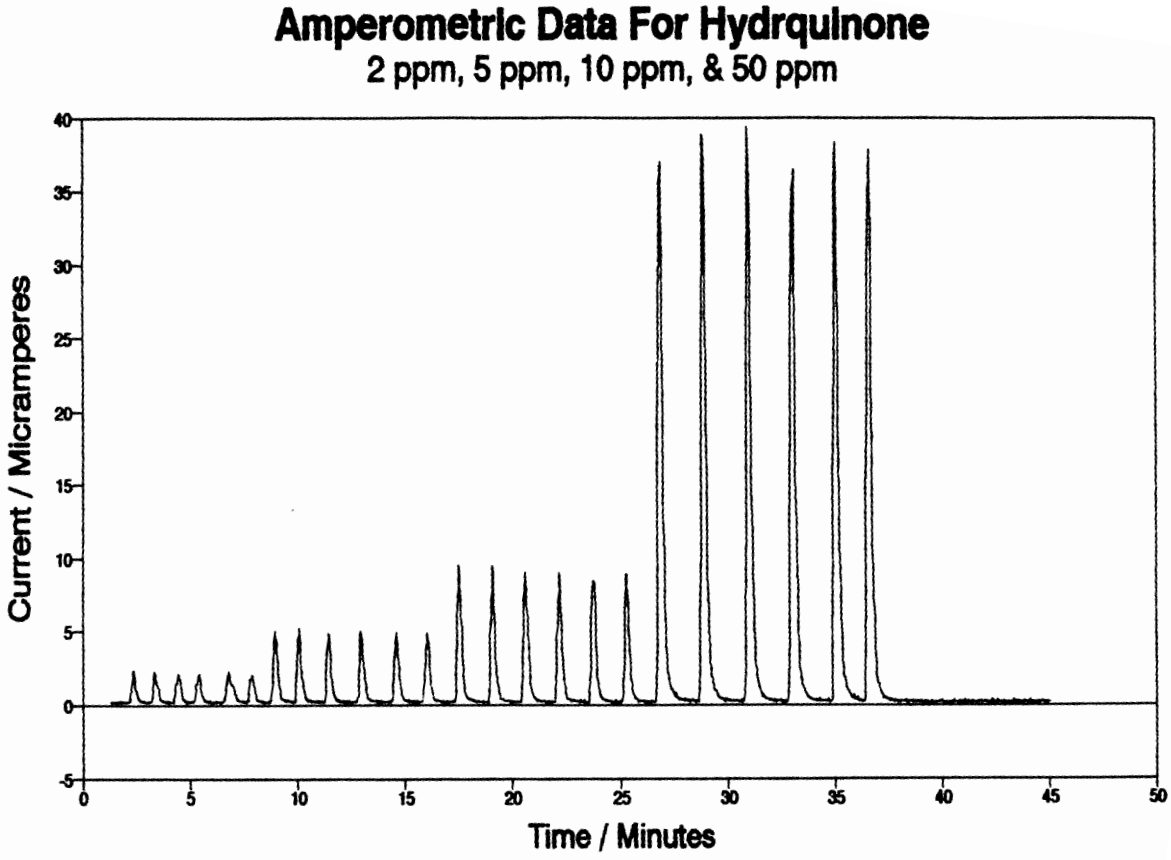

Data Set Used For Linear Dynamic Range Measurement
Sample Concentration (Left to Right)
2.00 ppm X 6 injections
5.00 ppm X 6 injections
10.00 ppm X 6 injections
50.00 ppm X 6 injections

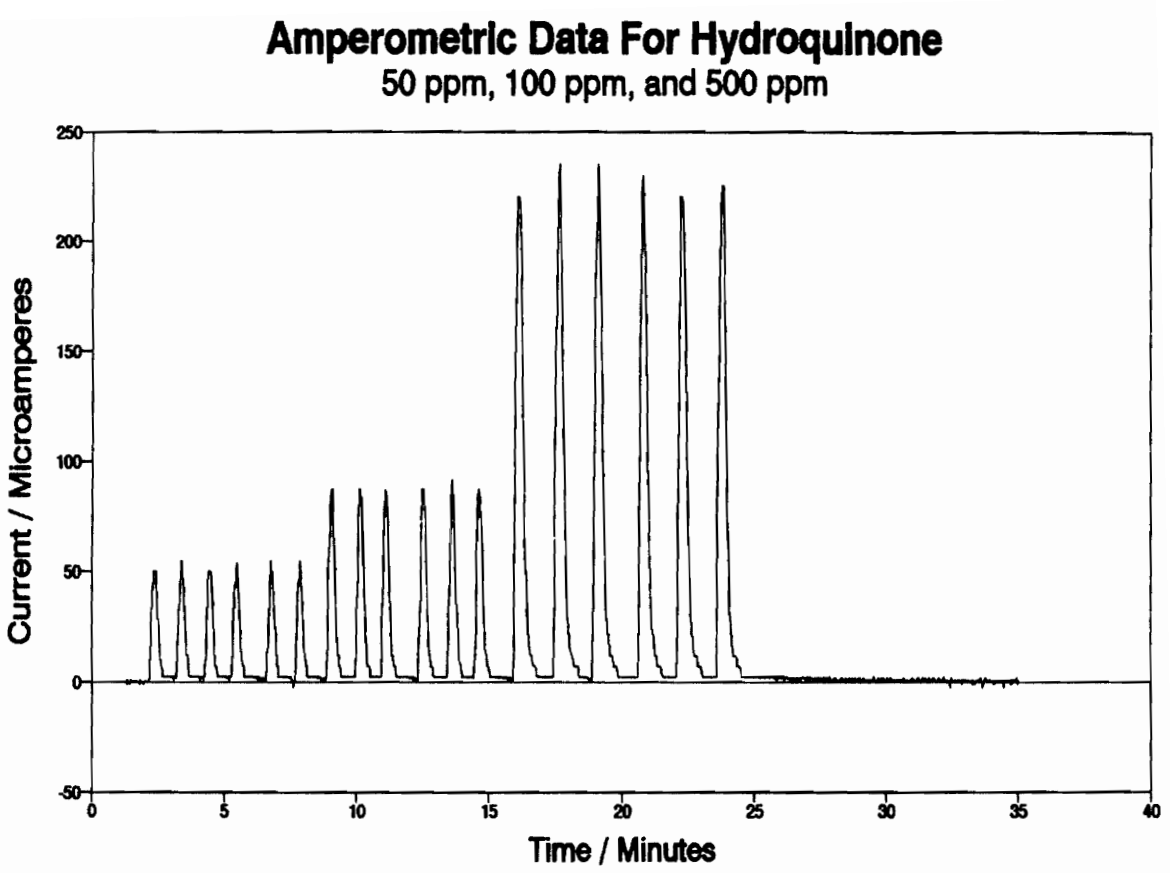

Data Set Used For Linear Dynamic Range Measurement
Sample Concentration (Left to Right)
50.00 ppm X 6 injections
100.0 ppm X 6 injections
500.0 ppm X 6 injections

APPENDIX E
QCM Data

QCM SIGNAL vs CONCENTRATION FOR KCl AT FIXED FLOW RATE
Crystal Modifier: 4-aminothiophenol
Solvent Composition: 20% acetonitrile, 80% water
Solvent Flow Rate: 26.6 μL/minute
Injection Volume: 20 μL
Data Values Are The Average of 3-4 Measurements per Sample

BARE CRYSTAL signal HZ	SAMPLE CONC. PPM	AMINE CRYSTAL signal Hz
257.7	1000	400.27
26.55	100	96.21
18.51	75	89.59
6.75	25	76.37
5.5	20	74.17
3.82	15	71.98
2.79	10	69.02
	8	63.17
1.62	6.7	57.29
	5	46.15
1.25	3.3	34.53
	2	20.57
	1	9.54

QCM SIGNAL vs CONCENTRATION FOR $KClO_4$ AT FIXED FLOW RATE
Crystal modifier: 4-aminothiophenol
Solvent Composition: 20% acetonitrile, 80% water
Solvent Flow Rate: 26.6 μL/minute
Injection Volume: 20 μL
Data Values Are The Average of 3-4 Measurements per Sample

BARE CRYSTAL signal HZ	SAMPLE CONC. PPM	AMINE CRYSTAL signal Hz
167.5	1000	205.2
13.4	100	85.9
9.5	75	82.9
3.6	25	71.3
1.7	15	66.9
0.89	10	59.6
	8	53.7
0.60	6.7	46.9
	5	37.4
0.0	3.3	24.9
	2	15.4
	1	6.5

QCM Response To Sugars As A Function of Solvent Flow Rate
Solvent Composition: 20% acetonitrile, 80% water
Crystal Modifier: 4-aminothiophenol
Injection Volume: 20 μL
Data Values Are The Average of 3-4 Measurements per Sample

RESPONSE HERTZ (1 g/L FRUCTOSE)	RESPONSE HERTZ (1 g/L SUCROSE)	FLOW RATE uL / MINUTE
31.2	42.3	13.3
27.6	36.3	26.7
24.7	33.3	40
22.2	29.8	53.3
20.6	27.6	66.7
19.2	25.7	80
18.2	24.7	93.3
17.3	23.3	106.7
16.5	22.5	120
16.5	22	133.3
14.9	20	166.7
14.1	18.2	233.3
	17.6	300

Response of the QCM for various phenols using a
4-aminothiophenol bonded crystal before addition of .001 M HCl
(data values row 1) and after addition of the acid (data values row 2)
solvent = 20% AcN, 80% H2O; 40 uL/min.
samples = 1000 ppm X 20 uL each
Data Values Are The Average of 3-4 Measurements per Sample

4-t-but phenol	4-i-prop phenol	4-ethyl phenol	phenol	
132.5	52.7	32.5	8.9	RESPONSE BEFORE ADDITION OF ACID
13.5	8.5	7.3	5.6	RESPONSE AFTER ADDITION OF ACID

Response of The QCM To Various Concentrations of 4-t-butylphenol As A Function of Solvent Composition.
Crystal Modifier: 4-aminothiophenol
Solvent Flow Rate: 40 μL/minute
Sample Volume: 20 μL
Data Values Are The Average of 2-4 Measurements per Sample

Sample Concentration ppm	QCM Response		
	20% acectonitrile 80% water	30% acetonitrile 70% water	40% acetonitrile 60% water
25	10.4	5.4	1.2
50	16.8	6.2	2.2
75	21.3	8.0	2.6
100	31.7	9.8	3.1
200	38.9		
250		19.5	6.8
500	69.4	26.9	14.8
1000	138.8	30.9	24.2

QCM Response To 4-ethylphenol and 4-isopropylphenol As A Function of Reduced Concentration.

Crystal Modifier: 4-aminothiophenol
Solvent Composition: 20% acetonitrile, 80% water
Solvent Flow Rate: 40 μL/minute
Sample Volume: 20 μL
Samples were prepared by first making saturated solutions of the test solutes in the carrier solvent and then diluting these to the appropriate concentration with the carrier solvent. For example, a sample with a reduced concentration of 0.4 would be prepared by mixing 4 parts saturated solution with 6 parts carrier solvent.

Data Values Are The Average of 3 Measurements per Sample

Reduced Concentration	QCM Response HERTZ	
	4-ethylphenol	4-isopropylphenol
0.5	69.3	50.6
0.4	52.0	38.9
0.3	40.5	31.3
0.2	27.5	20.6
0.1	14.3	10.0

Professional Vita
John Albert Roush

Born: August 14, 1957
Lafayette, Indiana

Education:

High School	Hernando High School Brooksville, Florida June, 1975
Undergraduate Education	King College Bristol, Tennessee Bachelor of Science, Chemistry May, 1979
Graduate Education	East Tennessee State University Johnson City, Tennessee September 1985 - May 1988
	Virginia Polytechnic Institute and State University Blacksburg, Virginia PhD, Chemistry September, 1992

Thesis:

"Development and Characterization of Novel Detectors For Use In Flow Injection Analysis Or Liquid Chromatography"
Advisor: Dr. Mark R. Anderson

Married: Kathleen D. LaGuardia
August 4,1979
Kingsport, Tennessee

Children: Jennifer Kathleen Roush, born November 10, 1982
John Albert Roush, Jr., born April 4, 1989

Employment
History: Giant Food Markets
Kingsport, Tennessee
May 1979 - December 1984
Director of Advertising, 1980 - 1984

Eastman Chemical Company
Kingsport, Tennessee
1988 - 1991 Summer Tech Program

Presentations:

John A. Roush and Mark R. Anderson, "Scanning Voltammetric Detector For Routine HPLC and Flow Injection Analysis", 43rd Annual Southeast Regional ACS Meeting, Richmond, Virginia, November, 1991

Mark R. Anderson, David Thacker, and John A. Roush "Selective Detection of Analytes In Flowing Streams Using Piezoelectric Quartz", ACS National Meeting, San Francisco, Ca., April, 1992

John A. Roush